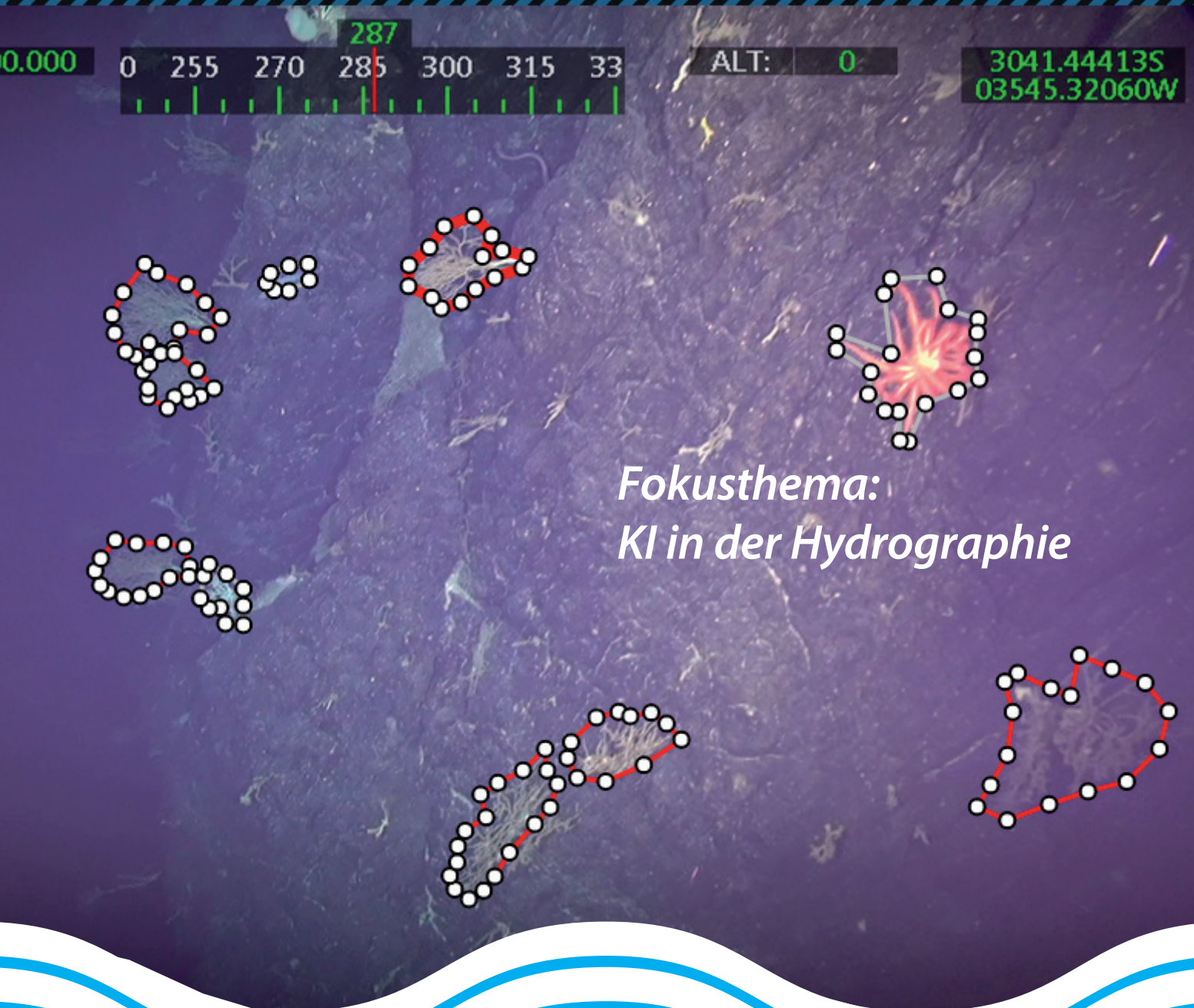


HYDROGRAPHISCHE NACHRICHTEN

Journal of Applied Hydrography

06/2021

HN 119



Consulting



Ocean engineering from space into depth

Realise your projects in cooperation with our hydrographic services

CTDs & SVPs



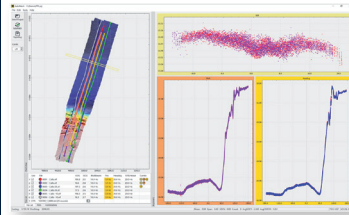
Our hydrography engineers are happy to develop systems tailored exactly to your needs and to provide professional advice and support for setting up your systems and training your staff.

MacArtney Germany benefits from being part of the MacArtney Group and enjoys unlimited access to cutting-edge engineering competences and advanced facilities.

Acoustic sensors



Software



Position and motion sensors



Integration



Liebe Leserinnen und Leser,

wir alle nutzen künstliche Intelligenz. Beinahe täglich. Meist ohne es zu merken. Wenn wir uns von Suchmaschinen durchs Web lotsen lassen, wenn wir online shoppen. Oder wenn wir für die Suche nach dem rechten Weg Navigationssystemen vertrauen.

In Navigationssystemen steckt künstliche Intelligenz übrigens gleich dreifach drin. Da wird der kürzeste Weg ermittelt. Da gibt es eine Sprachausgabe. Und da werden aktuelle Verkehrsinformationen mit in die Routenplanung einbezogen.

Ist das nun künstliche Intelligenz? Ja, auch. Aber eben nicht nur das. Der Begriff lässt sich bislang nicht wirklich klar definieren. Es geht irgendwie um Informatik, um abgefahrene Technologien und um immer mehr Anwendungen.

Mit Blick auf die Hydrographie schafft hoffentlich diese Ausgabe der *Hydrographischen Nachrichten* etwas mehr Klarheit. Wir haben die Frage gestellt, welche Rolle künstliche Intelligenz in der Hydrographie spielt. Die Antworten erfahren Sie in fünf Fachbeiträgen – zwei davon sind im Peer-Review-Verfahren begutachtet worden – und im Wissenschaftsgespräch mit Professor Alexander Reiterer vom Fraunhofer-Institut für Physikalische Messtechnik IPM in Freiburg (Seite 42).

In den Fachbeiträgen geht es um Steine auf dem Gewässerboden, die künstliche Intelligenz in Messdaten von Fächerecholoten bzw. Seitensichtsonaren erkennen soll (Feldens et al., Seite 6, und Christensen, Seite 24); es geht um die automatische »Erkennung und Klassifizierung von ben-

thischen Arten mittels Deep Learning« (Lütjens und Sternberg, Seite 18); es geht um den Mangel an echten Trainingsdaten und um den Versuch, die künstliche Intelligenz mit synthetischen Bildern zu trainieren (Steiniger et al., Seite 30); und es geht um Softwarelösungen, die dank maschinellem Lernen neue autonome Anwendungen in der Hydrographie ermöglichen (McPherson Kimø, Seite 36).

Auffallend ist, dass es bei den KI-Anwendungen vor allem um das Erkennen von Mustern geht. Und dass künstliche Intelligenz gar nicht von sich aus intelligent ist, sondern erst von Menschen trainiert werden muss. Von Science-Fiction keine Spur. Aber umso mehr von Science. Was in diesem Heft präsentiert wird, ist überwiegend Stand der Wissenschaft, noch nicht Stand der Technik. Die Anwendungen finden erst allmählich Einzug in die Praxis.

Außerdem im Heft: Die Beiträge von den beiden für den *DHyG Student Excellence Award* nominierten Absolventinnen der HCU. Cigdem Askar vergleicht verschiedene Sedimentecholote für die Anwendung in flachen Gewässern (Seite 54). Sophie Andree entwickelt Open-Source-Bibliotheken für die Prozessierung hydrographischer Daten (Seite 48).

Und Peter Ehlers blickt in einem angemessen langen Beitrag auf die hundertjährige Geschichte der IHO zurück (Seite 62).

Ich wünsche Ihnen eine erkenntnisreiche Lektüre dieser Ausgabe.



Lars Schiller

Hydrographische Nachrichten HN 119 – Juni 2021

Journal of Applied Hydrography

Offizielles Organ der Deutschen Hydrographischen
Gesellschaft – DHyG

Herausgeber:

Deutsche Hydrographische Gesellschaft e. V.
c/o Innomar Technologie GmbH
Schutower Ringstraße 4
18069 Rostock

ISSN: 1866-9204

© 2021

Chefredakteur:

Lars Schiller
E-Mail: lars.schiller@dhyg.de

Redaktion:

Peter Dugge, Dipl.-Ing.
Horst Hecht, Dipl.-Met.
Holger Klindt, Dipl.-Phys.
Dr. Jens Schneider von Deimling
Stefan Steinmetz, Dipl.-Ing.
Dr. Patrick Westfeld

Hinweise für Autoren und Inserenten:

www.dhyg.de > Hydrographische Nachrichten >
Mediadaten und Hinweise



R2SONIC Fächerlotsysteme



Sonic 2020



Sonic 2022



Sonic 2024



Sonic 2026

- **Beispiellose Leistungsfähigkeit** mit 256 Beams und 1024 Soundings bei 160° Öffnungswinkel (einstellbar) und einer Pingrate von 60 Hz
- **Breitbandtechnologie** mit Frequenzwahl in Echtzeit zwischen 200 bis 400 kHz sowie 700 kHz optional
- **Dynamisch fokussierende Beams** mit einem max. Öffnungswinkel von 0,5° x 1° bei 400 kHz bzw. 0,3° x 0,6° bei 700 kHz
- **Höchste Auflösung** bei einer Bandbreite von 60 kHz, bzw. 1,25 cm Entfernungsauflösung
- **Kombinierbar** mit externen Sensoren aller gängigen Hersteller
- **Flexibler Einsatz** als vorausschauendes Sonar und der Fächer ist vertikal um bis zu 30° schwenkbar
- **Zusätzliche Funktionen** wie True Backscatter und Daten der Wassersäule
- **MultiSpectral Modus™**, der es den R2Sonic-Systemen ermöglicht, Backscatter Daten mehrerer Frequenzen in einem einzigen Durchlauf zu sammeln

Nautilus Marine Service GmbH ist der kompetente Partner in Deutschland für den Vertrieb von R2Sonic Fächerecholotsystemen. Darüber hinaus werden alle relevanten Dienstleistungen wie Installation und Wartung kompletter hydrographischer Vermessungssysteme sowie Schulung und Support für R2Sonic Kunden angeboten.

R2Sonic ist ein amerikanischer Hersteller von modernen Fächerecholoten in Breitbandtechnologie. Seit Gründung des Unternehmens im Jahr 2009 wurden weltweit bereits mehr als 1.500 Fächerlote ausgeliefert und demonstrieren so eindrucksvoll die außergewöhnliche Qualität und enorme Zuverlässigkeit dieser Vermessungssysteme.

KI in der Hydrographie

Bolder detection I

- 6 **Automatic detection of boulders by neural networks**
 A comparison of multibeam echo sounder and side-scan sonar performance
A peer-reviewed paper by PETER FELDENS, PATRICK WESTFELD, JENNIFER VALERIUS, AGATA FELDENS and SVENJA PAPPENMEIER

Image classification

- 18 **Deep learning-based detection of marine images and the effect of data-driven influences**
A peer-reviewed paper by MONA LÜTJENS and HARALD STERNBERG

Boulder detection II

- 24 **Automatic boulder identification in side-scan sonar**
An article by JESPER HAAHR CHRISTENSEN

Synthetische Trainingsdaten

- 30 **Erzeugung von synthetischen Seitensichtsonar-Bildern mittels Generative Adversarial Networks**
Ein Beitrag von YANNIK STEINIGER, JANNIS STOPPE, DIETER KRAUS und TOBIAS MEISEN

Autonomous operations

- 36 **AI is enabling a transformation toward autonomous hydrographic operations**
An article by SARAFINA MCPHERSON KIMØ

Wissenschaftsgespräch

- 42 **»Die riesigen Flächen unterhalb der Wasseroberfläche bilden das perfekte Szenario für KI-basierte Ansätze«**
Ein Wissenschaftsgespräch mit ALEXANDER REITERER

DHyG Student Excellence Award I

- 48 **Interactive processing of MBES bathymetry and backscatter data using Jupyter Notebook and Python**
An article by SOPHIE ANDREE

DHyG Student Excellence Award II

- 54 **Comparison of different sub-bottom profiling systems to be used in very shallow and tide-influenced areas**
 A case study in the backbarrier tidal flat of Norderney, Germany
An article by CIGDEM ASKAR

Company presentation

- 60 **Meeting requirements for new types of on-demand survey campaigns**
An article by ANDRES NICOLA and DANIEL ESSER

IHO anniversary

- 62 **100 years of international cooperation in hydrography**
An article by PETER EHLERS

Die nächsten Fokusthemen

HN 120 (Oktober 2021)	Habitatkartierung
HN 121 (Februar 2022)	Häfen und Verkehre der Zukunft
HN 122 (Juni 2022)	Meerestechnik

Automatic detection of boulders by neural networks

A comparison of multibeam echo sounder and side-scan sonar performance

An article by PETER FELDENS, PATRICK WESTFELD, JENNIFER VALERIUS, AGATA FELDENS and SVENJA PAPENMEIER

Neural networks show great promise in the automatic detection of boulders on the seafloor. Maps derived from bathymetric data show better performance compared to backscatter mosaics in this study. However, we find the lack of training data ground-truthed to a high standard the largest challenge for automated object detection based on acoustic data.

boulder detection | neural networks | hydrographic surveying | bathymetry | backscatter
Erkennung von Felsbrocken | neuronale Netze | Seevermessung | Bathymetrie | Backscatter

Neuronale Netze sind sehr vielversprechend bei der automatischen Erkennung von Felsbrocken auf dem Meeresboden. Aus bathymetrischen Daten abgeleitete Karten zeigen in dieser Studie eine bessere Leistung im Vergleich zu Rückstreumosaiken. Die größte Herausforderung für die automatische Objekterkennung auf Basis akustischer Daten ist jedoch der Mangel an Trainingsdaten, die auf einem hohen Standard erprobt sind.

Authors

Dr. Peter Feldens, Agata Feldens and Dr. Svenja Papenmeier work at the Leibniz Institute for Baltic Sea Research Warnemünde. Dr. Patrick Westfeld and Jennifer Valerius work at the Federal Maritime and Hydrographic Agency (BSH) in Rostock and Hamburg.

peter.feldens@io-warnemuende.de

1 Introduction

Multibeam echo sounders (MBES) have been used for decades to provide high-quality bathymetric maps of the seafloor (Lurton 2002; Augustin et al. 1996; Pickrill and Todd 2003). The German Hydrographic Office (Federal Maritime and Hydrographic Agency, BSH) collects bathymetry and detects objects underwater by vessel-mounted MBES systems (Dehling and Ellmer 2012). The data surveyed in German waters are processed into official nautical charts and nautical publications to ensure navigational safety at sea. Accurate and reliable information of seabed's topography further forms a decisive basis for political and technical decisions relating to the sea, including applications depending on spatio-temporal-resolved 3-D geodata. Echo sounding is a measurement technique allowing for the 3-D reconstruction of the surface of the seafloor and all objects located on it. As a primary result, a digital surface model (DSM) is available. During the following data processing chain conducted at BSH, the task is to separate between the surface measured and the actual seabed, to derive a digital terrain model (DTM) of the seafloor. The detection and extraction of boulders are challenging. At BSH, it is realised in a semi-automatic process based on geometric filtering, with interactive post-processing and a final visual inspection by well-trained experts. This procedure is time-consuming and error-prone because of subjectiv-

ity and generalisation. Against a background of increasing user requirements (e.g. nautical information service needs a consistent separation of seabed and boulders for chart production; marine spatial planning requires information about conditions on the seabed to assess the impact of offshore construction projects) and the compliance with international standards (IHO S-44 Order 1a and 1b require the reliable detection of obstacles along all main shipping routes), automation of the processing chain is indispensable in terms of accuracy, reliability and reproducibility of the results. It is also required in the sense of an efficient evaluation of large areas.

Next to hydrographic applications, recent developments in habitat mapping require the detection of cobbles and larger hard substrates. The identification of marine hard substrates based on acoustic remote sensing is important for the detection, delineation and ecological assessment of seafloor habitats (Papenmeier et al. 2020) as well as for marine spatial planning. This need is accounted for in several international frameworks, such as the Convention on Biological Diversity and the Marine Strategy framework directives. Boulder detection in the German Baltic and the North Sea for these purposes is done using side-scan sonar (SSS) systems. Next to the ease of operation over large scales, the survey geometry of a side-scan sonar, towed above the seafloor,

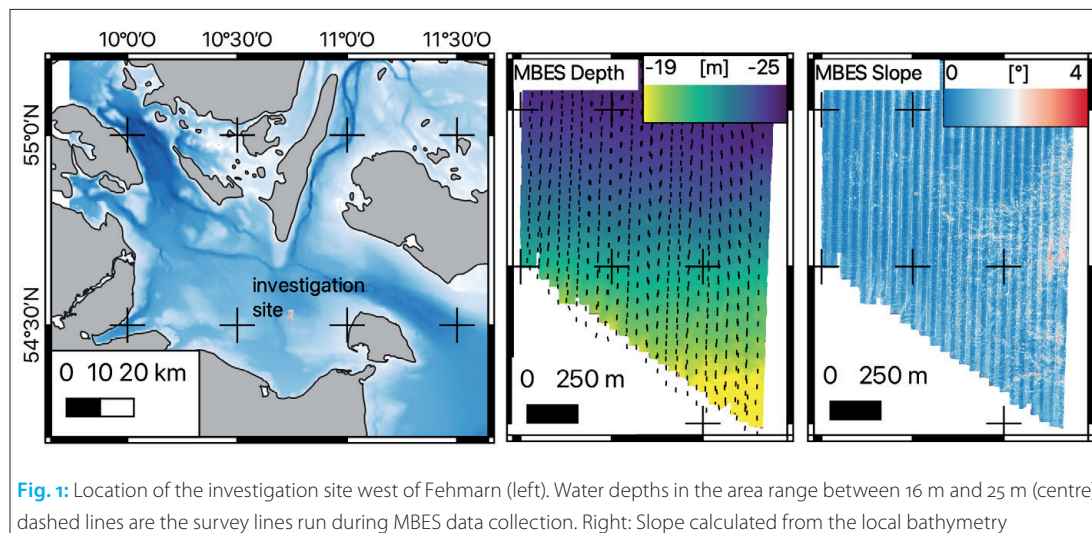


Fig. 1: Location of the investigation site west of Fehmarn (left). Water depths in the area range between 16 m and 25 m (centre), dashed lines are the survey lines run during MBES data collection. Right: Slope calculated from the local bathymetry

aids the detection of small objects. Both for manual and automatic methods, boulder detection was found to be more reliable, with an increasing number of pixels forming an object's representation in backscatter (BS) mosaics (Feldens et al. 2019). Acoustic shadows, which form behind boulders, increase the number of pixels of boulder representations in backscatter mosaics. Shadow sizes increase with grazing angle, thus favouring towed sonar systems (Papenmeier et al. 2020). Therefore, while the spatial resolution of modern MBES derived backscatter information can rival that of side-scan sonar systems in many relevant practical applications (depending on water depth), their survey geometry is unfavourable for boulder detection in backscatter data. However, the pixel-perfect co-registration of depth and backscatter and derived data sets may offset this disadvantage and facilitate boulder detection based on MBES data. Considering the interpretation of extensive areas, human experts have difficulties in combining information of multi-dimensional data sets, while machine learning algorithms are less limited by dimensionality and more efficient (Yokoya et al. 2017).

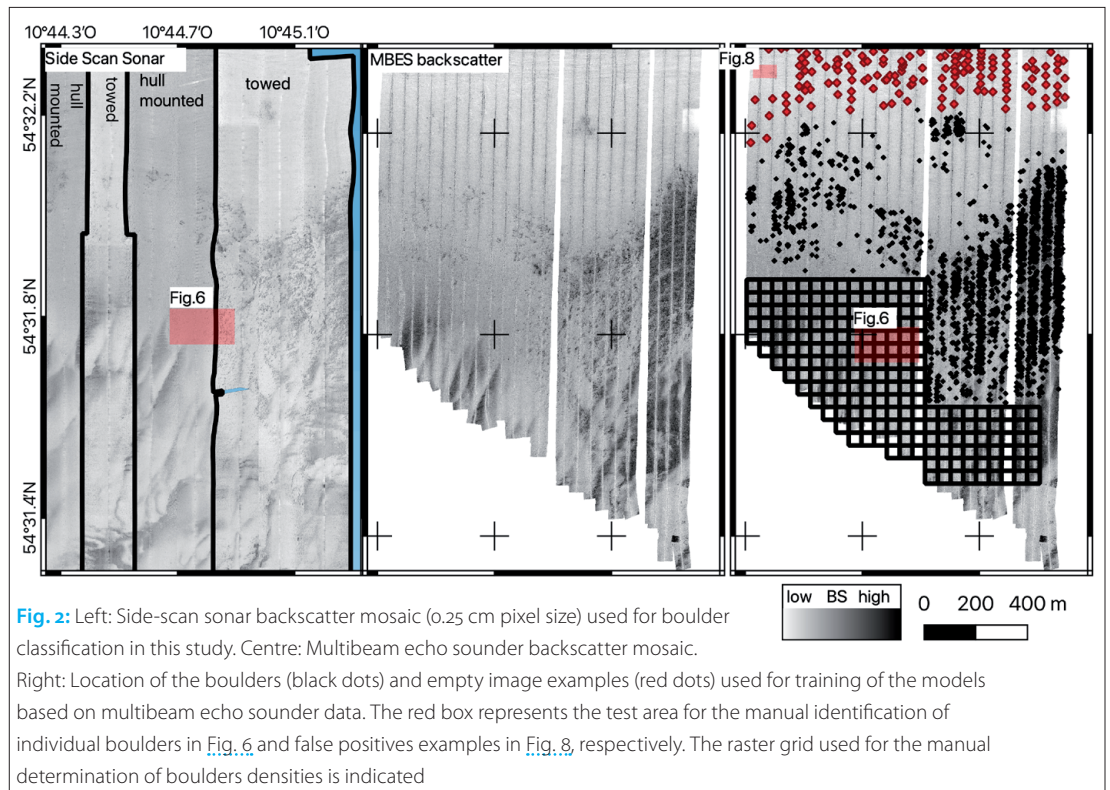
In the last decade, object detection frameworks based on convolutional neural networks (CNN) were applied to different topics, including remote sensing in the earth sciences (Ghamisi et al. 2017; Zhu et al. 2017) with great success. CNNs were used to find boulders in side-scan sonar backscatter mosaics, showing performance comparable to human experts in areas of moderate to good data quality (Feldens et al. 2019). It is the aim of this case study to compare the performance of multibeam echo-sounder and side-scan sonar to image boulders in single-band and multi-band data sets including depth, slope and backscatter intensity. An object detection framework based on a neural network is used to identify boulders in the data sets, and the results are compared with the interpretation of human experts.

2 Methods

2.1 MBES

Multibeam echo sounder data were collected in summer 2019 from the hydrographic survey vessel VWFS *Deneb*, operated by BSH, by a state-of-the-art MBES system Teledyne-Reson Seabat 7125-SV2. The system operates at 400 kHz with a 140° opening angle, a pulse length of 300 μ s and 512 beams per swath. The seafloor of the study area (Fig. 1, left) was fully covered by 50 survey lines with 100 % overlap (Fig. 1, centre). The software Teledyne PDS was used for real-time data acquisition. A combined GNSS (Global Navigation Satellite Systems; good global but poor relative accuracy) and INS (Inertial Navigation System; good local accuracy but drifts without external reference) forms the basis for an accurate and reliable real-time direct georeferencing of MBES measurements. MBES instruments require an accurate portrayal of the sound speed structure of the water column. In this campaign, the distribution of water sound velocity was determined by continuous profile measurements using the multi-parameter online probe Sea & Sun Technology CTD 60Mc. Bathymetry data were processed using Teledyne CARIS HIPS & SIPS. The processing chain holds techniques for i.a. correction of sound velocity induced effects, calculation of a georeferenced 3-D point cloud, generation of 3-D surface representation of the bottom topography, outlier detection and filtering.

To create backscatter grids with a resolution of 0.25 m based on the multibeam echo sounder data provided as s7k-files, angular variations in intensities were removed using the open-source processing toolbox MB-System (Caress and Chayes 1996). A grazing angle of 40° (here, minor variations in incidence angle have little effect on backscatter intensity) was used as a reference angle. A low pass Gaussian mean filter stretching five samples in the across-track and three samples in the along-track direction was applied once to



the data to remove high frequency speckle noise. Data gaps of up to 1.25 m were interpolated. The grid was built by applying a Gaussian Weighted Mean. As available profiles are overlapping, samples of higher grazing angles were given an increased priority during gridding. Profiles were run in both N-S and S-N directions on the same profile track. For the backscatter maps, one of these directions was used, the other line was discarded. Backscatter intensities were clipped at the 0.2 % and 99.8 % percentile to improve image contrast. In this study, higher backscatter intensities are displayed in darker colours. All backscatter intensities are uncalibrated, relative values (Lamarche and Lurton 2018) and were exported as 8-bit greyscale mosaics following processing. Multi-band images of MBES-derived grids of backscatter, slope and depth were created using the open source GDAL utilities (GDAL/OGR contributors 2021), by placing slope information in the green image channel (Fig. 1, right), backscatter information in the red image channel (Fig. 2, centre) and depth values in the blue image channel (Fig. 1, centre).

2.2 SSS

The side-scan sonar data were recorded in May 2019 during cruise #164 with the vessel *VWFS Deneb*. The Edgetech CSS-2000 was towed at an altitude of approximately 12 ± 3 m above the seabed. Due to technical problems with the CSS-2000 a change to the hull-mounted side-scan sonar (Edgetech 4300 MPX) became necessary during the cruise (Fig. 2 shows the coverage of both data sets). The vessel speed varied between 4 and

4.5 kn. Using a swath-width of 200 m the profile distance was set to 180 m to allow an overlap of approximately 10 % at the edges.

Processing of the backscatter amplitudes was done with the software package SonarWiz 7.3. Only the higher frequency of the CSS-2000 has been used (600 kHz). The 4300 MPX used a frequency of 410 kHz. After bottom tracking and empirical gain normalisation, the data of the towed system additionally required a correction of the navigation data. The sheave offset was adjusted, and a layback correction was executed basing on data of a cable counter and a pressure sensor. To generate a final backscatter mosaic both data sets were merged. The overlapping profiles were cut at the edges as far as possible without causing gaps. Finally, a mosaic (8-bit greyscale) with a spatial resolution of 25 cm was exported (Fig. 2, left).

2.3 Manual boulder count

Two experienced human interpreters did a manual count of individual boulders in a test area (Fig. 2, red box) based on the side-scan sonar mosaics. Human interpreters generally recognise boulders by an increased backscatter intensity facing towards the side-scan sonar, followed by an acoustic shadow forming behind. The human interpreters were not involved in picking the training data for the neural networks. To interpret larger areas, a raster approach is used. For $50 \text{ m} \times 50 \text{ m}$ cells (Fig. 2, black raster grid), the same human experts decided whether it includes no boulders, one to five boulders, or over five boulders. This procedure is in line with currently published recommenda-

tions for mapping geogenic reefs (Heinicke et al., in press), used to characterise geogenic reefs over larger areas. The agreement between the human experts is calculated using the F_1 score of the resulting confusion matrix. An F_1 score of 1.0 indicates perfect agreement, while the lowest value is 0, when either precision or recall are 0. The F_1 score is calculated from the confusion matrix by $F_1 = 2 \times (\text{precision} \times \text{recall}) / (\text{precision} + \text{recall})$. Values for each class (no boulders, one to five boulders and more than five boulders) were averaged.

2.4 Automatic boulder count

2.4.1 Neural network

Artificial neural networks are composed of series of interconnected layers of artificial neurons. In a trained neural network, input signals are transformed by changing weights at each connection, until the last layer of the network reports the result of the computation. Convolutional neural networks are a subset of neural networks and were developed for image classification with overwhelming success. While the architecture of CNNs varies, all include a series of convolutional layers, that operate by convolving a small part, often 3×3 pixels, of the underlying image (or the output of an earlier layer in the network) with weights initialised at random. This assumes that pixels in close vicinity are more likely to form patterns significant for the image context than those pixels with greater distance. The weights are adjusted during model training with annotated images to minimise a loss function. Loss functions compare the predictions of the neural network to the annotations. To allow CNNs learning non-linear features, activation functions change the output of layers in the network, while regular downsampling of the image size allows the network to learn features of larger scales.

The automated boulder count was done using the YOLO (You Look Only Once) framework, developed by Joseph Redmon (Redmon et al. 2015), with the current implementation available under a permissive license on GitHub (<https://github.com/AlexeyAB/darknet>). Lary et al. (2016) and Schmidhuber (2015) give a detailed description of convolutional neural networks and their application for image interpretation.

The YOLO network was developed for object detection. To identify and locate different objects in images is more complicated than the classification of entire images and requires a different network architecture. YOLO is a one-stage detector, meaning it analyses images in one pass (hence the abbreviation, You Only Look Once) while keeping high accuracy. One-stage detectors are a faster approach compared to other object detection frameworks that rely on multiple stages for object detection in images. The YOLO architecture is described by Bochkovskiy et al. (2020). In principle, it uses a series of different convolutional layers (the

backbone and neck) to extract object features and divide the input image into grids at three different resolutions. For each grid cell at each resolution, it predicts the probability that the cell includes a learned object within anchor boxes of predefined size. These probabilities and the corresponding bounding box coordinates are the output of the trained model. YOLO networks are available in different configurations of the backbone, of which we here utilise the standard configuration of YOLO version 4.

2.4.2 Model training and application

To create the training data sets, a human interpreter identified bounding boxes of boulders in training areas in QGIS 3.16. Boulders were required to have a shadow. The boulders were exported as an SQLite database. The training database for the SSS model includes 13,847 boulder instances. A model was trained on a data set with an emphasis on small boulders comprising only a few pixels. This data set comprises 4,070 entries. The MBES training database was only started with the investigation site reported here (Fig. 2). It is not possible to use the same training data sets for MBES and SSS models, since the position accuracy of the side-scan sonar is not good enough to co-locate features of only a few pixels in size. Therefore, the MBES training data set comprises 2,654 instances of boulders (Fig. 2), with typical sizes of 3×3 to 8×15 pixels including shadows. The training mosaics were cut into small georeferenced images of 64×64 pixels (corresponding to approximately $16 \text{ m} \times 16 \text{ m}$ in this study), overlapping by six pixels to minimise the number of training boulders that are cut by image boundaries. In the following, the pixel coordinates of the annotated examples were calculated and used as an input for training. Besides the annotated boulder examples, 182 examples of empty images (defined as containing no boulders) were selected for the MBES data set and 2,349 examples of empty images for the SSS data set.

For training, we used the YOLO network version 4, in contrast to earlier case studies that used the two-stage RetinaNet framework (Lin et al. 2017). We adhered to suggestions published on the project's GitHub page and changed the default configuration of the YOLO network. Therefore, the maximum number of training batches was reduced to 6,000 for MBES models and 24,000 for SSS models, the number of classes reduced to one, and the filter number of the convolutional layers before the object detection layers reduced to 18. Images were magnified to 512×512 pixels before training. Random variations in hue, exposure and saturation applied to the image were reduced from their standard settings to 0.1. The size of the input image was changed by 40 % every ten batches at random, and the size and aspect

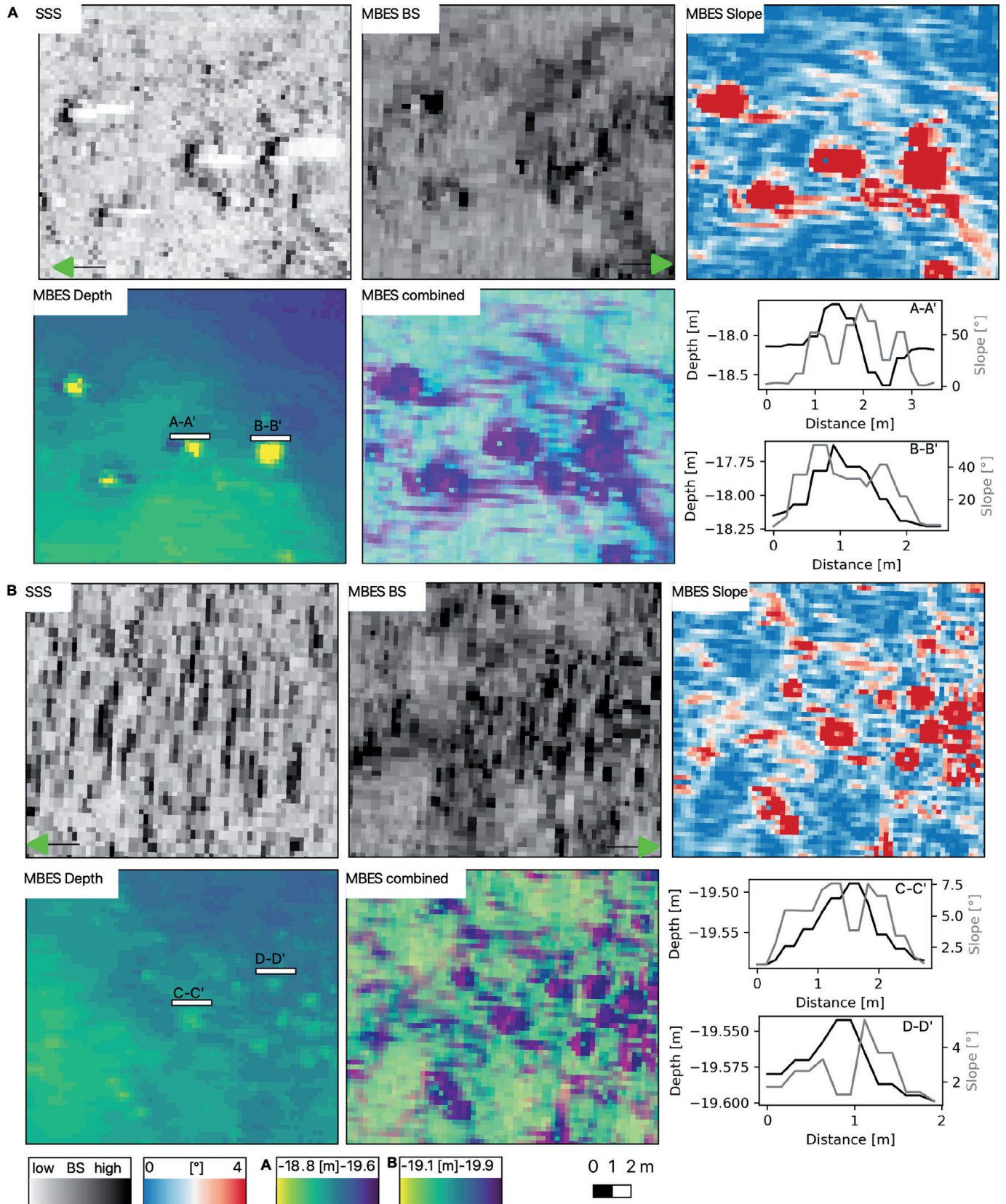


Fig. 3: The appearance of boulders in the different data sets. A) At a distance of 45 m to the nadir individual boulders are recognised in SSS backscatter. The same boulders (27 m to the nadir) are more difficult to recognise in MBES backscatter. The boulders are visible in bathymetry, slope, and combined data sets. B) Small boulders as imaged in the outer part (75 m to nadir) of a side-scan sonar swath. The characteristic boulder pattern is hard to recognise and appears smeared in the along-track direction, due to yaw movements or decreasing along-track resolution. The appearance of boulders is difficult to interpret in MBES (20 m to nadir) backscatter, but the objects are recognised in slope, bathymetry and combined data sets. The position of SSS images was shifted by several metres to account for positional differences to the MBES. The green arrow points to the nadir. SSS data was recorded with a CSS-2000

ratio were also changed by $\pm 60\%$ for each image. The optimal anchor sizes for the YOLO network were calculated. 15% of the training samples were randomly selected for validation and used to calculate the average precision for the boulder class (AP) of the different networks. After the image set for validation was separated, a Python script rotated every image in 45° steps to account for variable survey directions. The training took place on a NVIDIA 2080 TI graphic card (11 GB RAM). Training of the MBES models required about twelve hours for the MBES models and 40 hours for the large SSS model.

For model application, the training procedure is reversed. The (single or multi-band) mosaic is cut into small georeferenced image tiles of 64×64 pixels. Threshold values for include objects were set to 0.2 for all models except the SSS model for small objects, which was set to 0.35. The model is run on these small tiles. The detection of objects on a single image requires about 10 ms on an NVIDIA 2080 TI. The pixel-coordinates of the resulting bounding boxes are converted to geographic coordinates and displayed using QGIS. To emulate the raster approach used by human experts to cover large areas, detected boulders in each grid cell are counted.

3 Results

3.1 Local geology and appearance of boulders

Water depths in the investigation site (approximately 2 km^2) vary between 16 m and 25 m, with depths increasing towards the north. Backscatter maps derived from MBES and SSS show different seafloor facies at the site (Fig. 2), with fine-grained deposits and intensive disturbance by bottom trawling activities in the north (low backscatter). High backscatter intensities characterise glacial lag deposits towards the south and east. A high number of boulders are part of these deposits. Intermediate backscatter intensities towards south and west characterise fine to medium sands and partial outcrops of glacial lag deposits. In the side-scan sonar mosaics, which cover a larger area, a series of elongated, elevated ridges exist in the southeast. The general sedimentological build-

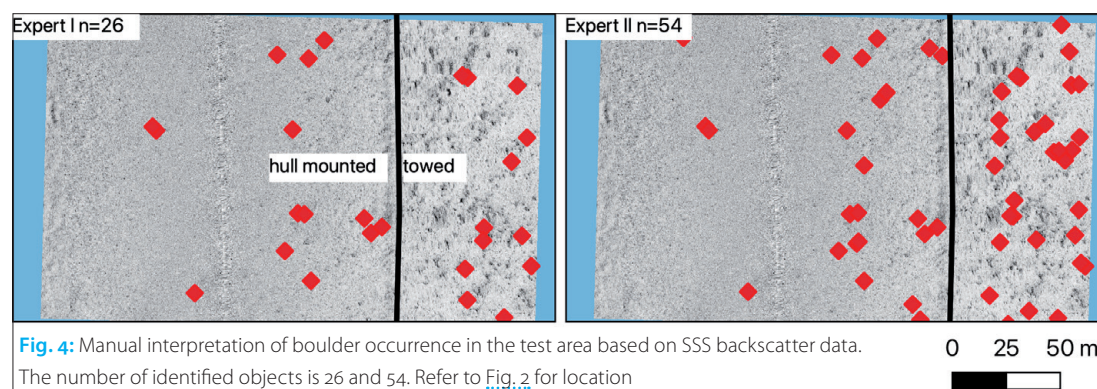
up also controls the local slope shown in Fig. 1. While high pixel-to-pixel slopes exceeding 60° at maximum prevail in the areas of glacial lag deposits due to the presence of boulders and near the trawl marks, the remaining area is flat with slope values below 2° .

Based on a visual inspection, we find most boulders in the area composed of glacial lag deposits, with some also present in the sandy facies. The boulders have different characteristics in the data sets that are displayed in Fig. 3. In the SSS-derived backscatter mosaics, boulders can be recognised by a high backscatter front, an intermediate intensity signal behind and an acoustic shadow at the back, relative to the side-scan sonar position. However, small boulders are often more difficult to interpret. This is caused either by their small size or their position in the outer part of the swath (a combination of which is shown in Fig. 3B). In addition, artefacts in side-scan sonar data can resemble smaller boulders. Such artefacts include scatter from water column stratification or areas near the side-scan sonar nadir.

In MBES-derived backscatter, boulders are recognised by an increase in backscatter intensity compared to the surrounding seafloor (Fig. 3) but are often lacking a pronounced acoustic shadow. The backscatter representation of boulders is less distinct compared to SSS imagery in close to intermediate distance to the nadir. Boulders are imaged as circular to elliptic features in maps of the local slope. Slope values for boulders range from 3.5° to more than 60° degrees, related to the large variety of boulder shapes in transported lag deposits transported by glaciers. Also, boulders may be partially buried in the subsurface. However, not all circular features correspond to increased backscatter intensities, for example in the areas of overlapping profiles. In MBES-derived maps of depth, boulders are displayed as circular features elevated 2.5 cm to over 50 cm compared to the adjacent seafloor.

3.2 Manual boulder identification

For a test area of about $30,000 \text{ m}^2$, two experienced human interpreters picked boulders on the side-scan sonar backscatter mosaic (Fig. 4). The test area showcases instances of water column



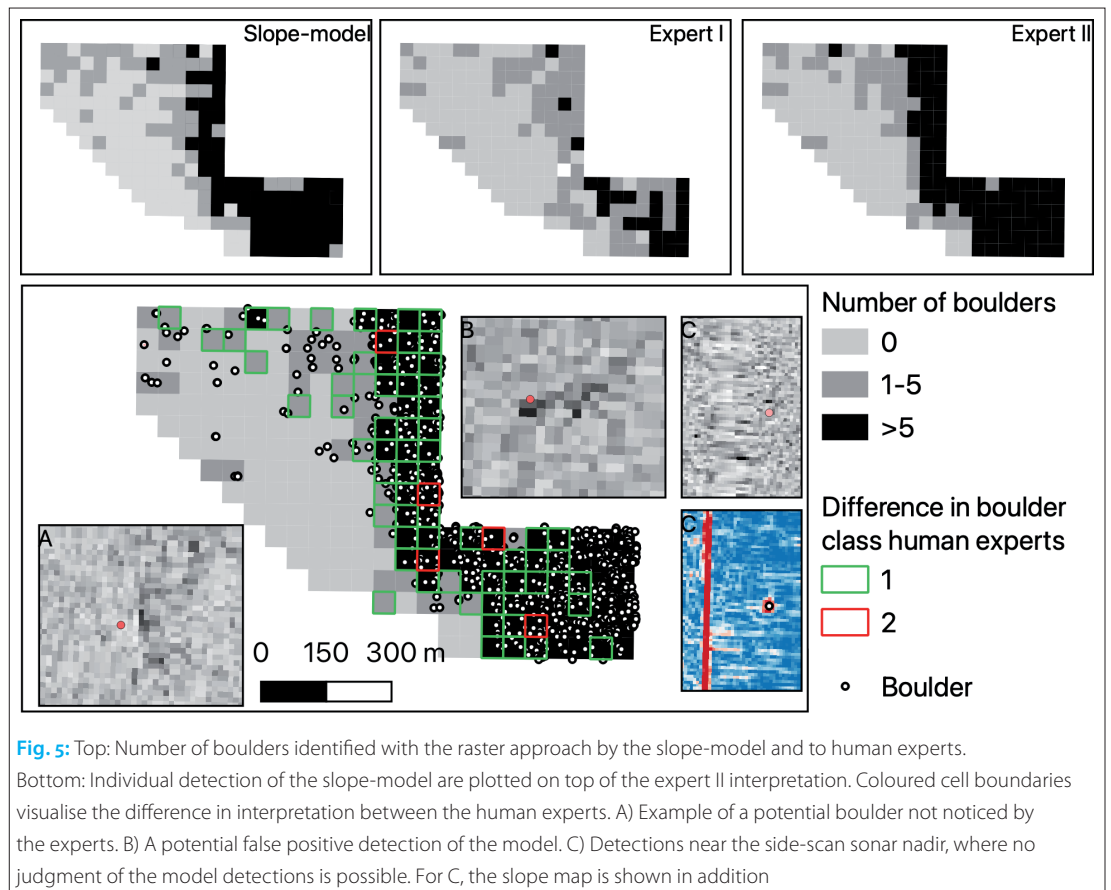


Fig. 5: Top: Number of boulders identified with the raster approach by the slope-model and to human experts. Bottom: Individual detection of the slope-model are plotted on top of the expert II interpretation. Coloured cell boundaries visualise the difference in interpretation between the human experts. A) Example of a potential boulder not noticed by the experts. B) A potential false positive detection of the model. C) Detections near the side-scan sonar nadir, where no judgment of the model detections is possible. For C, the slope map is shown in addition

stratification on the eastern side, a nadir stripe in the centre of the area and an overlap of two different profiles recorded with different side-scan sonars towards the west. The experts found 26 and 54 boulders. No human misinterpreted the water column artefacts, nadir stripes or overlapping profiles as boulders. A higher variability exists in the outer parts of the swath near the overlapping profiles, where the appearance of potential boulders varies. The same human experts interpreted boulder densities over a larger area using the raster approach applied to 50 m × 50 m cells (Fig. 5). Dense boulder assemblages were confirmed in the east towards the outcropping glacial till, while boulders are sparse towards west. Corresponding to the different number of individual boulders found in the test area, expert I identified a larger area covered by one to five boulders compared to expert II. The

Data set	Model AP
MBES SLOPE	64 %
MBES DEPTH SLOPE BACKSCATTER	61 %
SSS BACKSCATTER large objects	43 %
SSS BACKSCATTER small objects	37 %
MBES DEPTH	36 %
MBES BACKSCATTER	18 %

Table 1: Overview of performance on the validation data set (measured in AP) for the different models and data sets

F_1 score, measuring the agreement between the two experts, is 0.61 based on 196 raster cells.

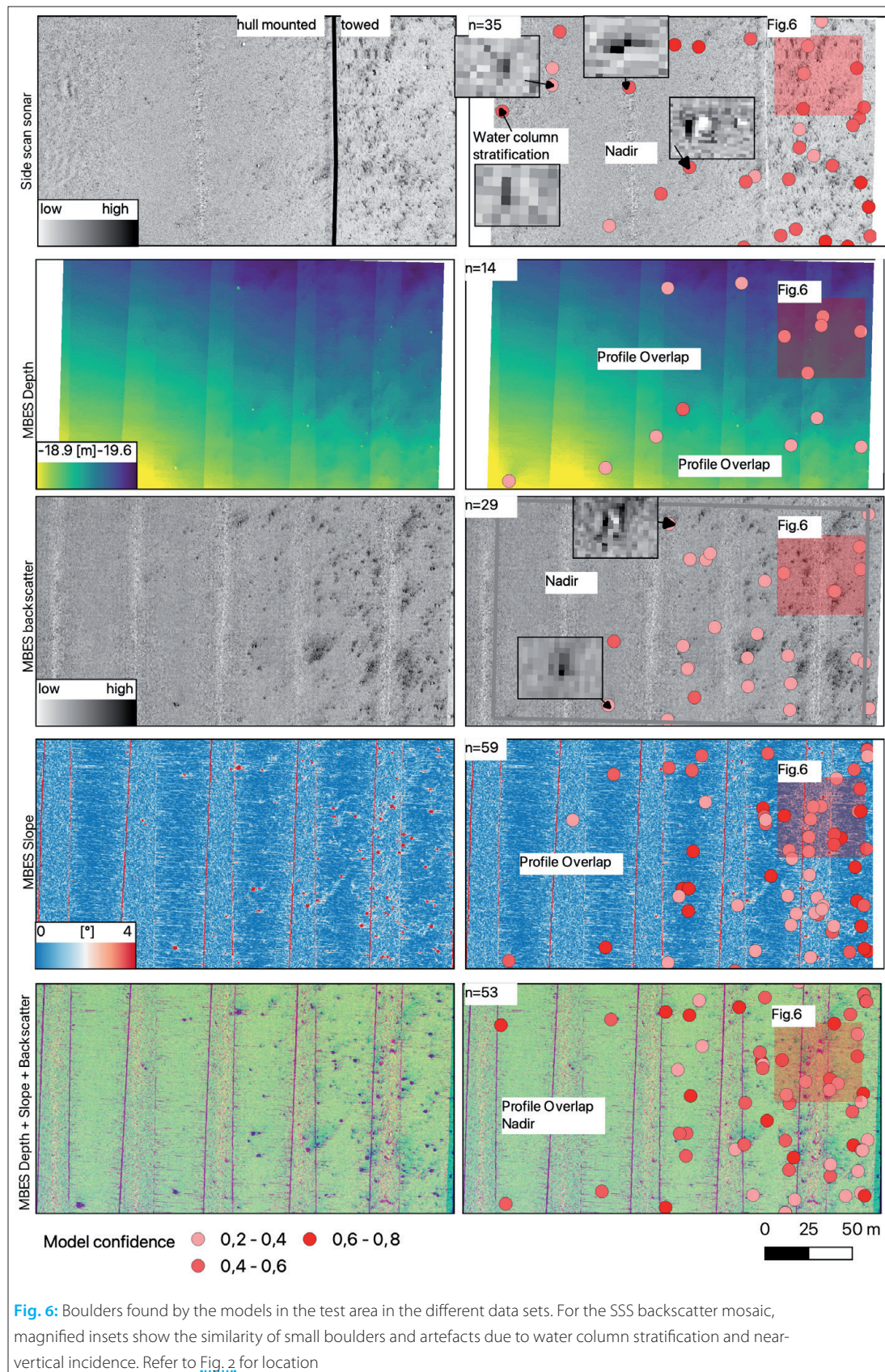
3.3 Automated boulder detection

The Average Precision (AP) of the models on the validation data is shown in Table 1. The highest performance is 64 % by the slope-only model, followed by a model working on a 3-band data set comprising MBES backscatter, slope and depth with 61 % AP. The MBES backscatter-only model achieves an AP of 18 %. The side-scan sonar performance is 37 % to 43 %, with the lower AP for the training data set with a focus on small objects. The detections of the best-performing slope-model are plotted on top of boulder densities as determined by human experts (Fig. 5).

The resulting detections of the models in the test area are shown in Fig. 6. The SSS models find a total of 35 boulders, all including a discernible shadow on visual inspection. One likely false positive occurs around water column stratification artefacts and one false positive in the nadir region. The MBES backscatter model finds a total of 29 boulders. Of these, seven have no discernible shadow, while the remaining display at least one pixel of acoustic shadows behind. The model working on the area-wide bathymetric grids detects 14 boulders with elevations of 6 cm to 40 cm compared to the surrounding seafloor, albeit most boulders smaller than 15 cm are not recognised in the data set. The slope model finds

59 objects at the test site, characterised by slopes ranging from 35° to less than 3.5°. However, most identified boulders show slope values of over 4°. The model running on the combined data set of backscatter, slope and depth detects 53 boulders. Most of these boulders are also recognised in the

slope data set. However, several potential boulders found in the slope data set were not found by the combined model and vice versa, with examples shown in Fig. 7. Here, a comparison with the independently recorded side-scan sonar data – barring some uncertainty because of the positional

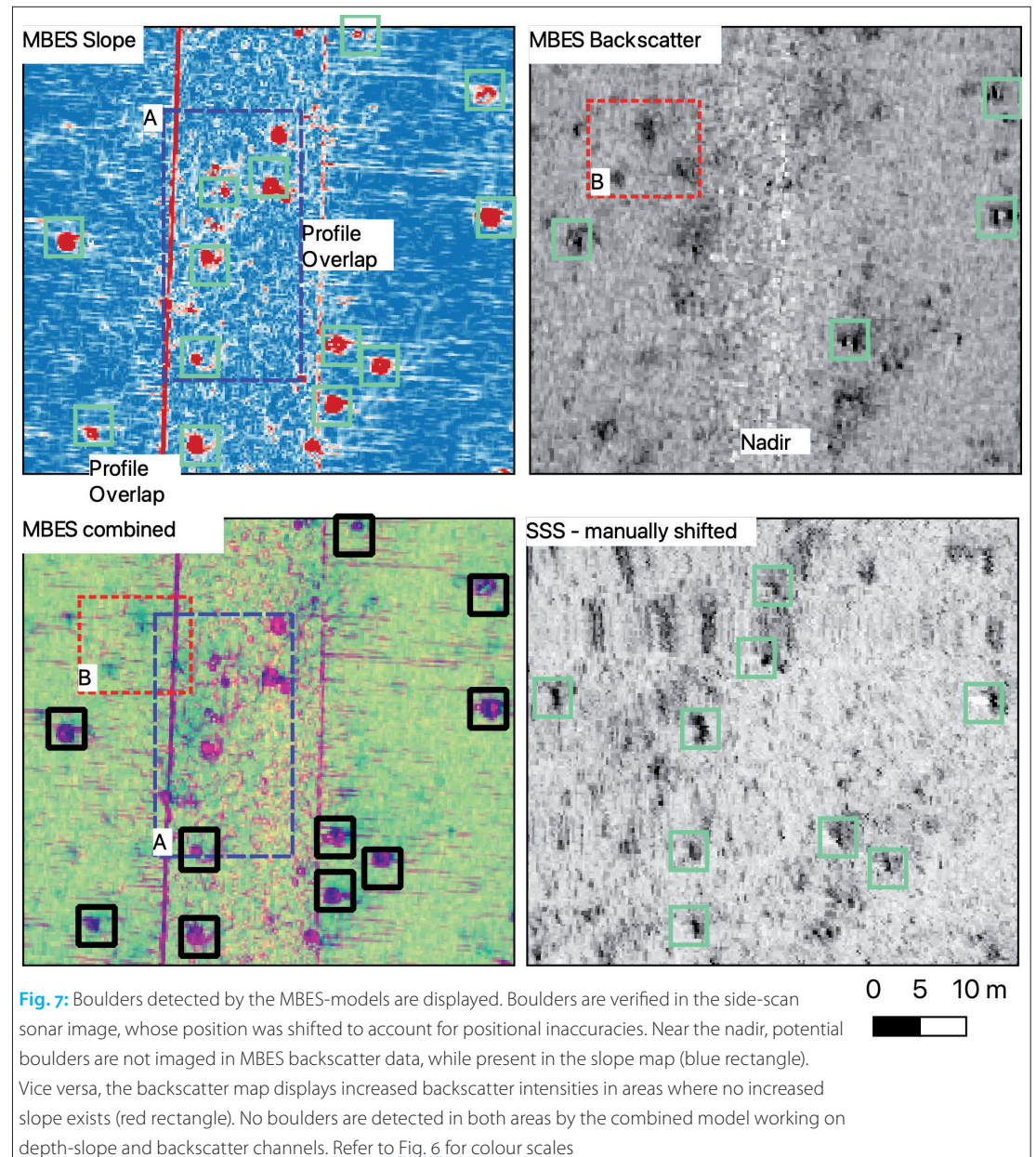


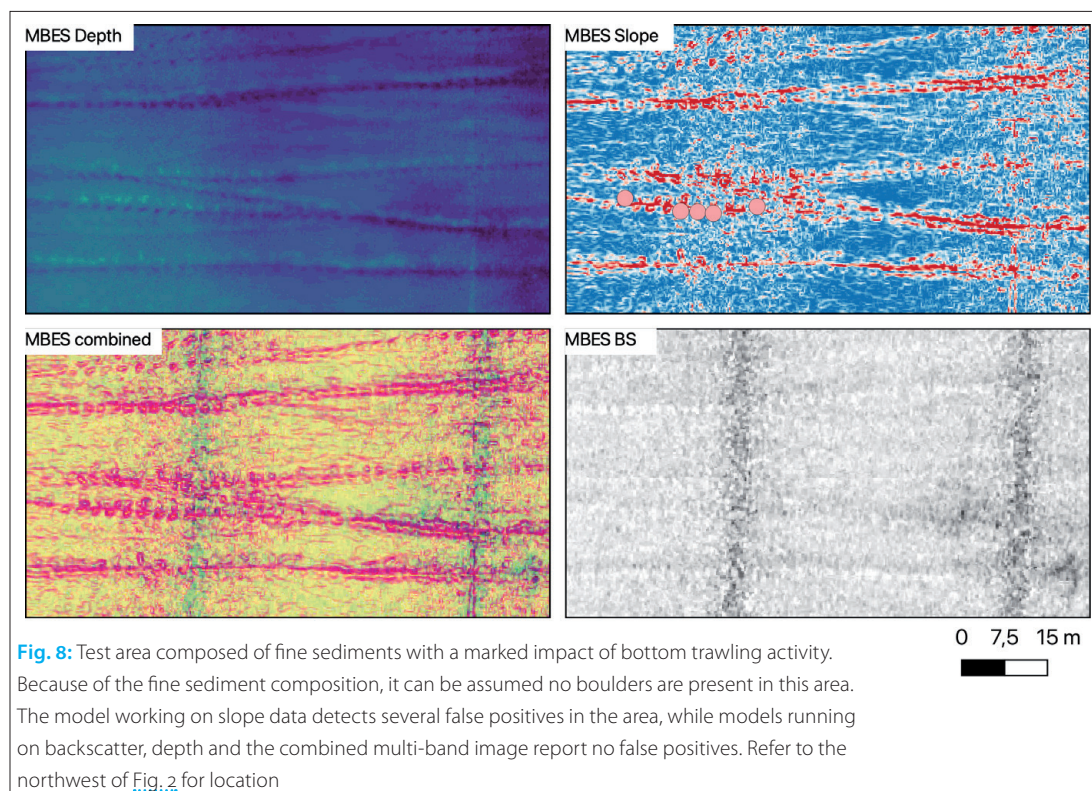
inaccuracy that required shifting the side-scan sonar mosaic location by a few metres – seems to show that the slope data is correct, and these objects should have been identified as boulders. In contrast, in the northern test area (Fig. 8), circular elevated features are identified as boulders by the slope-model. We find similar examples, not displayed here, in areas with remaining outliers in morphological data which have a similar appearance. Such outliers cause artificial slopes but do not affect backscatter data information.

The results of the raster approach using the model with the highest AP (the slope-model) are shown in Fig. 5. The slope-model identifies between 0 and 42 boulders in the 50 × 50 m cells. The agreement with the human experts I and II as measured by the F₁ score for 182 cells (cells where both SSS and MBES data are available) is 0.75 and 0.63, respectively.

4 Discussion

The high difference of boulder detection by very experienced human interpreters (Fig. 3) shows the need for an objective, automatic method for boulder detection. The different count of individual boulders transfers to an agreement of 0.61 (F₁ score) over 196 cells that were interpreted with the raster approach. This poses a significant challenge both for quantification of model performance and for the establishment of correctly annotated training images, a problem faced by many other applications of neural networks to remote sensing data (Zhu et al. 2017). The same person interpreting the training database and the reference sites for boulder detection (Feldens et al. 2019) partially mitigates the problem. However, this approach does not scale to more than one involved person or to applications where objective results without interpreter bias are required. Almost no study includes an extensive ground truthing for boulders





in acoustic data, and – except for obvious instances – the interpretation of a human interpreter of what is and what is not a boulder varies based on his/her experience, with no possibility to judge what is the correct interpretation. The appearance and visibility of boulders in backscatter data can change with swath width and incidence angle (Papenmeier et al. 2020; von Rönn et al. 2019). While a methodological description on how to assess geogenic reefs exists (Heinicke et al., in press), it defines no sufficient criteria to decide which objects are to be identified as boulders in acoustic data.

Still, our case study allows qualitative insight into the advantages and disadvantages of SSS and MBES-based boulder mapping by neural networks. To mitigate the impact on AP for the different models, a single person confirmed all samples in the training database used for this study. Therefore, model performance is only compared relative to the interpretation of the acoustic data by one human expert and not to the true seafloor conditions. Both SSS and MBES systems supply backscatter information. A problem of SSS-based boulder detection are artefacts (Wilken et al. 2012), e.g., near the nadir or in areas of water column stratification that can in their structure resemble small boulders (Fig. 6). Due to the requirements to detect tiny objects comprising only 7 to 9 pixels in the examples shown here and even less if objects of 25 cm in size are to be detected in acoustic data (von Rönn et al. 2019), there is limited information to differentiate between artefacts and real objects. This causes a trade-off during the training of side-scan sonar-based models: if the sensitivity of the

model to detect small boulders – as required by regulations – is increased, the amount of false positive identifications increases as well. Because of the absence of well ground-truthed reference sites, a calculation of meaningful precision-recall curves to find optimal threshold values is not possible. Tuning the threshold level of the model to the local conditions (e.g., the number of artefacts in the data) is done manually, which is a subjective procedure. A possible solution is to include nadir and water column stratification effects as distinct classes and define these areas as insufficient for boulder detection. While MBES snippet-derived backscatter data is not affected by water column stratification and is used for object detection (e.g., Kunde et al. 2018), individual boulders are not displayed in the specular regime (Fig. 7) at near-vertical incidence angle and are resolved in less detail compared to side-scan sonar images in the data (Fig. 2). The loss of detail may be caused by a different along-track resolution due to different opening angles of the used systems (0.5° at 400 kHz for the Reson 7125, CSS-2000: 0.26° at 600 kHz, respectively 0.29° at 410 kHz for the 4300 MPX). Combined with the less pronounced acoustic shadows, the AP of the MBES backscatter model data set, therefore, is worse compared to the model trained on side-scan sonar backscatter data (Table 1). MBES-based backscatter maps cannot be recommended as the principal data source for boulder detection based on our case study.

An obvious problem related to the use of MBES bathymetry and derived slope values is the required thorough cleaning of the data, with outli-

ers or morphological features having similarities to small boulders in slope maps. An example of such morphological feature in the German Baltic Sea is related to bottom trawling (Fig. 8). The trawl doors create steep local, almost circular morphological features when lifted off the seafloor. These features are misinterpreted by the slope-only model as boulders. The backscatter model correctly ignores these features. The combination of backscatter and slope data also prohibit false positives in the combined model. Therefore, while the AP of the slope model is the best on the validation data overall (Table 1), it also produced undesirable false positives in areas where boulders are very unlikely to appear (Fig. 7). The pixel-perfect coregistration of depth and backscatter information by multibeam echo sounders can mitigate this downside. Being the best model in our case study, the slope-model results were compared with the human raster-based interpretation of a larger area. The F_1 score of the model compared to the human experts is 0.75 and 0.62. Both scores are higher than the score for the direct comparison of the human experts, although the number of raster cells counted is not identical due to the different extension of available SSS and MBES data. Positional inaccuracies between the side-scan sonar and multibeam echo sounder data of approximately 5 m may negatively impact the comparison of cells where boulders are situated close to the edges. In hindsight interpretation of the model-human differences, potential errors on both sides were identified (examples shown in Fig. 5). In addition, the slope data is less affected than backscatter intensity by survey geometry and finds boulders that could not be identified in the side-scan sonar data because they are located close to the nadir.

The poorer performance of the MBES depth-derived model compared to the slope model is not surprising, given that the maximum resolution of the input image is the regional depth interval divided by the available discrete pixel values. In our study, this is 9 m divided by 256 (28 bpp, bit per pixel), artificially limiting the vertical resolution to ca. 0.035 m in the single band 8-bit image. Given that many boulders have smaller elevations (Fig. 2) and are visible in slope maps, the performance of the depth model is good and may have great potential for models operating on point clouds and derived statistics which became available in the last years (Held and Schneider von Deimling 2019; Guo et al. 2020). The advantages and disadvantages of including absolute depths as an input channel for neural networks must be considered, however. In the Baltic Sea, for example, finding boulders in deeper muddy basins is unlikely, but

possible (Beisiegel et al. 2019), and changing depth intervals between different sites (and thus changing resolution in colour-coded depth images) may be problematic. We suggest exploring the use of further depth-derived information, such as the bathymetric position index, or texture parameters derived from backscatter mosaics in the future.

Models working on a combination of depth, slope and backscatter data produced false negatives in the near-nadir region, as boulders are not imaged in the backscatter channel. They also show fewer false positives and are less susceptible to remaining outliers in bathymetric data. Therefore, while the performance of the joint depth-slope-backscatter data set is worse than for the slope-only model (due to validation examples in the nadir region) in our case study, its inherent robustness to false positives by combining independent data sets makes it the method of choice for practical applications in the future. Ideally, and needed for many commercial applications anyway, an over 100 % overlap would remove the near-vertical incidence backscatter data and is expected to improve model results. Multi-band images with calibrated backscatter data collection (Lamarche and Lurton 2018) would also allow for a quantitative definition of boulders, e.g., by measuring increase of backscatter intensity in addition to local slope and local bathymetric position index.

5 Conclusion

Our case study shows that boulders are detected with higher precision in bathymetric data compared to backscatter mosaics recorded by either multibeam echo sounder or side-scan sonar. The results of the best model are comparable to the range of results achieved by human interpreters. We recommend combining bathymetry and backscatter data into a multi-band image to limit false positive detections. However, the limiting factor for the automated detection of boulders in acoustic data is not the technology, but the domain knowledge and the availability of accurately annotated training images. Future activities should involve the careful choice of sites for ground-truthing and acoustic surveys, to create a high-quality training data set. //

Acknowledgment

The authors thank Elham Al-Akrami for initial preparation of MBES-related training data set, and Merle Hennig for support in digitising boulders on the SSS mosaics. We thank the crew of VWFS *Deneb* for their great support during the measurement campaigns, and the two reviewers who provided helpful and constructive comments.

References

- Augustin, Jean-Marie; Raymond Le Suavé et al. (1996): Contribution of the multibeam acoustic imagery to the exploration of the sea-bottom. *Marine Geophysical Researches*, DOI: 10.1007/BF00286090
- Beisiegel, Kolja; Franz Tauber et al. (2019): The potential exceptional role of a small Baltic boulder reef as a solitary habitat in a sea of mud. *Aquatic Conservation: Marine and Freshwater Ecosystems*, DOI: 10.1002/aqc.2994
- Bochkovskiy, Alexey; Chien-Yao Wang, Hong-Yuan Mark Liao (2020): YOLOv4: Optimal Speed and Accuracy of Object Detection. arXiv: 2004.10934
- Caress, David W.; Dale N. Chayes (1996): Improved processing of Hydrosweep DS multibeam data on the R/V Maurice Ewing. *Marine Geophysical Researches*, DOI: 10.1007/BF00313878
- Dehling, Thomas; Wilfried Ellmer (2012): Zwanzig Jahre Seevermessung seit der Wiedervereinigung. *AVN Vol. 119, Nr. 7, S. 243–248*
- Feldens, Peter, Alexander Darr et al. (2019): Detection of Boulders in Side Scan Sonar Mosaics by a Neural Network. *Geosciences*, DOI: 10.3390/geosciences9040159
- GDAL OGR contributors (2021): GDAL/OGR Geospatial Data Abstraction software Library. Open Source Geospatial Foundation
- Ghamisi, Pedram; Javier Plaza et al. (2017): Advanced Spectral Classifiers for Hyperspectral Images: A review. *IEEE Geoscience and Remote Sensing Magazine*, DOI: 10.1109/MGRS.2016.2616418
- Guo, Yulan; Hanyun Wang et al. (2020): Deep learning for 3d point clouds: A survey. *IEEE Transactions on Pattern Analysis and Machine Intelligence*, DOI: 10.1109/TPAMI.2020.3005434
- Heinicke, Kathrin; Tim Bildstein; Dieter Boedecker (in press): Leitfaden zur großflächigen Abgrenzung und Kartierung des LRT 1170 »Riffe« in der deutschen Ostsee (Untertyp: geogene Riffe)
- Held, Philipp; Jens Schneider von Deimling (2019): New Feature Classes for Acoustic Habitat Mapping – A Multibeam Echosounder Point Cloud Analysis for Mapping Submerged Aquatic Vegetation (SAV). *Geosciences*, DOI: 10.3390/geosciences9050235
- Kunde, Tina; Philipp Held et al. (2018): Ammunition detection using high frequency multibeam snippet backscatter information. *Marine Pollution Bulletin*, DOI: 10.1016/j.marpolbul.2018.05.063
- Lamarche, Geoffray; Xavier Lurton (2018): Recommendations for improved and coherent acquisition and processing of backscatter data from seafloor-mapping sonars. *Marine Geophysical Research*, DOI: 10.1007/s11001-017-9315-6
- Lary, David J.; Amir H. Alavi et al. (2016): Machine learning in geosciences and remote sensing. *Geoscience Frontiers*, DOI: 10.1016/j.gsf.2015.07.003
- Lin, Tsung-Yi; Priya Goyal et al. (2017): Focal Loss for Dense Object Detection. arxiv: 1708.02002
- Lurton, Xavier (2002): An introduction to underwater acoustics: principles and applications. Springer Science & Business Media
- Papenmeier, Svenja; Alexander Darr et al. (2020): Hydroacoustic Mapping of Geogenic Hard Substrates: Challenges and Review of German Approaches. *Geosciences*, DOI: 10.3390/geosciences10030100
- Pickrill, Richard A.; Brian J. Todd (2003): The multiple roles of acoustic mapping in integrated ocean management, Canadian Atlantic continental margin. *Ocean & Coastal Management*, DOI: 10.1016/S0964-5691(03)00037-1
- Redmon, Joseph; Santosh Divvala et al. (2015): You Only Look Once: Unified, Real-Time Object Detection. DOI: 10.1109/CVPR.2016.91
- Schmidhuber, Juergen (2015): Deep learning in neural networks: An overview. *Neural Networks*, DOI: 10.1016/j.neunet.2014.09.003
- von Rönn, Gitta Ann; Klaus Schwarzer et al. (2019): Limitations of Boulder Detection in Shallow Water Habitats Using High-Resolution Sidescan Sonar Images. *Geosciences*, DOI: 10.3390/geosciences9090390
- Wilken, Dennis; Peter Feldens et al. (2012): Application of 2D Fourier filtering for elimination of stripe noise in side-scan sonar mosaics. *Geo-Marine Letters*, DOI: 10.1007/s00367-012-0293-z
- Yokoya, Naoto; Claas Grohnfeldt; Jocelyn Chanussot (2017): Hyperspectral and Multispectral Data Fusion: A comparative review of the recent literature. *IEEE Geoscience and Remote Sensing Magazine*, DOI: 10.1109/MGRS.2016.2637824
- Zhu, Xiao Xiang; Devis Tuia et al. (2017): Deep learning in remote sensing: A comprehensive review and list of resources. *IEEE Geoscience and Remote Sensing Magazine*, DOI: 10.1109/MGRS.2017.2762307

Deep learning-based detection of marine images and the effect of data-driven influences

An article by MONA LÜTJENS and HARALD STERNBERG

Throughout recent years convolutional neural networks have been applied for various image detection tasks. Training data thereby plays an important role for the performance of those models. Not only the amount of images is crucial but also the number of annotations, classes as well as image dimensions. In view of changing underwater environments, the study of benthic communities is increasingly important especially in the Southern Ocean as they provide a key link for ecosystem shifts. This study concentrates on the automatic detection and classification of benthic species using deep learning. It could be shown that glass sponges, brittle stars and soft corals could successfully be detected even on few input data and highly biased class distributions in varying underwater scenes. Further analyses considering data-driven influences show significant performance declines regarding the training on single objects and classes per image and the evaluation on large image dimensions.

deep learning | automatic detection | underwater imagery | benthos
Deep Learning | automatische Detektion | Unterwasserbilder | Benthos

In den letzten Jahren wurden gefaltete neuronale Netze für verschiedene Aufgaben der Bilderkennung eingesetzt. Die Trainingsdaten spielen dabei eine wichtige Rolle für die Leistungsfähigkeit dieser Modelle. Dabei ist nicht nur die Menge der Bilder entscheidend, sondern auch die Anzahl der Annotationen, Klassen sowie die Bilddimensionen. Angesichts sich verändernder Unterwasserumgebungen wird die Untersuchung benthischer Lebensgemeinschaften vor allem im Südlichen Ozean immer wichtiger, da sie hier vor allem sensibel auf Veränderungen reagieren. Diese Arbeit konzentriert sich auf die automatische Erkennung und Klassifizierung von benthischen Arten mittels Deep Learning. Es konnte gezeigt werden, dass Glasschwämme, Schlangensterne und Weichkorallen selbst bei wenigen Eingabedaten und stark unterrepräsentierten Klassen in unterschiedlichsten Unterwasserlandschaften erfolgreich erkannt werden. Weitere Analysen zu datengetriebenen Einflüssen zeigen deutliche Leistungseinbußen bei einzelnen Objekten und Klassen pro Bild während des Trainings und großen Bilddimensionen während der Evaluation.

Authors

Mona Lütjens is Research Associate at HafenCity University in Hamburg. Harald Sternberg is Professor for Hydrography at HafenCity University in Hamburg.

mona.luetjens@hcu-hamburg.de

1 Introduction

Global ocean temperature rise and ocean acidification are ubiquitous and threaten especially benthic communities in the Southern Ocean where many species survive only in a narrow thermal range (Griffiths et al. 2017). To detect current ecosystem shifts, studies regarding the abundance of megabenthic species can provide information as they are very sensitive to environmental change (Piepenburg et al. 2017). Sponges should be especially investigated as they create and shape habitats for other species like brittle stars and a decrease in sponges might directly lead to a decrease in many other species as well (Mitchell et al. 2020).

One of the main methods to study megabenthic species is through optical imagery. It is a fast and non-destructive sampling method and optical systems are typically mounted on towed or remotely operated vehicles. In light of its advantages,

an increasing amount of underwater imagery has emerged raising the need for automatic analytical methods. Recent research in full automatic detection and classification of marine images deploy deep learning algorithms as they show superior results for unconstrained underwater environments, non-iconic images and variant image deformations (Gonzalez-Cid et al. 2017). The latter is one of the main challenges as objects in marine images are greatly changing due to different lightning conditions, rotation of the camera system, lens distortion and noise (Pavoni et al. 2021). To account for this, multilayer convolutional neural network (CNN) models are introduced. Learned features can be recognised regardless of their position or imaging condition and without previous image preprocessing or human supervision. In computer vision tasks, two main methods for recognising multiple objects have emerged: object detection and in-

stance segmentation. The output of an object detector is a set of bounding boxes around detected objects whereas instance segmentation computes pixel-accurate masks around detected objects and is thus able to grasp the shape of objects. Generating training data for instance segmentation is very laborious and masks are typically generated in a second step after the bounding box detection. Since this study simply focuses on the detection of marine species without the necessity to capture shapes of features, instance segmentation was not implemented. Several previous works deal with the classification and detection of fish (Salman et al. 2016; Christensen et al. 2018) or benthic communities (Boulais et al. 2020) using state-of-the-art models such as LeNET, SSD via MobileNet and RetinaNet via ResNet50, respectively.

For CNNs the amount of training data is considered to be the main driver for accurate network inference. Also, better results are achieved with deeper layered networks because features can be learned at more diverse levels of abstractions. As more layers of neurons are added to the network, different feature details ranging from low-level features such as lines or dots to high-level features such as common objects or shapes are trained to be recognised. Networks with multiple layers are thus better at generalising because they learn more discriminative features (Pauly et al. 2017). However, deeper layered networks typically consists of several million of parameters, increasing the demand of more training data. Therefore, training data sets are commonly augmented by changing the rotation, sharpness, perspective and brightness (Huang et al. 2019) to produce more input data in a cost and time effective way. In view of successful training, it is further important to consider data related design choices such as number of annotations and classes per image during training as well as the image input size. While considering image sizes ranging from 96 to 224 pixels, it could be shown that the accuracy linearly increases (Mishkin et al. 2017).

This paper investigates the effect of data driven influences on the model accuracy in an attempt to create a road map for optimal input training data with regards to number of annotations and classes per image, class imbalance and image sizes exceeding those in previous mentioned studies. For the detection of benthic morphotypes the state-of-the-art network CenterMask (Lee and Park 2019) via ResNeXt-101 (Xie et al. 2017) was utilised which is trained on the three classes: glass sponges, soft corals and brittle stars.

2 Data

2.1 Underwater imagery data set

A seabed survey to investigate the epibenthos was carried out during the PS118 cruise of RV *Polarstern*



Fig. 1: Synthetically derived image compositions by placing cut out foregrounds onto cropped backgrounds

in the western Weddell Sea in 2019 (Purser et al. 2021). Seafloor images were obtained using the towed Ocean Floor Observation and Bathymetric System (Purser et al. 2019). For this study images from seven different sampling stations at distinct depths and with diverse seafloor types were used to incorporate various environmental alterations in the network training process. The original 3840×5760 sized images were tiled rather than down sampled to 1440×960 to keep the input resolution but decreasing the need for computational resources during training. Image annotation for the three object classes was conducted on 1000 images using the web-based annotation tool COCO Annotator (Brooks 2019). The selected image set was split so that 700 images belong to the training set, 100 images to the validation set and 200 images to the test set. After labelling it was evident that a high class imbalance persists because of the 3550 annotations from the training set, 87 % of the labels belong to the class brittle stars, 8 % to the class glass sponges and 5 % to the class soft corals.

2.2 Data augmentation

Data augmentation was conducted using the image generator COCO Synth (Kelly 2019) which composes new images by placing cut out objects as foreground over plain seafloor images. The foregrounds are randomly altered in brightness, rotation, scale and amount. For training, a total of 12,000 synthetic images were created from 30 foregrounds per class and 30 background images (Fig. 1). It is noted, that the selected foregrounds and backgrounds originate from images that are not part of the original training set mentioned in section 2.1. Also, to alleviate class imbalance 4000 images of the 12,000 images are solely composed of glass sponges and soft corals changing the ratio

to 33 %, 33 % and 34 % for glass sponges, soft corals and brittle stars.

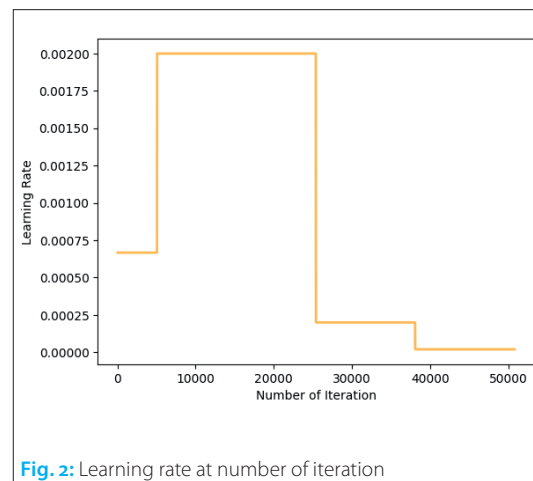
3 Method

3.1 Deep learning architecture

The neural network which was utilised for the detection of benthic species in section 4.1. and 4.2 is the object detector CenterMask (Lee and Park 2019) in combination with the backbone ResNeXt-101 (CM-X-101) (Xie et al. 2017). Backbone refers to the part of the network which is used to extract basic features and creates the feature map representation of the input data. They are typically initialised by ImageNet pre-trained weights. The detection head uses the feature map to perform the task of object detection and classification. It computes bounding boxes on identified objects for each image and calculates the classification confidences. Both architectures used in this study received excellent results in recent benchmarks such as COCO (Lin et al. 2014). For the experiments conducted in section 4.3 and 4.4 the more light-weight backbone VoVNetV2-99 (CM-V-99) (Lee und Park 2019) was used instead of ResNeXt-101 as it comprises fewer network parameters such as weights of connections which reduces the computing time.

3.2 Training details

Training was executed on five NVIDIA Tesla V100 GPUs of a 64-bit Linux machine equipped with an Intel Xeon Gold 6254 CPU @ 3.10 GHz. The base learning rate was set to 0.002. To reduce the effect of early overfitting on highly differentiated data sets, the learning rate was reduced for the first 5080 iterations by one third (Fig. 2). After 25,400 and again after 38,100 iterations the base learning rate was reduced by a factor of ten. The maximum number of iterations one image batch was passed forward and backward through the neural network was 50,800 which corresponds to 20 epochs defined as the number where the entire data set is passed through the network.



3.3 Performance metrics

The performance was assessed based on the evaluation metrics adopted for COCO which are based on the average precision and average recall scores (Lin et al. 2014). Both, precision as well as recall are evenly important metrics for the classification of benthic communities. While precision is the ratio of correctly predicted specimen out of all predicted specimen, recall indicates whether all correct specimen could be detected and how many were missed. Consequently, the precision P defines the proportion of false positives FP and the recall R reflects the proportion of false negatives FN . With TP being the number of true positives they can be mathematically computed as follows:

$$P = \frac{TP}{(TP + FP)} \quad \text{and} \quad R = \frac{TP}{(TP + FN)}$$

Precision and recall scores are then computed into average scores (AP and AR) over all classes and at varying intersection over union (IoU) thresholds which are used to measure the overlap between ground truth and predicted bounding boxes. The defined IoU are 0.5 and the average of ten IoU levels starting from 0.5 to 0.95 with a step size of 0.05 (the latter is further denoted as: .50:.95). AP and AR are also calculated for varying object sizes (small: $< 72^2$ pixels, medium: $> 72^2$ and $< 214^2$ pixels, large: $> 214^2$ pixels) and for different maximum number of detections per image (1, 10, 100). AR_1 computes the mean average recall across all classes and IoU thresholds for images where at most one detection was made while AR_{10} and AR_{100} compute the mean average recall for images where at most ten or at most 100 detections were made, respectively. Additional adopted metrics are the accuracy to assess the total number of predictions that are correct and the F_1 measure which evenly weighs between precision and recall (Manning et al. 2009):

$$\text{accuracy} = \frac{TP + TN}{(TP + TN + FP + FN)} \quad \text{and} \quad F_1 = \frac{2PR}{P + R}$$

4 Experiments and results

Main experiments in section 4.1 and 4.2 were executed across varying data sets summarised in Table 1.

Data set	Training set composition
Baseline	Original data set (700 images)
Synth-B	Synthetic images with equal class distribution & Baseline composition (12,700 images)
Synth-GS	Synthetic images composition including extra glass sponges and soft corals & Baseline (12,700 images)

Table 1: Data set compositions for main experiments

The corresponding test runs were performed on the 200 original image test set. Further ablation studies performed in section 4.3 and 4.4 were con-

Model/Data	AP _{.50:.95}	AP _{.50}	AP _{small}	AP _{medium}	AP _{large}	AR ₁	AR ₁₀	AR ₁₀₀	AR _{small}	AR _{medium}	AR _{large}
CM-X-101/Baseline	41.7	68.2	25.3	29.3	54.7	21.6	51.6	55.2	25.4	45.1	70.8
CM-X-101/Synth-B	48.8	71.0	27.4	39.1	62.8	24.7	58.8	64.2	27.9	57.3	77.1
CM-X-101/Synth-GS	51.8	76.7	27.5	40.2	66.1	25.7	59.0	63.9	27.9	55.7	77.9

Table 2: Summary of detection results with bounding boxes (in percent)

ducted on 20 epochs using a smaller synthetically derived training set of 2000 images with varying image sizes, number of annotations and classes considering the respective experiment. Corresponding testing was performed with respective 300 synthetically derived images.

4.1 Detection results

To investigate the detection results of the trained network, the average precision and average recall exhibit best scores around 76.7 % AP for an IoU_{.50} and 63.9 % AR₁₀₀ on the Synth-GS data set (Table 2). Further, deploying synthetically derived images to support the training increases the performance of AP_{.50:.95} by 17 % and AR₁₀₀ by 16 % emphasising the importance of more input data.

With regards to recall scores at varying numbers of detections, it can be noted that more detections per image will lead to better recall evalu-

ations. Additionally, smaller object sizes receive lower precision as well as recall scores throughout all testing strategies (Table 2). Those low performances might be caused by down sampling operations inside pooling layers that are applied on each feature map in the model. Down sampling output feature maps makes them more robust to changes in the translation of a feature in the image but fewer features might get extracted as resolution decreases with repeated convolutional and pooling layers. Also, there is a relatively large ratio between pixel size and object size for smaller objects which quickly increases the possibility to predict bounding boxes with positional deviations from ground truth boxes. Those positional deviations might already be too large to pass the threshold defined for the IoU.

Considering qualitative results, Fig. 3 shows detection results for various stations with differ-

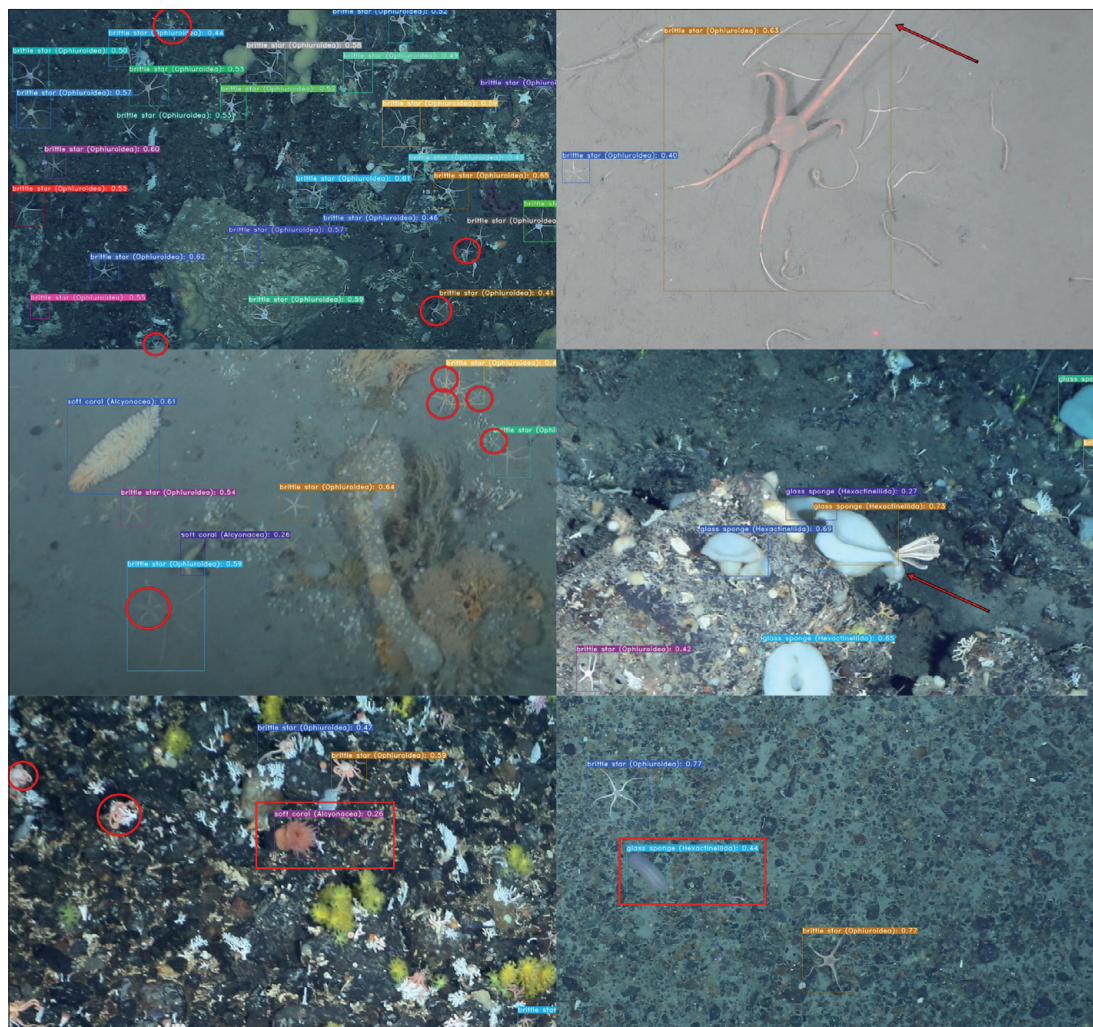


Fig. 3: Detection results and confidences of the model CenterMask – ResNeXt-101. Red circles show missing brittle stars, red arrows indicate inaccurate bounding boxes predictions and red rectangles reveal wrong species detections. Images belong to the test set and originate from different diving locations of the PS118 cruise

Model/Data	Glass sponges		Soft corals		Brittle stars	
	F ₁	AP _{.50:.95}	F ₁	AP _{.50:.95}	F ₁	AP _{.50:.95}
CM-X-101/Baseline	67.7	41.4	70.3	36.8	80.2	46.9
CM-X-101/Synth-B	67.8	45.3	69.8	48.8	79.2	52.4
CM-X-101/Synth-GS	71.4	51.4	76.8	51.5	79.9	52.6

Table 3: Summary of performance results per class (in percent)

ent seafloor types, camera distances, variant illuminations and sharpness. It can be seen, that the trained model is able to correctly detect almost all specimen belonging to the three classes. Even blurred images pose no problem in detection just very small specimen or such that are lying closely to one another might be wrongly detected as one.

4.2 Influence of class imbalance

The influence of class imbalance where class distributions are biased is a known problem in deep learning applications (Guo et al. 2008). There are many approaches to combat class imbalance such as oversampling, undersampling or setting class weights to emphasise minority classes. In this study the underrepresented classes glass sponges and soft corals were oversampled because this method has proven to be very effective (see Guo et al. 2008; Buda et al. 2018). After adopting the data augmentation strategy with additional distributions of underrepresented classes, the F₁ and AP scores are increased by 5 % and 13 % for glass sponges and by 10 % and 6 % for soft corals, respectively (Table 3). Consequently, AP and AR scores across all classes are boosted with a percentage increase of 24 % AP_{.50:.95} and 16 % AR₁₀₀ compared to the Baseline data set

4.3 Influence of number of annotations and classes

Ablation studies with respect to number of annotations show that single annotations per image have a precision reduction of 27 % when evaluating on images with five annotations and 71 % when evaluating on images showing up to 20 annotations (Fig. 4). Training performed on five and

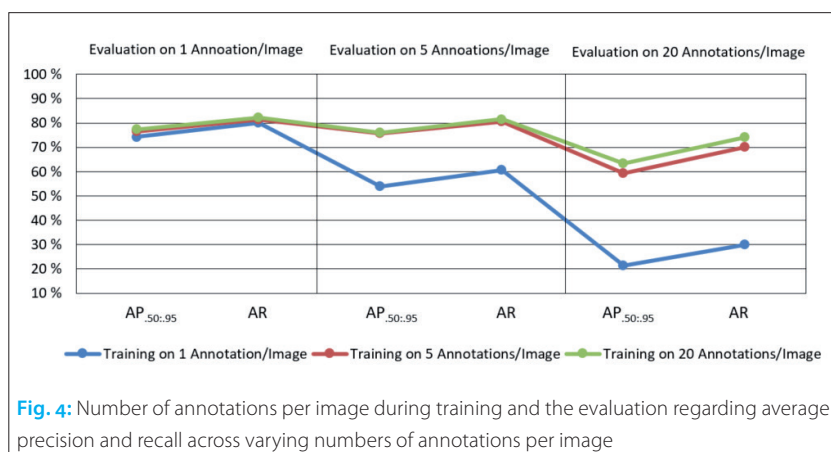


Fig. 4: Number of annotations per image during training and the evaluation regarding average precision and recall across varying numbers of annotations per image

20 annotations show a reduction in precision of 22 % (59.5 % AP_{.50:.95}) and 18 % (63.3 % AP_{.50:.95}), when testing on images with 20 annotations, respectively. Hence, best AP results are received when training is performed on images with up to 20 annotations, and worse results are scored when images contain only single objects during training. Also, it can be argued that images with lots of specimen not necessarily need to be implemented for training as the gap between 59.5 % AP_{.50:.95} and 63.3 % AP_{.50:.95} is rather low. Overall, precision and recall rates are slightly lower for multiple annotations in comparison to single annotations per image. A reason could be that synthetically derived data sets tend to compose overlapping foregrounds the more foregrounds are being used which poses incorrect detection results as also stated in section 4.1. Considering the number of classes, it is evident that multiple classes per image yield an increase in AP and AR by 280 % and 158 %, respectively (Table 4). Therefore, images with single classes on images should be avoided.

	AP _{.50:.95}	AR
Single classes	19.9	31.2
Multiple classes	75.6	80.6

Table 4: Performance for number of classes per image during training (in percent)

4.4 Influence of image pixel dimension

For the investigation regarding different image pixel dimensions, the original image was tiled into sizes ranging between 1440 × 1280 and 960 × 768 pixels as training for larger image sizes result in GPU memory issues and smaller sizes tend display only single or cut objects for original data. The evaluation was performed also on the original image size of 5760 × 3840 pixels to investigate whether tiling has to be performed also for model inference. In general, the evaluation on image sizes larger than 1440 × 1280 yield a sharp drop in precision (Fig. 5) which might occur because region of interests could be assigned to unsuitable feature levels. Also, as image sizes increase, the more GPU memory and inference time is being used. Meanwhile, same image sizes adopted for both training and evaluation show not necessarily a performance boost which demonstrate that images deployed for the evaluation may vary in size and aspect ratio from the input training set. Highest precision results are achieved by the 1440 × 960 image size trained with adequate (6 GB) GPU memory usage. Further, it can be certain that original images may contain multiple objects and classes.

5 Conclusion and outlook

In conclusion, this study shows that deep convolutional neural networks are a suitable choice to automatically detect and classify benthic species in varying underwater environments. Further, large

amount of training data can be synthetically derived to feed deep networks with sufficient information without risking overfitting. The implemented data augmentation strategy is thus not only useful to extend the input data set but also to alleviate class imbalances boosting the performance considerably. When preparing input data, images not necessarily need to exhibit lots of specimen decreasing time spend for annotation. However, images with single specimen and single classes should be avoided as performance may drop significantly. Therefore, larger image sizes such as 1440 × 960 pixels may be used where chances are high that image tiles contain multiple objects. On the contrary, greater image sizes consume more GPU memory and if image sizes exceed a critical threshold, the precision will drop as region of interests may be assigned to wrong feature levels. Next to this challenge, future

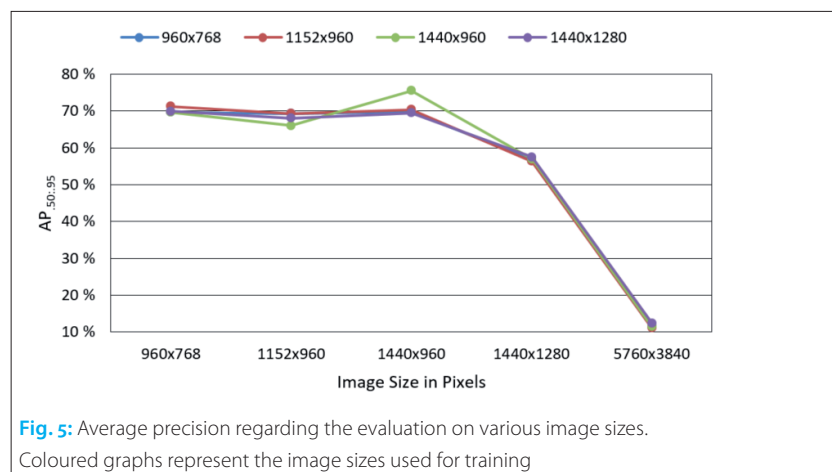


Fig. 5: Average precision regarding the evaluation on various image sizes. Coloured graphs represent the image sizes used for training

studies will incorporate more benthic classes and concentrate on their count. //

References

- Boulais, Océane; Ben Woodward et al. (2020): FathomNet: An underwater image training database for ocean exploration and discovery. <http://arxiv.org/pdf/2007.00114v3>
- Brooks, Justin (2019): COCO Annotator: GitHub. <https://github.com/jsbroks/coco-annotator/> (accessed 7 January 2020)
- Buda, Mateusz; Atsuto Maki; Maciej A. Mazurowski (2018): A systematic study of the class imbalance problem in convolutional neural networks. *Neural Networks*, DOI: 10.1016/j.neunet.2018.07.011
- Christensen, Jesper H.; Lars V. Mogenssen et al. (2018): Detection, Localization and Classification of Fish and Fish Species in Poor Conditions using Convolutional Neural Networks. 2018 IEEE/OES Autonomous Underwater Vehicle, DOI: 10.1109/AUV.2018.8729798
- Gonzalez-Cid, Yolanda; Antoni Burguera et al. (2017): Machine learning and deep learning strategies to identify Posidonia meadows in underwater images. *OCEANS 2017*, DOI: 10.1109/OCEANSE.2017.8084991
- Griffiths, Huw J.; Andrew J. S. Meijers; Thomas J. Bracegirdle (2017): More losers than winners in a century of future Southern Ocean seafloor warming. *Nature Climate Change*, DOI: 10.1038/nclimate3377
- Guo, Xinjian; Yilong Yin et al. (2008): On the Class Imbalance Problem. 2008 Fourth International Conference on Natural Computation, DOI: 10.1109/ICNC.2008.871
- Huang, Hai; Hao Zhou et al. (2019): Faster R-CNN for marine organisms detection and recognition using data augmentation. *Neurocomputing*, DOI: 10.1016/j.neucom.2019.01.084
- Kelly, Adam (2019): COCO Synth: GitHub. <https://github.com/akTweleve/cocosynth> (accessed 22 February 2020)
- Lee, Youngwan; Jongyoul Park (2019): CenterMask: Real-Time Anchor-Free Instance Segmentation. <http://arxiv.org/pdf/1911.06667v1>
- Lin, Tsung-Yi; Michael Maire et al. (2014): Microsoft COCO: Common Objects in Context. <http://arxiv.org/pdf/1405.0312v3>
- Manning, Christopher D.; Prabhakar Raghavan; Hinrich Schütze (2009): Introduction to information retrieval. Cambridge University Press, ISBN: 0521865719
- Mishkin, Dmytro; Nikolay Sergievskiy; Jiri Matas (2017): Systematic evaluation of CNN advances on the ImageNet. *Computer Vision and Image Understanding*, DOI: 10.1016/j.cviu.2017.05.007
- Mitchell, Emily G.; Rowan J. Whittle; Huw J. Griffiths (2020): Benthic ecosystem cascade effects in Antarctica using Bayesian network inference. *Communications biology*, DOI: 10.1038/s42003-020-01310-8
- Pauly, Leo; Harriet Peel et al. (2017): Deeper Networks for Pavement Crack Detection. *Proceedings of the 34th International Symposium on Automation and Robotics in Construction (ISARC)*, DOI: 10.22260/ISARC2017/0066
- Pavoni, Gaia; Massimiliano Corsini et al. (2021): Challenges in the deep learning-based semantic segmentation of benthic communities from Ortho-images. *Applied Geomatics*, DOI: 10.1007/s12518-020-00331-6
- Piepenburg, Dieter; Alexander Buschmann et al. (2017): Seabed images from Southern Ocean shelf regions off the northern Antarctic Peninsula and in the southeastern Weddell Sea. *Earth System Science Data*, DOI: 10.5194/essd-9-461-2017
- Purser, Autun; Simon Dreutter et al. (2021): Seabed video and still images from the northern Weddell Sea and the western flanks of the Powell Basin. *Earth System Science Data*, DOI: 10.5194/essd-13-609-2021
- Purser, Autun; Yann Marcon et al. (2019): Ocean Floor Observation and Bathymetry System (OFOBS): A New Towed Camera/Sonar System for Deep-Sea Habitat Surveys. *IEEE Journal of Oceanic Engineering*, DOI: 10.1109/JOE.2018.2794095
- Salman, Ahmad; Ahsan Jalal et al. (2016): Fish species classification in unconstrained underwater environments based on deep learning. *Limnology and Oceanography Methods*, DOI: 10.1002/lom3.10113
- Xie, Saining; Ross Girshick et al. (2017): Aggregated Residual Transformations for Deep Neural Networks. 2017 IEEE Conference on Computer Vision and Pattern Recognition (CVPR), Honolulu, DOI: 10.1109/CVPR.2017.634

Acknowledgements

We thank the annotators of the images: Gavin DMello, Diana Rubio and Seyed Lialestani. Further we thank the captain and crew of RV *Polarstern* as well as the scientific party of the cruise PS18 for their support. Special thanks go to Autun Purser and Huw Griffiths for their support, the data collection on board and the identification of benthic organisms.

Automatic boulder identification in side-scan sonar

An article by JESPER HAAHR CHRISTENSEN

Boulder surveys seek to identify prominent boulders which position may collide with planned cable routes, offshore wind farms or other subsea construction activities. Data is collected using suitable sensor technologies such as bathymetry from multibeam echo sounders and side-scan sonar imaging. Currently, the boulder identification process is a labour-intensive job that requires domain expertise to interpret the data and provide each identified target with accurate annotations. With this work, we propose to automate the majority of this process by training neural networks to identify boulders in side-scan data. Our preliminary work estimates the area covered by each boulder instance and further generates metadata for each identified target for filtering, sorting and report generation. In addition to being an automated process, our method can process several kilometres of side-scan data and identify thousands of boulders in less than a minute. Not only does this provide results of high accuracy but it also performs orders of magnitude faster than human processors.

boulder identification | AUV | SeaCat | artificial intelligence | deep learning | side-scan sonar imaging
Erkennung von Felsbrocken | AUV | SeaCat | künstliche Intelligenz | Deep Learning | Side-Scan-Sonar-Bilder

Bei der Vermessung von Felsblöcken geht es darum, markante Felsblöcke zu identifizieren, deren Position mit geplanten Kabeltrassen, Offshore-Windparks oder anderen Bauten unter Wasser kollidieren könnten. Die Daten werden mit Hilfe geeigneter Sensortechnologien gesammelt, wie z. B. Bathymetrie von Fächerecholoten und Side-Scan-Sonar-Bildern. Derzeit ist es eine arbeitsintensive Aufgabe, Felsbrocken zu erkennen, die Fachwissen erfordert, um die Daten zu interpretieren und jedes identifizierte Ziel mit genauen Anmerkungen zu versehen. Mit dieser Arbeit schlagen wir vor, den Großteil dieses Prozesses zu automatisieren, indem wir neuronale Netze trainieren, um Felsbrocken in Side-Scan-Daten zu identifizieren. Unsere vorläufige Arbeit schätzt die Fläche, die von jedem Felsbrocken abgedeckt wird, und generiert darüber hinaus Metadaten für jedes identifizierte Ziel zum Filtern, Sortieren und Erstellen von Berichten. Da es sich um einen automatisierten Prozess handelt, kann unsere Methode in weniger als einer Minute mehrere Kilometer an Side-Scan-Daten verarbeiten und Tausende von Felsbrocken identifizieren. Dies liefert nicht nur Ergebnisse von hoher Genauigkeit, sondern arbeitet auch um Größenordnungen schneller als Menschen.

Author

Jesper Haahr Christensen is Ph.D. student and works at Atlas Maridan ApS in Denmark, a subsidiary of Atlas Elektronik GmbH, Germany.

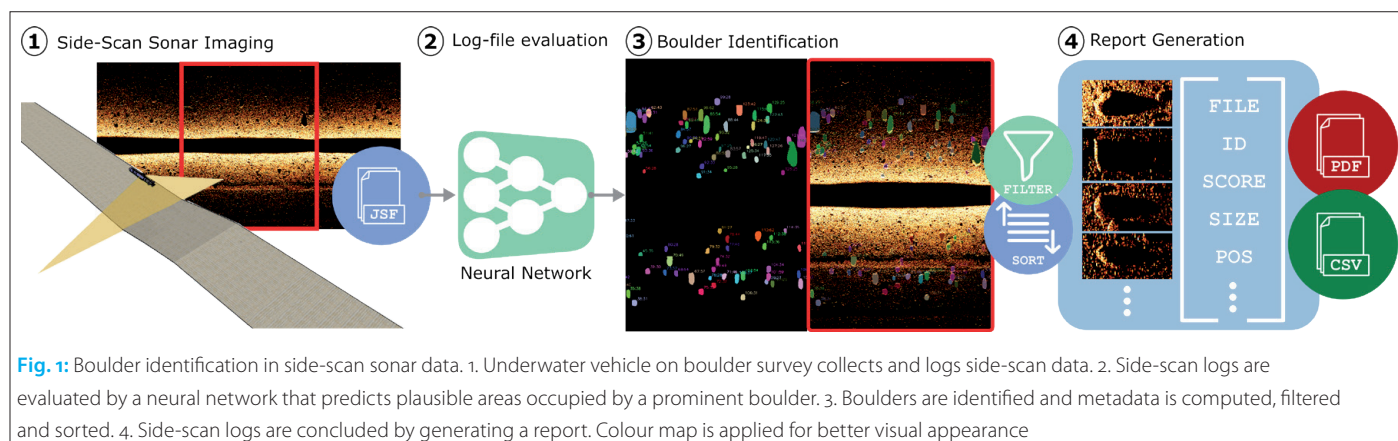
jhc@atlasmaridan.com

1 Introduction

Collecting side-scan data of large areas using autonomous underwater vehicles (AUVs), operators seek to utilise the vehicle's total endurance to cover as much area as possible by following a predefined trajectory or by traversing back and forth in a lawnmower pattern. This is accomplished with a carefully chosen set of parameters relating to vehicle trajectory, attitude, velocity and sensor settings to align for sufficient coverage, overlap, data resolution and data quality. As work is done in GNSS-denied environments, positioning and navigation are estimated by high-quality acoustically-aided subsea inertial navigation systems. During operation, communication with the vehicle is limited to low-bandwidth acoustic data links typically used to monitor only a few important vehicle parameters.

We describe subsea surveying as the process of mapping the ocean floor by collecting highly ac-

curate georeferenced data points. Boulder surveys, more specifically, seek to identify prominent boulders whose positions may collide with planned cable routes or offshore wind farms. Such surveys are performed using suitable sensor technologies such as bathymetry from multibeam echo sounders and side-scan sonar imaging. The ever-accumulating log files are first available for review after mission completion where boulders, defined as salient objects on the seabed, need identification. This identification process is a labour-intensive job and does not only require domain expertise for interpreting the data, but each identified target needs further to be measured in size and mapped to its exact location. The processing job is typically concluded by compiling a report of all prominent targets and their metadata, providing the client with detailed information needed for making informed decisions on the next steps.



As shown in Fig. 1, we propose to automate the majority of this process by leveraging neural networks for processing side-scan logs. More specifically, recorded logs are passed through our model that estimates the positions and areas of prominent boulders. Due to the design nature of the neural network, all estimated boulders are separable at an instance level. This allows us to count the number of boulders in the log file and analyse each separate boulder in relation to georeferenced position, size and confidence. By further filtering the outputs, we can remove most false positives and eliminate cases where a boulder is identified and counted several times. The latter case occurs due to overlap in the data, which typically is created and desired by design. We currently make a naive assumption on size and calculate a pseudo area for each boulder using the coverage obtained by the estimated segmentation masks and can thus sort boulders by size. Future work will be making more accurate predictions on boulder sizes and hence give complete control over which sizes (width, height and length) are desired to report.

Our method does not only benefit from being an automated process but also promises substantially shorter processing times. Quantitatively, our model can process several kilometres of side-scan data and identify thousands of boulders in less than a minute. In addition, the number of boulders that our model identifies is significantly higher than any human processor would possibly have time to process. The presented work is ongoing, but we estimate that saved time and effort will be substantial even in the current state.

2 Side-scan sonar data set

We collect available side-scan logs from previous completed in-house surveys and prepare them in a format suitable for training neural networks, as detailed below.

2.1 Hardware and data details

All side-scan data is recorded using EdgeTech 2205 sonar systems integrated on our SeaCat AUVs (Kalwa 2019). Data is recorded using high- and low-

frequency channels and is available in EdgeTech's JSF file format. Typically, side-scan logs are split into line segments where turns are excluded. The spatial size of each line segment varies with velocity, altitude and sensor settings. Our complete data set consists of more than 1500 km worth of line segments recorded at many different locations. However, only a tiny fraction of this has been given annotations suitable for learning boulder identification. In total, we have annotated about 1300 prominent boulders with varying settings and visual variations. In Fig. 2, we show two side-scan snippets with corresponding segmentation masks. We note that the objective of segmentation masks is to cover the complete area occupied by prominent boulders in order to, at a later stage, separate each of these areas into a boulder and shadow region.

2.2 Preprocessing of acoustic images

With the protocol description from EdgeTech, we read raw JSF files using Python to load the sonar trace data into matrices for high- and low-frequencies and port- and starboard-side channels. We further collect the navigational data, pulse information and weighting factor for each cross-track line.

With the weighting factor and additional sensor information, we restore each data sample to its original floating-point value and perform slant-range correction to match along-track and cross-track resolutions. Each sonar image is further nor-

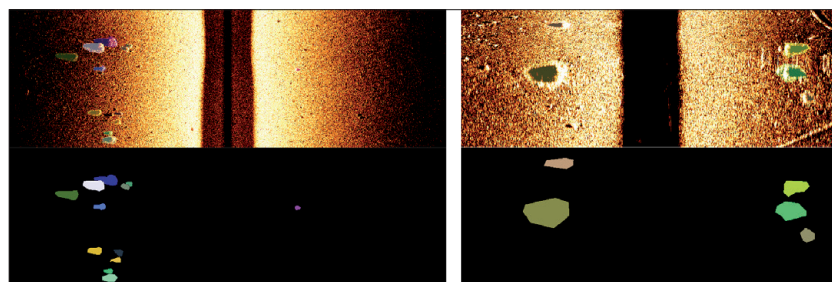


Fig. 2: Side-scan snippets with corresponding segmentation masks. For each boulder, we draw a segmentation mask that covers the boulder itself and its shadow. Colour map is applied for better visual appearance

malised and stored as PNG images split into 200 m long segments. When applying colour maps for visualisation, we use the `cmapy` Python module with the `afm-hot` colour scheme.

3 Boulder identification model

We aim to train a neural network that, given an input, predicts plausible areas occupied by boulders not only by placing rectangular boxes around the object but by a per-pixel classification of the input. Typically segmentation models consist of an encoder-decoder style architecture like U-Net (Ronneberger 2015). However, while U-Net style networks are fast and easy to train, they fail to offer object-instance separation. Consequently, segmentation masks predicted by the model are essentially one object and thus need further processing to identify and analyse each separate boulder. Especially when boulders are located in close proximity, this is a difficult task. To avoid inaccuracies from hard-coding object separation algorithms, we base our model on Mask R-CNN (He et al. 2017) for instance segmentation. As shown in Fig. 3, several neural networks are used as explained in the following.

3.1 Feature extraction

To generate feature maps of our input, we use a Feature Pyramid Network (FPN) (Lin et al. 2017) build on a ResNet (He et al. 2016) CNN with 50 layers. The FPN is used to extract features at different scales from our single-scale input efficiently. This is analogous to processing our input image at different scales but much more efficient in terms of computation. The complete ResNet-50-FPN backbone is pre-trained on the Microsoft COCO: Common Objects in Context data set (Lin et al. 2014), and is not updated during training for boulder identification.

3.2 Region proposals

Region proposals are generated by a Region Proposal Network (RPN). This evaluates the input

feature map and predicts a set of rectangular regions and their objectness (score of object vs. background). The regions are generated by sliding a fixed set of windows, called anchors, with varying aspect ratios and scales over the available (differently scaled) feature maps generated by the FPN. We refer to Ren et al. (2015) for more details on RPNs.

3.3 RoI pooling

The Region of Interest (RoI) pooling layer accepts the feature map generated by our ResNet-50-FPN feature extractor and the proposals from the RPN. The proposals from the RPN are a set of regions, each defined as a four-tuple $(r; c; h; w)$ that specifies top-left corner $(r; c)$ and its height and width $(h; w)$. As such, RoI pooling has the objective of »cropping« out regions of the feature map in which the RPN has estimated an object and passing it on to the final output heads.

3.4 Box and score prediction head

This accepts the feature map of the regions proposed by the RPN, i.e., the regions most likely to contain a boulder. We have two objectives for this head: (i) bounding-box regression and (ii) object classification/score. The bounding-box regression refines the region proposed by the RPN to enclose the object better. The score is a measure of the network's estimated probability of this object being a boulder.

3.5 Mask prediction head

For generating segmentation masks of our object instances, a Fully Convolutional Network (FCN) (Long et al. 2015) is used to estimate binary masks for each RoI. This prediction is 1-channel and binary, and thus class-agnostic. Therefore, we rely on the classification score from the above prediction head to identify the object correctly. As we currently focus on boulders as a whole, we only have two options for the classification (background or

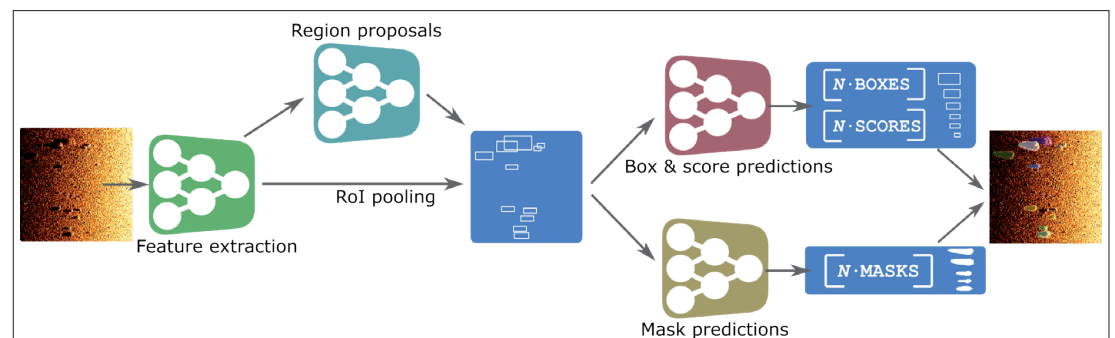


Fig. 3: Boulder identification model overview. A feature extraction network generates feature maps of the input image. These are the input to a region proposal network (RPN), predicting regions in the input likely to contain an object. Using the region proposals, a region of interest (RoI) pooling layer »crops« the feature map and passes the regions on to our prediction heads. The box and score prediction head refines the bounding-boxes for the regions and estimates the probability of each region being a boulder. The mask prediction head performs a per-pixel classification of the proposed regions and thus outputs a segmentation mask for each proposed region. Colour map is applied for better visual appearance

boulder). However, in future work, we can use this same architecture for expanding the scope to include more low-level predictions, e.g., separating boulders into boulder and shadow regions. For more detailed information on the mask prediction head, we refer to He et al. (2017).

3.6 Loss functions

As we train our entire network end-to-end, we employ a multitask loss that seeks to minimise the error in each sub-network simultaneously. We can define the total loss as:

$$L = L_{\text{RPN}} + L_{\text{loc}} + L_{\text{cls}} + L_{\text{mask}},$$

where $L_{\text{RPN}} = L_{\text{loc}}^{\text{RPN}} + L_{\text{cls}}^{\text{RPN}}$ constitutes bounding-box regression loss and objectness score of the RPN, L_{loc} and L_{cls} are the bounding-box regression and classification loss of the box and score prediction head, and L_{mask} is the average binary cross-entropy loss over the per-pixel classification of the RoI for the final segmentation mask (mask prediction head). For more details on loss functions and their implementation, we refer to Girshick (2015), Ren et al. (2015) and He et al. (2017).

4 Experiments

4.1 Training details

Our models are implemented in PyTorch and trained using four NVIDIA RTX 2080 Ti GPUs. During training, we load from our data set the 200-m tracks with corresponding segmentation masks

and »mine« regions in which boulders are located. We do this by random cropping 256×256 pixel areas at locations that contain at least one annotated boulder. Since our annotations are sparse in the sense that not all boulders in a 200-m track have been carefully annotated, we ignore areas with no corresponding annotated segmentation mask. We further apply image transformations at random during training time to represent as many visually varying examples as possible. Finally, before entering the network, the input image is resized to 800×800 pixels. We use a batch size of eight per GPU and train our complete model end-to-end for about 5×10^3 update iterations.

4.2 Results

During inference, as illustrated in Fig. 4, we process side-scan data line-by-line by sliding a 256×256 pixel window over it. We note that we can process input images of arbitrary size during inference time and are not limited to non-postprocessed (raw) lines. Hence, if a post-processing step is used to generate side-scan mosaics and mitigate errors from erroneous navigation or correct position offsets due to uneven seabed, we can utilise this as input to our model. We use a sliding window approach to generate overlap of the processed data. This ensures that objects receive maximum exposure to the network and are therefore identified as a whole and not only partly identified. The stride of the window is an adjustable parameter that balances processing time and accuracy. We use a stride of 100 pixels for our experiments.

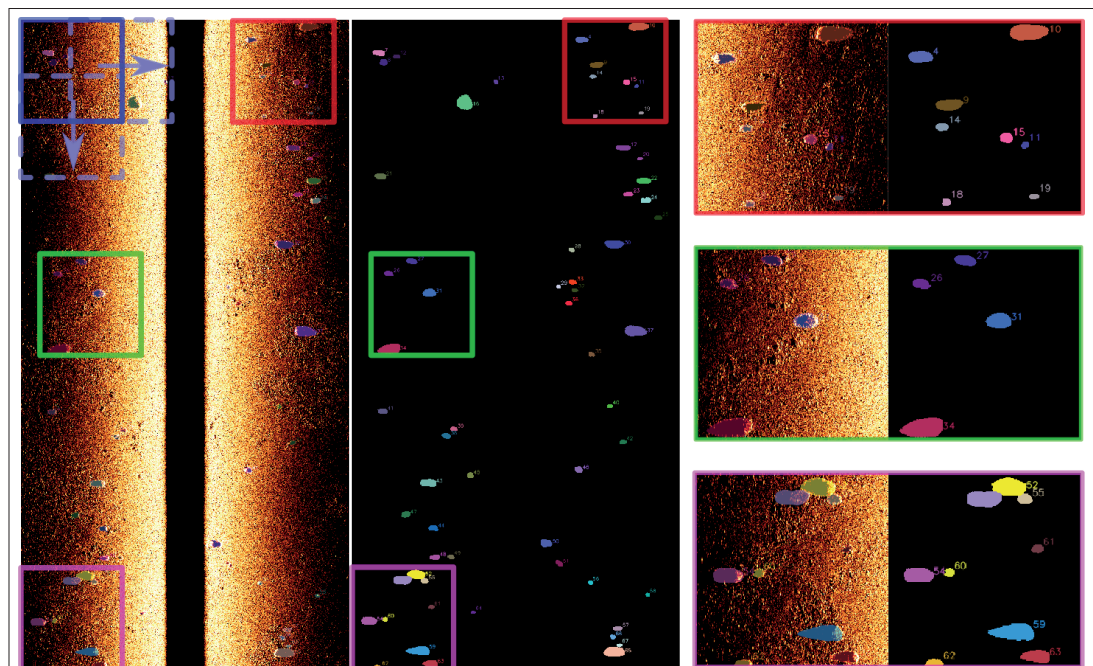


Fig. 4: Result from processing a 200-m side-scan line. Inputs to the model are generated by sliding a 256×256 pixel window over the data as illustrated by blue squares. The red, green and purple squares are enlarged results and shown to the right. Note that the input to the model is greyscale, but a colour map is applied for better visual appearance. The input image used here has a length of 200 m, a width of 80 m and a resolution of 0.1 m/px. This was processed on a single GPU in 13 s. The amount of identified boulders does not affect the processing time

Test data set	Non-filtered	Filtered
Accuracy (annotated vs. identified)	91.7 %	91.7 %
Accuracy (non-annotated vs. identified)	87.8 %	94.8 %
Model gain (annotated vs. identified)	× 62	× 27

	Human	Model (stride = 100 px)
Average processing speed	0.5 m/s	22 m/s
Average time per boulder	21.7 s	0.1 s

Table 1: Comparison of accuracy and performance on the test data set. See section 4.3 for details on the metrics presented

After processing each window separately, we reassemble outputs corresponding to the input by mapping each locally detected boulder into its global coordinate. Due to the sliding window approach, many boulders will be identified several times. To keep only the best segmentation mask for the identified boulders, we use non-maximum suppression (NMS) that filters overlapping objects based on their intersection over union (IoU) and keeps only the best scoring.

During inference, we also collect all available metadata relevant to each identified boulder. This is currently logfile name/path, id, position, confidence and »pseudo«-area. The »pseudo«-area is calculated as the area covered by the estimated segmentation mask and is for sorting purposes assumed to correlate with the actual size of the boulder. From the metadata, human operators can further filter and sort the outputs to obtain the desired output. Finally, the information can be compiled into a report, e.g., as CSV or PDF files.

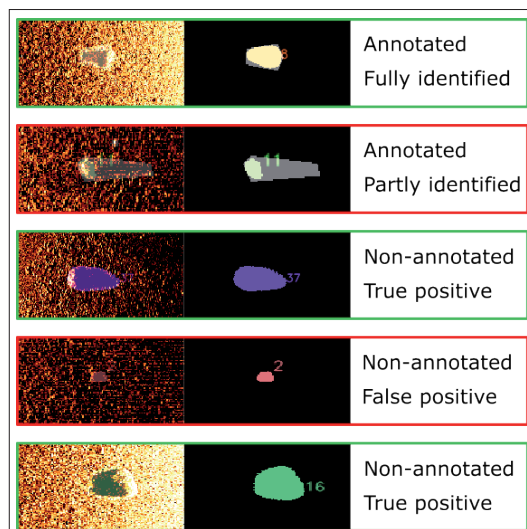


Fig. 5: Representative samples from the test data set. True positives have masks that capture the shape of targets (boulder and shadow) with high accuracy. False positives fail to capture the entire object or estimate objects at positions where there are none. Annotated masks are shown in faded white as an overlay. Each example has been resized, and sizes are therefore not relative to each other

For the input shown in Fig. 4, the time used for the complete processing steps from input to output on a single GPU is 13 s. The input has a length of 200 m, a width of 80 m and a resolution of 0.1 m/px. The amount of identified boulders does not affect the processing time.

4.3 Comparison against human-annotated data

To provide quantitative metrics on the performance of our model, we compare the targets found by our model against the human-annotated targets on our test data set. Table 1 shows the accuracy with which our model identifies targets annotated in the test data set, i.e., the proportion of annotated targets the model correctly identifies. Since our model further identifies many targets beyond the annotated targets, we also provide the accuracy of these being correct, i.e., the proportion of correctly identified non-annotated targets. The model gain denotes the gain or increase in identified targets compared to the number of annotated targets, e.g., a gain value of × 62 refers to the model identifying × 62 more targets than have been annotated. Finally, we report the processing speed as a measure of metre per second using a single GPU and time spend on generating segmentation masks using human annotators and our model. We note that these measures are an average over our test data set collected using a window stride of 100 px and are not entirely representative. They are more dependent on sensor/vehicle/data parameters than the number of boulders identified. The column »Non-filtered« denotes that all outputs from the model have been used without modification, and »Filtered« refers to the outputs being filtered. The filtering is currently removing identified boulders with an area smaller than the smallest of the annotated targets.

In Fig. 5, we show representative examples of the different cases, which is the basis for the metrics reported in Table 1. True positives, annotated or non-annotated, are shown as masks that capture targets' shapes (boulder and shadow) with high accuracy. We note that the estimated masks typically enclose the objects better than our annotated masks (shown in faded white as overlay). False positives, annotated or non-annotated, are shown as objects only partly identified or by estimated masks that do not cover any objects. We note that false positives relate mostly to small areas, further supported by the increase in accuracy of the filtered metrics as shown in Table 1.

5 Conclusion

We have presented our preliminary work on automatic boulder identification in side-scan sonar data. With our method, we currently identify prominent boulders by estimating a segmentation mask that accurately captures the entire area of the boulder and its shadow. As our model is based on

instance segmentation, we retrieve and analyse each boulder separately to provide each detected target with metadata used for filtering, sorting and report generation purposes. Using only a single GPU, our model can process several kilometres of side-scan data and identify thousands of boulders in less than a minute. We envision that even in its current state, our presented work has the potential to drastically reduce the effort of industry professionals even if human-in-the-loop is still required to some extent.

6 Future work

In improving our method, several steps may be considered. To improve the accuracy, we can use our current model to label our entire data set of more than 1500 km side-scan sonar data in a semi-supervised manner. This potentially generates millions of annotated boulders to retrain on instead of the 1300 targets used for this work. To report

more accurate measures on size (width, height, length), the segmentation masks may be extended to separate the currently estimated masks into a boulder and shadow area. Our model architecture readily supports this addition and thus only needs labels for learning. Finally, for accurate side-scan object positioning, we currently assume a flat seabed, and to remove duplicate identifications on separate side-scan lines with overlap, we must assume good navigation. To mitigate these assumptions, either post-processed mosaics must be used (already supported), or further work may investigate cross-referencing data points with accurate bathymetry from, e.g., multibeam echo sounders. //

Acknowledgements

We thank Fugro Germany Marine GmbH for providing support and insights in boulder identification.

References

- Girshick, Ross (2015): Fast R-CNN. 2015 IEEE International Conference on Computer Vision (ICCV), DOI: 10.1109/ICCV.2015.169
- He, Kaiming; Xiangyu Zhang et al. (2016): Deep residual learning for image recognition. 2016 IEEE Conference on Computer Vision and Pattern Recognition (CVPR), DOI: 10.1109/CVPR.2016.90
- He, Kaiming; Georgia Gkioxari et al. (2017): Mask R-CNN. 2017 IEEE International Conference on Computer Vision (ICCV), DOI: 10.1109/ICCV.2017322
- Kalwa, Jörg (2019): Unter-Wasser-Drohnen für Hydrographie und Seebodenerkundung. Hydrographische Nachrichten, DOI: 10.23784/HN114-02
- Lin, Tsung-Yi; Michael Maire et al. (2014): Microsoft COCO: Common Objects in Context. In: Computer Vision – ECCV 2014, DOI: 10.1007/978-3-319-10602-1_48
- Lin, Tsung-Yi; Piotr Dollár et al. (2017): Feature pyramid networks for object detection. 2017 IEEE Conference on Computer Vision and Pattern Recognition (CVPR), DOI: 10.1109/CVPR.2017.106
- Long, Jonathan; Evan Shelhamer; Trevor Darrell (2015): Fully convolutional networks for semantic segmentation. 2015 IEEE Conference on Computer Vision and Pattern Recognition (CVPR), DOI: 10.1109/CVPR.2015.7298965
- Ren, Shaoqing; Kaiming He et al. (2015): Faster R-CNN: Towards real-time object detection with region proposal networks. Advances in Neural Information Processing Systems, DOI: 10.1109/TPAMI.2016.2577031
- Ronneberger, Olaf; Philipp Fischer; Thomas Brox (2015): U-net: Convolutional networks for biomedical image segmentation. In: Medical Image Computing and Computer-Assisted Intervention (MICCAI), Springer, <http://lmb.informatik.uni-freiburg.de/Publications/2015/RFB15a>

Erzeugung von synthetischen Seitensichtsonar-Bildern mittels Generative Adversarial Networks

Ein Beitrag von YANNIK STEINIGER, JANNIS STOPPE, DIETER KRAUS und TOBIAS MEISEN

Für die Anwendung von Deep-Learning-Methoden zur automatischen Auswertung von Daten bildgebender Sonare stellt die nicht vorhandene Verfügbarkeit größerer Trainingsdatensammlungen nach wie vor ein Problem dar. In den letzten Jahren wurden jedoch sogenannte Generative Adversarial Networks (GAN) als ein Werkzeug aus dem Bereich Deep Learning für die Erzeugung synthetischer Daten entwickelt. In dieser Arbeit wird untersucht, inwieweit sich GANs zur Erzeugung künstlicher Sonarbilder eignen. Um das GAN auch mit wenigen Beispielen trainieren zu können, wird eine Art des Transfer-Lernens mit Hilfe von einfachen simulierten Bildern entwickelt. Es zeigt sich, dass die Performance eines Klassifikators durch Hinzunahme der künstlichen Bilder gesteigert werden kann.

Seitensichtsonar | Autonomes Unter-Wasser-Fahrzeug | Deep Learning | generative Netzwerke | Transfer-Lernen
side-scan sonar | autonomous underwater vehicle | deeplearning | generative adversarial network | transfer-learning

A remaining problem is the lack of large-scale sonar image data sets when applying deep learning algorithms for the automatic analysis of these data. However, over the past few years, generative adversarial networks (GAN) were developed as a tool for generating synthetic data. This work investigates how GANs can be used to generate synthetic sonar images. In order to train the GAN with only a few available samples, a transfer-learning approach is applied which uses simple simulated images. Using the additional synthetic sonar images, the performance of a classifier can be increased.

Autoren

Yannik Steiniger und Dr. Jannis Stoppe arbeiten am Institut für den Schutz maritimer Infrastrukturen des DLR in Bremerhaven.

Prof. Dr. Dieter Kraus leitet das Institut für Wasserschall, Sonartechnik und Signaltheorie an der Hochschule Bremen.

Prof. Dr. Tobias Meisen hat den Lehrstuhl für Technologien und Management der Digitalen Transformation an der Universität Wuppertal inne.

yannik.steiniger@dlr.de

1 Einleitung

Seitensichtsonare sind spezielle unterwasser-akustische Sensoren, die unter anderem an autonomen Unter-Wasser-Fahrzeugen (englisch: autonomous underwater vehicle, AUV) montiert werden, um den Meeresboden zu inspizieren und beispielsweise nach Objekten zu suchen. In den letzten Jahren wurde die Erkennungsrate von Objekten in Bildaufnahmen stetig verbessert. Grundlage hierfür sind maschinelle Lernverfahren, genauer Deep Convolutional Neural Networks (CNN), mittels derer heute Erkennungsraten erreicht werden, die der des Menschen in diesen Anwendungsbereichen entspricht (Wang et al. 2020). Sollen CNNs für die automatische Auswertung von Seitensichtsonar-Bildern herangezogen werden, stellt sich jedoch häufig das Problem einer zu geringen Datenlage für ein verlässliches Training. Das Sammeln von Seitensichtsonar-Bildern von Objekten ist besonders aufwendig, da im Allgemeinen die Position von Objekten unter Wasser im Vorfeld unbekannt ist. Auch das manuelle Auslegen von Objekten und die anschließende Aufnahme von Sonardaten ist, aufgrund der Zeit- und Kostenintensität, nur eine äußerst aufwendige Möglichkeit, einen umfangreichen und variablen Datensatz zu erstellen.

Während also die Technologie zur Unterstützung der Auswertung aufgenommener Sonardaten immer weiter voranschreitet, ist deren Anwendung auf Sonardaten als recht schwierig einzustufen, da nicht genügend Daten für das Training moderner, selbstlernender Algorithmen vorhanden sind.

Andererseits haben sich in den letzten Jahren generative neuronale Netze, sogenannte Generative Adversarial Networks (GAN) (Goodfellow et al. 2014), aus dem Bereich des Deep Learnings als eine gute Methode zum Generieren künstlicher Bilder erwiesen (Isola et al. 2017; Karras et al. 2020). GANs wurden bereits in anderen Arbeiten zur Generierung von Seitensichtsonar-Bildern (Steiniger et al. 2020) oder Synthetisches-Aperture-Sonar-Bildern (Reed et al. 2019) verwendet. Die Herausforderung, die sich jedoch ergibt, ist, dass auch GANs auf künstlichen neuronalen Netzen beruhen und entsprechend einen umfangreichen Trainingsdatensatz benötigen. Als Lösungsansatz greifen die beiden genannten Verfahren daher zunächst auf Simulationsdaten zurück. Für die Simulation kann beispielsweise ein Raytracer verwendet werden. [Abb. 1](#) zeigt zum einen ein reales Sonarbild eines Reifens und zum anderen ein mit dem Raytracer POV-Ray simuliertes Bild. Die simulierten Bilder

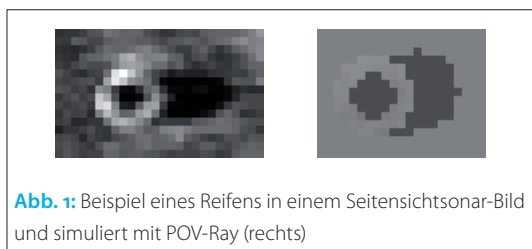


Abb. 1: Beispiel eines Reifens in einem Seitensichtsonar-Bild und simuliert mit POV-Ray (rechts)

weisen zwar die in einem echten Seitensichtsonar-Bild zu erwartenden geometrischen Formen für die Highlight- und Schattenregionen auf, enthalten aber weder weitere Details noch anwendungstypisches Rauschen oder Ähnliches.

Reed et al. verwenden in ihrem Ansatz ein GAN, um die simulierten Bilder in Sonarbilder zu »übersetzen«. Im hier vorgestellten Ansatz werden die simulierten Bilder stattdessen in einem ersten Schritt für ein Vortrainieren des GANs verwendet. Dadurch lernt das künstliche neuronale Netz, die geometrischen Formen der Highlight- und Schattenregionen zu erzeugen. Erst in einem zweiten Schritt, dem Transfer-Lernen, werden die echten Sonarbilder zum Trainieren verwendet, sodass das GAN die Verteilung der Pixelintensitäten in den jeweiligen Regionen im Bild lernt.

2 Aufnahme der Seitensichtsonar-Bilder

Für die Datenerzeugung wird das AUV SeaCat Mk1 der Atlas Elektronik GmbH verwendet (Kalwa 2019). Das AUV bietet die Möglichkeit, zuvor geplante Missionen weitgehend autonom abzufahren und dabei Messdaten mit Hilfe unterschiedlicher Sensoren zu erzeugen. Das AUV ist mit einem Doppler Velocity Log für die Messung der Geschwindigkeit über Grund, einem Drucksensor für die Messung der Tiefe und einem GNSS-System zur Positionierung über Wasser ausgestattet. In Kombination mit einem hochgenauen Inertial Navigation System (INS) ermöglichen diese Sensoren eine Positioniergenauigkeit des AUVs von bis zu 0,1 % der unter Wasser zurückgelegten Wegstrecke, wodurch eine präzise Lokalisierung von Zielobjekten unter Wasser möglich ist. Außer dem Seitensichtsonar Edge-tech 2205 am Rumpf führt das AUV in seinem modularen Sensorkopf eine Kamera mit künstlicher Beleuchtung, ein hochauflösendes Fächerecholot und einen parametrischen Sub-Bottom-Profiler mit. Das Seitensichtsonar erlaubt grundsätzlich das gleichzeitige Scannen mit zwei unterschiedlichen Frequenzen. Die Daten dieser Messung wurden mit einer Frequenz von 850 kHz erhoben, die eine Auflösung im Zentimeterbereich und eine Reichweite von 75 m zu jeder Seite erlaubt.

In der Regel werden parallel zur Aufnahme der Daten mit dem Seitensichtsonar Bathymetriedaten mit einem Fächerecholot aufgenommen. Je nach Auflösung der Daten besteht die Möglichkeit, über die einfache Bathymetrie hinaus 3D-Punktwolken von Objekten zu generieren (Heuskin 2020). Mit



Abb. 2: AUV SeaCat Mk1 der Atlas Elektronik beim Zu-Wasser-Lassen

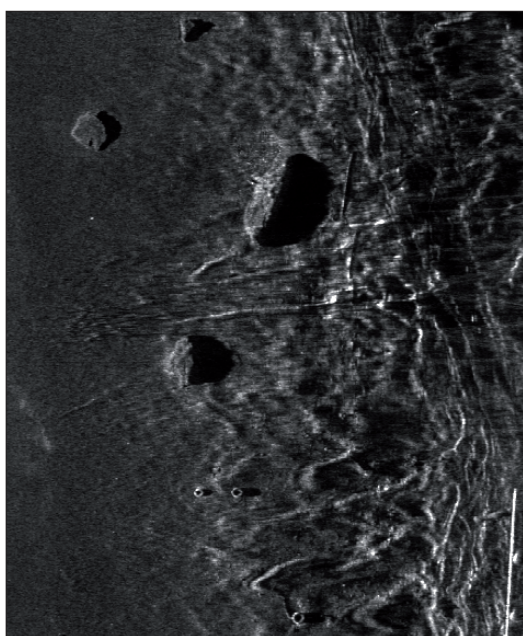


Abb. 3: Beispiel eines aufgenommenen Seitensichtsonar-Bildes

einer experimentellen Signalverarbeitungskette werden die während einer Mission aufgenommenen Rohdaten des Seitensichtsonars in Sonarbilder des Meeresbodens, wie in [Abb. 3](#) dargestellt, umgewandelt.

Die aus den erstellten Sonarbildern extrahierten Objekte sind in [Tabelle 1](#) aufgeführt. Zusätzlich ist die für die spätere Anwendung der neuronalen Netze relevante Aufteilung in Trainings- und Testbeispiele angegeben. Es ist zu erkennen, dass vor allem für die Klasse Reifen besonders wenig Bei-

Objekt	Anzahl der Trainingsbeispiele	Anzahl der Testbeispiele
Reifen	18	17
Stein	36	210
Hintergrund	36	210

Tabelle 1: Annotierte Objekte und Anzahl dieser im Trainings- bzw. Testdatensatz

spiele zur Verfügung stehen. Synthetische Bilder dieser Klasse können genutzt werden, um dieses Ungleichgewicht auszugleichen.

3 Künstliche Sonarbilder für die Klassifikation

Wie zuvor bereits geschrieben, sind insbesondere Objektklassen, die sehr selten auftreten, eine zusätzliche Herausforderung für Lernverfahren. In dieser Arbeit widmen wir uns daher der Synthese von Bildern derartiger Klasse, in diesem Fall also der Klasse Reifen. Obwohl sich diese Arbeit speziell mit dem Objekt Reifen befasst, lässt sich das Verfahren auch auf beliebige andere Objekte übertragen. Für komplexere Objekte wird jedoch gegebenenfalls die Simulation zum Erzeugen der Daten für das Vortrainieren aufwendiger.

Der entwickelte Trainingsprozess des GANs mit Vortrainieren und Transfer-Lernen ist in Abb. 4 schematisch dargestellt. Das GAN ist aus zwei neuronalen Netzen aufgebaut: dem Generator und dem Discriminator. Der Generator erhält als Eingangsdaten ein Bild mit zufällig verteilten Pixelintensitäten. Das formulierte Lernziel besteht

darin, diesen Eingang in ein Sonarbild zu transformieren. Der Discriminator hingegen sieht entweder ein echtes Bild aus dem Trainingsdatensatz oder ein vom Generator erzeugtes Bild und weist dem jeweiligen Bild eine Wahrscheinlichkeit P zu, die angibt ob er das Bild für ein echtes Bild ($P = 1$) oder generiertes Bild ($P = 0$) hält. Während des Trainings ist das Ziel des Generators, den Discriminator glauben zu lassen, dass das generierte Bild echt ist. Somit nähert sich die Verteilung der Pixelintensitäten der generierten Bilder im Laufe des Trainings immer mehr der der Trainingsdaten an.

Beim hier betrachteten Transfer-Lernen besteht der Trainingsdatensatz zunächst aus 10 000 simulierten Bildern. In der Simulation werden Parameter wie Abstand zum Sonar oder Größe des Objekts variiert, um einen differenzierten Datensatz zu erhalten. Wie in Abb. 4 (b) zu erkennen, weisen die generierten Bilder nach diesem Vortrainieren eine deutliche Highlight- und Schattenregion auf, wie sie für Seitensichtsonar-Bilder zu erwarten ist. Für das Transfer-Lernen wird dieses GAN mit den echten Seitensichtsonar-Bildern trainiert, wobei zuvor die Gewichte der letzten Schicht im neuro-

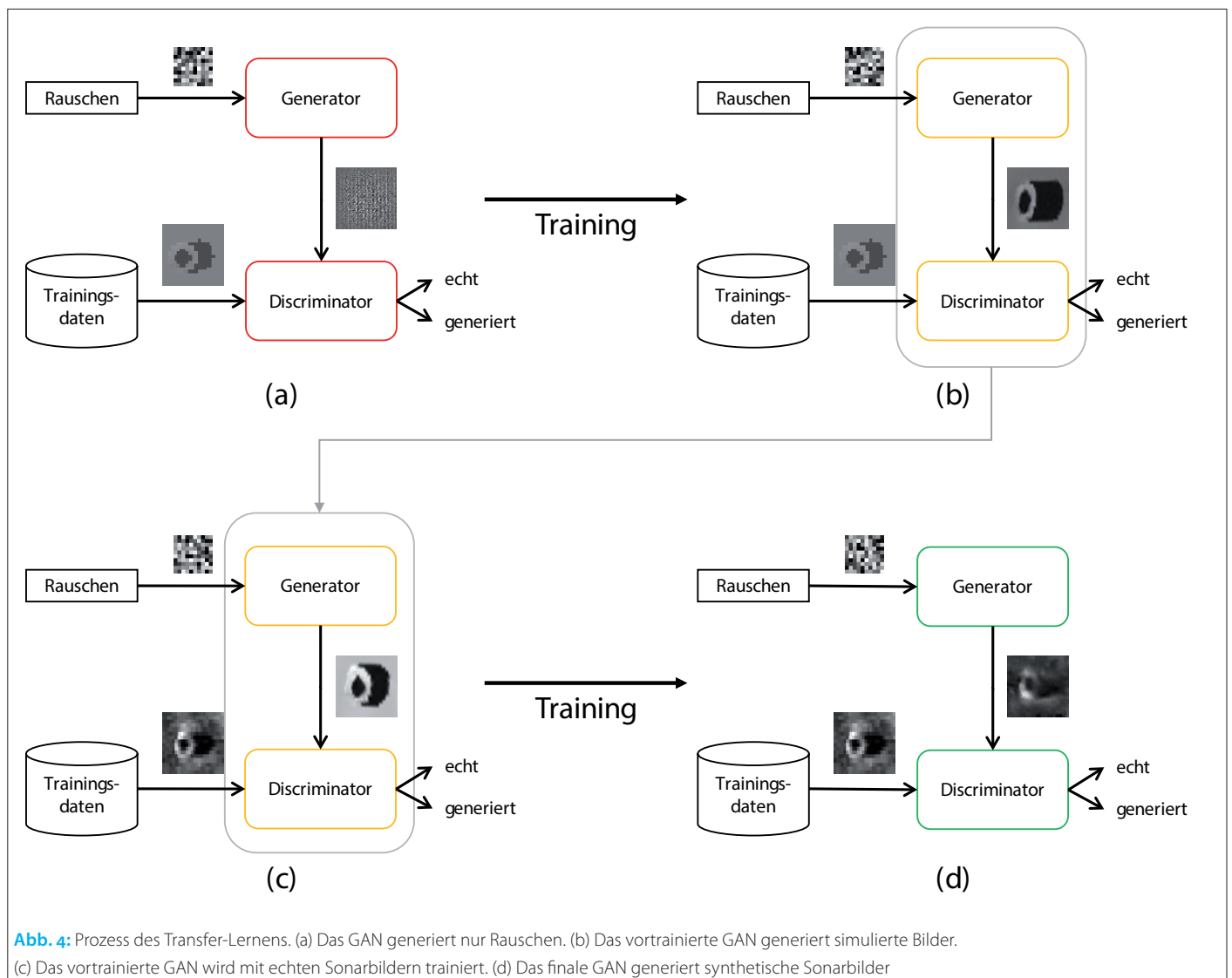


Abb. 4: Prozess des Transfer-Lernens. (a) Das GAN generiert nur Rauschen. (b) Das vortrainierte GAN generiert simulierte Bilder. (c) Das vortrainierte GAN wird mit echten Sonarbildern trainiert. (d) Das finale GAN generiert synthetische Sonarbilder

nalen Netz des Discriminators neu initialisiert werden, um eine Überanpassung und so ein Verschwinden des Gradienten während des Trainings zu verhindern. Die [Abb. 4 \(d\)](#) zeigt, dass das finale GAN nicht nur die geometrische Form, sondern auch die Pixelintensitäten in dem Bild realistisch generiert.

Das beschriebene Verfahren, basierend auf der Methodik des Transfer-Lernens, verringert das für GANs typische Problem des Mode-Collapse. Da nur wenige reale Trainingsbeispiele zur Verfügung stehen, würde ein direktes Lernen der Transformation von Eingangsruschen zu Sonarbild dazu führen, dass das GAN in einen Zustand kollabiert, in dem lediglich ein (nicht zwingend realistisches) Bild unabhängig vom Rauschen generiert wird. Der Discriminator lernt nur noch dieses eine Bild zurückzuweisen. Daraufhin muss der Generator seine Transformation nur minimal ändern, um den Discriminator zu täuschen. Somit führt ein Fortsetzen des Trainingsprozesses nicht mehr aus diesem Zustand des Mode-Collapse heraus. Die einzige Lösung ist es, das gesamte Training neu zu starten. Um dies zu umgehen, muss das Kollabieren des GANs verhindert werden.

Aber: Obwohl das Transfer-Lernen zwar das Problem des Mode-Collapse verhindert, kann die Variabilität in den generierten Daten dennoch gering sein. Wie verschieden die Daten, die von dem GAN generiert werden, letztlich sind, ist dabei von vielen Faktoren abhängig und muss noch genauer untersucht werden. Das Verhindern des Kollabierens des GANs hin zu einer einzigen Konfiguration der Ergebnisse stimmt jedoch zuversichtlich, dass durch eine Anpassung der Parameter auch die gewünschte Variabilität erreicht werden kann.

4 Performance des Klassifikators

Ziel der Erzeugung künstlicher Sonarbilder ist es letztendlich, die Performance eines Klassifikators durch die zusätzlichen Daten zu verbessern. Für

Anzahl synthetischer Bilder	ACC _{bal}	F1 _{macro}
0	0,6298	0,6302
9	0,6388	0,6379
18	0,6376	0,6364
36	0,6379	0,6368

Tabelle 2: Klassifikationsperformance des CNN für verschieden starke Augmentierungen

diese Klassifikation wird im Folgenden ein CNN verwendet. Die Augmentierung des Trainingsdatensatzes des CNN ist in [Abb. 5](#) dargestellt. Mit Hilfe der synthetischen Sonarbilder von Reifen wird der Datensatz aus [Tabelle 1](#) ausgeglichen.

Die Performance des CNN wird durch die ausbalancierte Genauigkeit (englisch: balanced accuracy, ACC_{bal}) und den Makro-F1-Wert (englisch: macro F1 score, F1_{macro}) gemessen. Die [Tabelle 2](#) gibt die Performance für eine unterschiedliche Anzahl an synthetischen Bildern im augmentierten Trainingsdatensatz an. Mit 18 synthetischen Bildern ergibt sich ein ausgeglichener Trainingsdatensatz. Alle vier Experimente wurden mit zehn verschiedenen Initialisierungen des CNN durchgeführt. In [Tabelle 2](#) sind die Mittelwerte der Metriken aufgelistet.

Das Hinzunehmen der synthetischen Daten zeigt eine leichte Steigerung in beiden Metriken von circa einem Perzentil. Es ist jedoch auch zu erkennen, dass mehr künstliche Bilder nicht zu einer weiteren Steigerung führen. Dies lässt darauf schließen, dass die Variabilität in den generierten Daten nicht ausreichend ist, um einen großen synthetischen Datensatz zu erzeugen. Es ist hierbei jedoch zu beachten, dass zum Trainieren des GANs – entsprechend der Ausgangsproblematik von nur spärlich verfügbaren Trainingsdaten – lediglich 18 reale Seitensichtsonar-Bilder verwendet wurden.

Die Performancesteigerung durch das Verwenden der synthetischen Daten ist messbar,

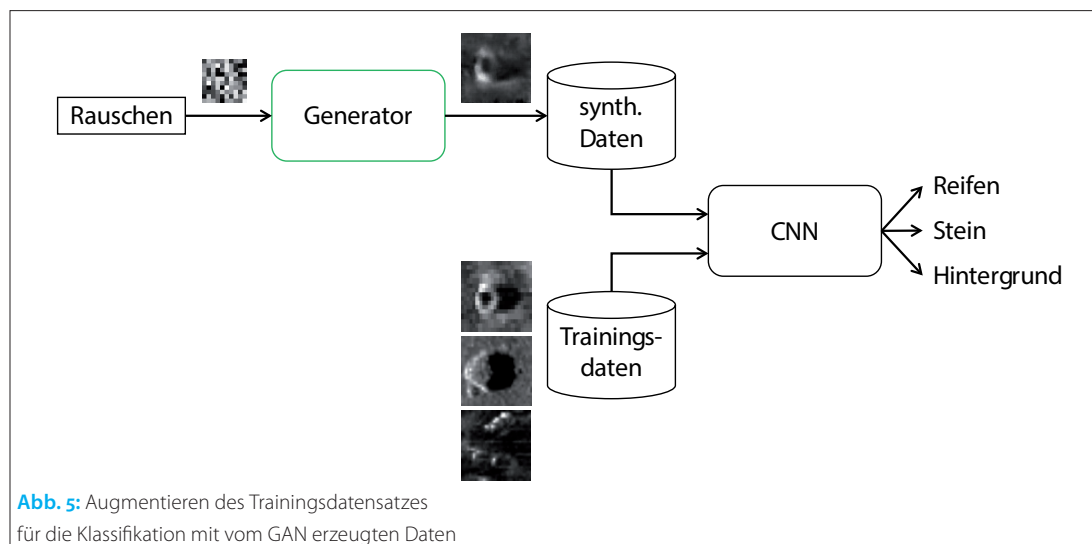


Abb. 5: Augmentieren des Trainingsdatensatzes für die Klassifikation mit vom GAN erzeugten Daten

verwandelt dabei jedoch – umgangssprachlich formuliert – einen passabel arbeitenden Detektor keineswegs in ein Patentrezept. Während für das Trainieren von CNNs zur automatischen Auswertung von Seitensichtsonar-Bildern die ausgiebige Erfassung von Daten nach wie vor das Mittel der Wahl darstellt, lassen sich mit synthetischen Daten gegebenenfalls noch ein paar Register ziehen, falls die Datenlage nicht verbessert werden kann.

5 Zusammenfassung und Ausblick

In diesem Artikel wurde ein Verfahren vorgestellt, um mittels Methoden des maschinellen Lernens synthetische Seitensichtsonar-Bilder zu erzeugen. Speziell wurde ein GAN mit Bildern eines Raytracers vortrainiert und anschließend ein Transfer-Lernen mit echten Sonarbildern durchgeführt. Die synthetischen Bilder weisen die zu erwartenden geometrischen Formen und Pixelintensitäten auf. Es konnte gezeigt werden, dass die Verwendung dieser synthetischen Daten zusätzlich zum Trainingsdatensatz eines Klassifikators die Performance steigern kann.

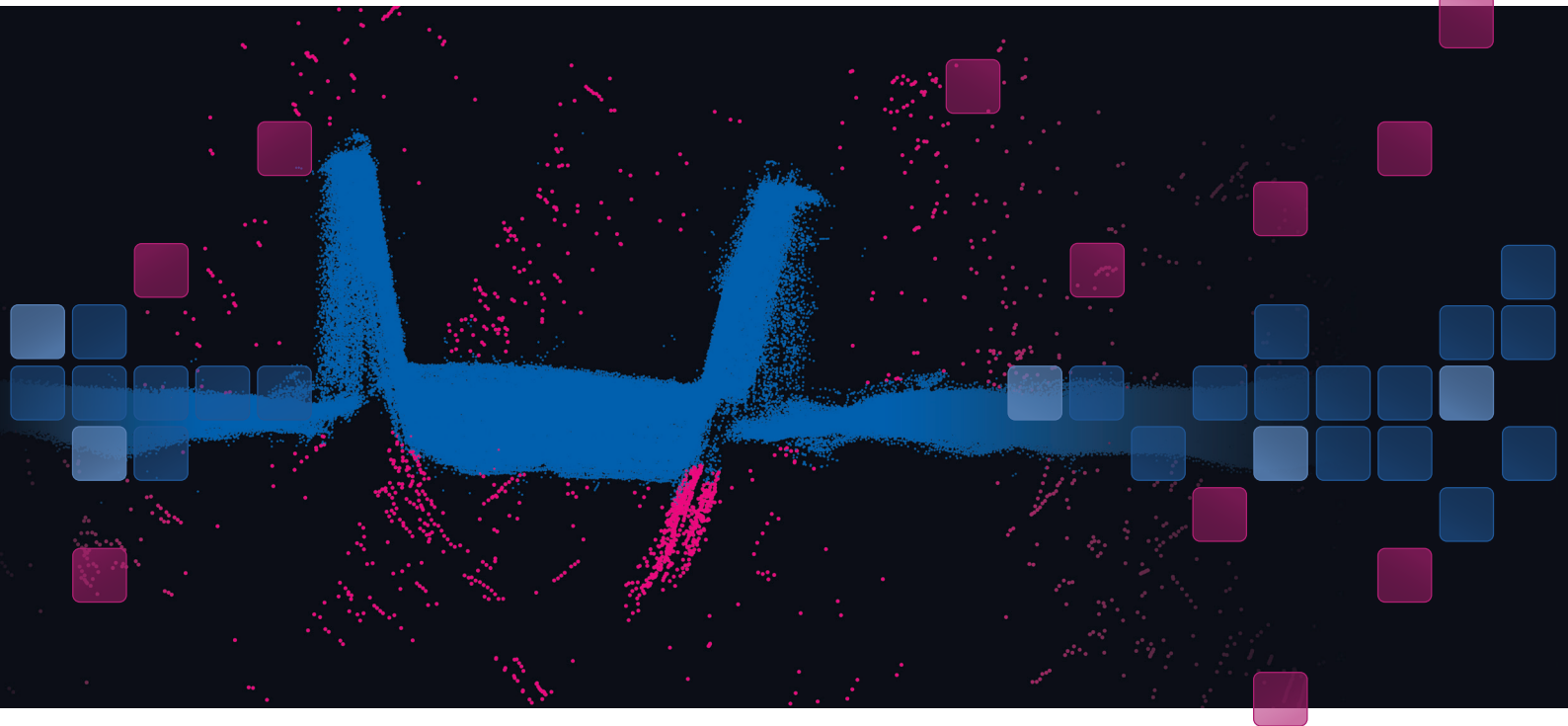
Um die Methodik weiter zu verbessern, ist ein primäres Ziel, die Variabilität in den generierten Daten zu erhöhen. Dies kann zum einen dadurch erreicht werden, dass auch der Hintergrund, sprich der Meeresboden, in einem weiteren Vortrainingschritt generiert wird. Zum anderen können bekannte Eigenschaften der Verteilungen der Pixelintensitäten in den Highlight- und Schattenregionen genutzt werden (Lehmann 2013). Damit lassen sich die Bilder nach dem Vortrainieren bereits realistischer gestalten und so etwas an Komplexität aus dem Schritt des Transfer-Lernens nehmen.

Generell sind GANs eine vielversprechende Methode, nicht um die Erfassung echter Trainingsdaten zu substituieren, sondern um fehlende Daten, die nicht ohne weiteres gewonnen werden können, zu synthetisieren. Echte Daten bleiben das Mittel der Wahl – aber sollten insbesondere für bestimmte Objekttypen eines Datensatzes mehr Beispiele benötigt werden, stellen GANs eine Möglichkeit zur Verbesserung der Datenlage als Alternative zu eventuell kostspieligen weiteren Kampagnen dar. //

Literatur

- Goodfellow, Ian; Jean Pouget-Abadie et al. (2014): Generative Adversarial Nets. *Advances in Neural Information Processing Systems* 27, MIT Press, DOI: 10.1145/3422622
- Heuskin, David; Frank Lehmann (2020): Drohnengestützte Erfassung von maritimen Infrastrukturen. *Hydrographische Nachrichten*, DOI: 10.23784/HN116-05
- Isola, Philipp; Jun-Yan Zhu et al. (2017): Image-to-Image Translation with Conditional Adversarial Networks. 2017 IEEE Conference on Computer Vision and Pattern Recognition (CVPR), DOI: 10.1109/CVPR.2017.632
- Kalwa, Jörg (2019): Unter-Wasser-Drohnen für Hydrographie und Seebodenerkundung. *Hydrographische Nachrichten*, DOI: 10.23784/HN114-02
- Karras, Tero; Samuli Laine et al. (2020): Analyzing and Improving the Image Quality of StyleGAN. 2020 IEEE/CVF Conference on Computer Vision and Pattern Recognition (CVPR), DOI: 10.1109/CVPR42600.2020.00813
- Lehmann, Benjamin (2013): Beiträge zur automatisierten Objekterkennung und insbesondere zur Bild-Segmentierung in hochaufgelösten Sonarbildern. Logos Verlag Berlin
- Reed, Albert; Isaac D. Gerg et al. (2019): Coupling Rendering and Generative Adversarial Networks for Artificial SAS Image Generation. *OCEANS 2019 MTS/IEEE SEATTLE*, DOI: 10.23919/OCEANS40490.2019.8962733
- Steiniger, Yannik; Jannis Stoppe et al. (2020): Dealing With Highly Unbalanced Sidescan Sonar Image Datasets for Deep Learning Classification Tasks. *Global OCEANS 2020 MTS/IEEE Singapore – U.S. Gulf Coast*, DOI: 10.1109/IEEECONF38699.2020.9389373
- Wang, Chien-Yao; Alexey Bochkovskiy; Hong-yuan Mark Liao (2020): Scaled-YOLOv4: Scaling Cross Stage Partial Network. <https://arxiv.org/abs/2011.08036v2>

Introducing CARIS Mira **AI**



Bring the Noise

The Sonar Noise Classifier is a Gamechanger

Powered by the CARIS Mira AI engine and available now in CARIS HIPS and SIPS 11.3.

The Sonar Noise Classifier automatically identifies noise providing significant reductions in manual cleaning and quickly propels data from acquisition to review.

Reduce manual cleaning by up to 10x at an accuracy of 95%.

Try it now with a **FREE 30-Day Trial!**



LEARN MORE about the Sonar Noise Classifier
www.teledynecaris.com/caris-mira/



TELEDYNE CARIS
Everywhereyoulook™

Part of the Teledyne Imaging Group

AI is enabling a transformation toward autonomous hydrographic operations

An article by SARAFINA MCPHERSON KIMØ

It has been possible to advance AI thanks to factors like increased access to massive computing power. In the same way, the increase in automation, which AI facilitates, advances the development of unmanned, autonomous hydrographic operations. This is an exciting prospect, as the advantages of such operations are many: efficiency gains, reduction in costs in the form of vessel time and man hours, as well as the minimisation of environmental impacts. We are working towards autonomous hydrographic operations by developing software tools, which provide automatic, real-time data processing and navigation-aiding. In 2017, we established a dedicated software development team with engineers specialising in machine learning, machine vision and deep learning. The first official EIVA software version utilising AI was released in 2018, when we made it possible to use NaviSuite Deep Learning for automatic interpretation of data in NaviSuite Nardoa, our software bundle for pipeline inspections. In this article, we will dive into how we are using machine learning to create software solutions that support autonomous hydrographic operations.

NaviSuite Deep Learning | artificial intelligence | autonomous hydrographic operations | AI software
NaviSuite Deep Learning | künstliche Intelligenz | autonome hydrographische Anwendungen | KI-Software

Die Weiterentwicklung der KI wurde durch Faktoren wie den verbesserten Zugang zu massiver Rechenleistung möglich. In gleicher Weise treibt die zunehmende Automatisierung, die KI ermöglicht, die Entwicklung unbemannter, autonomer hydrographischer Anwendungen voran. Dies ist eine spannende Perspektive, denn die Vorteile solcher Anwendungen sind vielfältig: Effizienzsteigerung, Kostenreduzierung in Form von Schiffszeit und Mannstunden sowie die Minimierung von Umweltauswirkungen. Wir arbeiten auf autonome hydrographische Anwendungen hin, indem wir Software entwickeln, die eine automatische Echtzeit-Datenverarbeitung und Navigationshilfe bietet. Im Jahr 2017 haben wir ein eigenes Software-Entwicklungsteam mit Ingenieuren gegründet, die auf maschinelles Lernen, maschinelles Sehen und Deep Learning spezialisiert sind. Die erste offizielle EIVA-Software mit KI wurde 2018 veröffentlicht, als wir die Nutzung von NaviSuite Deep Learning für die automatische Interpretation von Daten in NaviSuite Nardoa, unserem Softwarepaket für Pipeline-Inspektionen, ermöglichten. In diesem Artikel stellen wir vor, wie wir maschinelles Lernen nutzen, um Softwarelösungen zu erstellen, die autonome hydrographische Anwendungen unterstützen.

Author

Sarafina McPherson Kimø
is Content Writer at EIVA a/s
in Denmark.

smk@eiva.com

1 Teaching computers to name what they see

NaviSuite Deep Learning is a software tool which can identify objects from images. It is based on a neural network model, which is trained on thousands of images from various providers, typically NaviSuite users. To train the network, a human must manually mark objects of interest in images using our Annotation Tool (Fig. 1). Objects can be anything from a pipeline joint to a particular species of coral.

In a project with São Paulo University, we are training NaviSuite Deep Learning to identify coral species and their habitats. Currently, an expert from the university is marking the various coral species in images to teach the neural network to identify them. Once developed, this NaviSuite Deep Learning capability may be used for moni-

toring and maintaining sustainable marine ecosystem services.

We are in the process of planning another application: monitoring mussel farms to ensure they are operating optimally. This is for a developmental project in partnership with Wittrup Seafood, WSP and several others, and with the support of the Danish ministry of environment and food. So far, we have designed a set-up to perform surveys of mussel farms, and the next step is to train NaviSuite Deep Learning to identify important factors, such as how many mussels are growing in different locations, whether they are sick or if there are pests, such as starfish, on them.

It takes a lot of time and data to teach a neural network to recognise such complex objects. During the development of NaviSuite Deep Learning for its first application: pipeline inspections, it has

been possible for us to train it to identify over 20 different events which occur along a pipeline. For example, it can mark pipe visibility, anodes, field joints, debris, marine life, damage and more. This has been possible thanks to the help of our customers, who have shared data of their pipelines.

1.1 Putting the tool to work

There are three ways to incorporate NaviSuite Deep Learning into your operations. Firstly, it can be used on a cloud service hosted by EIVA, which is typically a good solution for onshore data processing staff. Secondly, it can be used on a rack server, useful for processing on board a vessel. Finally, it can be used on an on-board computer, which can be integrated into an AUV or USV. The on-board computer is ideal for autonomous operations, as this makes it possible to let the AUV or USV change mission based on objects detected via NaviSuite Deep Learning.

When using NaviSuite Deep Learning, it is incorporated into NaviSuite software. This means that when it identifies objects of interest, it can systematically organise this information for ease of use (Fig. 2).

1.2 Automatically identifying targets on the seabed

In addition to NaviSuite Deep Learning, we have developed other software tools for identifying targets on the seabed, such as rocks/boulders, debris and man-made objects. Identifying such objects is vital when planning construction on the seabed or removing abandoned fishing gear, which harms marine life if left in the waters. The tools can be used in NaviModel, our software solution for data modelling and visualisation. Objects identified with these tools can be automatically compiled in an intuitive overview, along with information, such as their type and location (Fig. 3).

In the future, NaviModel will not only be able to automatically register targets on the seabed, but also register the seabed type. Together with several customers, we are developing a tool which uses backscatter data to segment areas of the seabed based on their material type, for example clay, gravel, sand or rock. These different materials reflect sound with different intensities, which can be seen and detected automatically in the backscatter data. This is yet another way we are developing software to make the most of available data and support subsea operations.

2 Autonomous navigation methods

With the ability to interpret data automatically, the next step is to use that information to automate navigation and survey planning. NaviPac is our software solution for positioning and navigation of surface and subsea vessels.

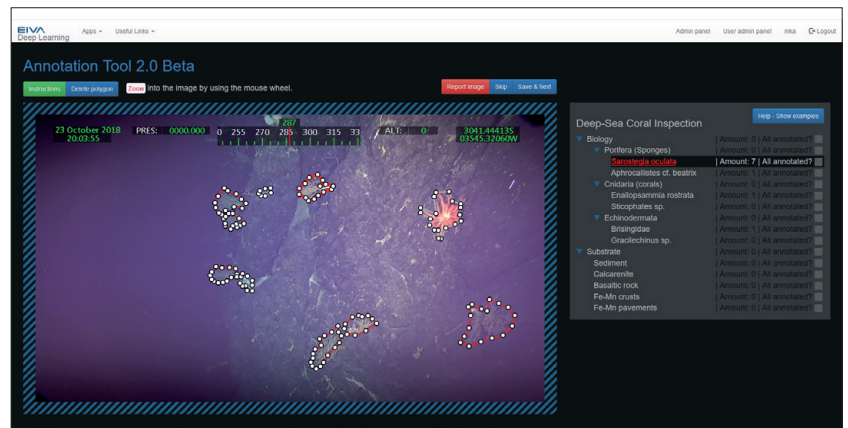


Fig. 1: Several coral species are marked on an image, using the NaviSuite Deep Learning Annotation Tool

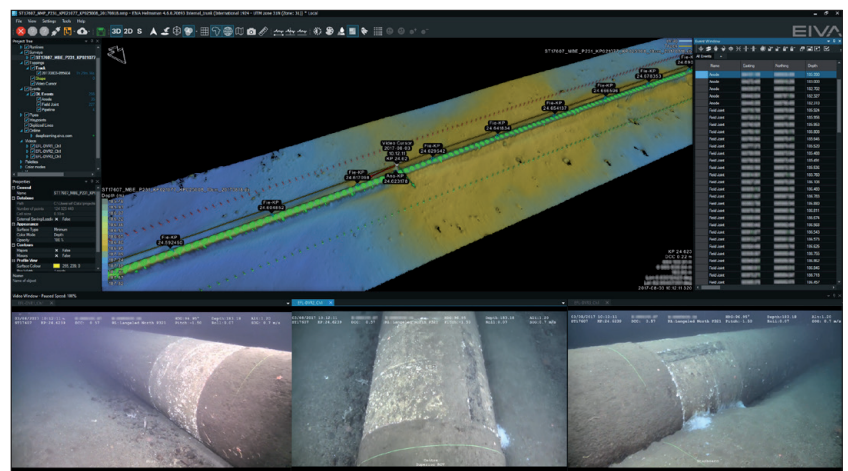


Fig. 2: Events marked along 3D model of pipeline, with video views of an anode shown at the bottom. In the upper right, you can see the full list of events

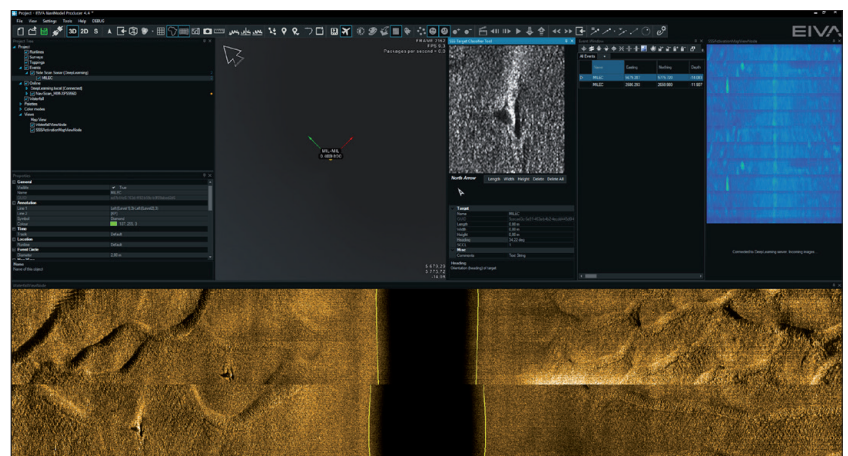


Fig. 3: The Automatic Target Recognition (ATR) tool uses a variety of NaviModel functions to identify objects – in addition to DTMs, it can be used on side-scan sonar data, as shown here, where two objects have been automatically registered as events, as shown in the event window (upper right)

NaviPac currently facilitates automatic navigation through the Coverage Assist tool. This tool automatically plans navigation runlines in real-time based on the detected depth, to ensure optimal coverage when scanning an area. The operator

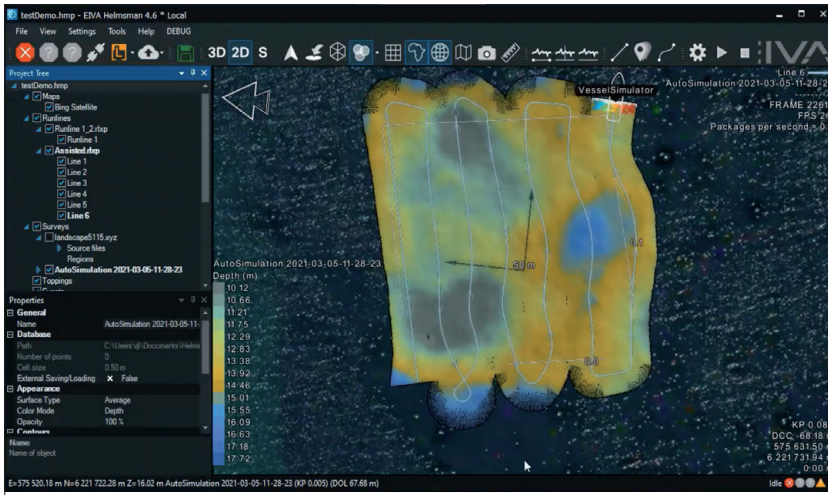


Fig. 4: A demonstration of the runlines and scan results of a survey completed using the Coverage Assist tool

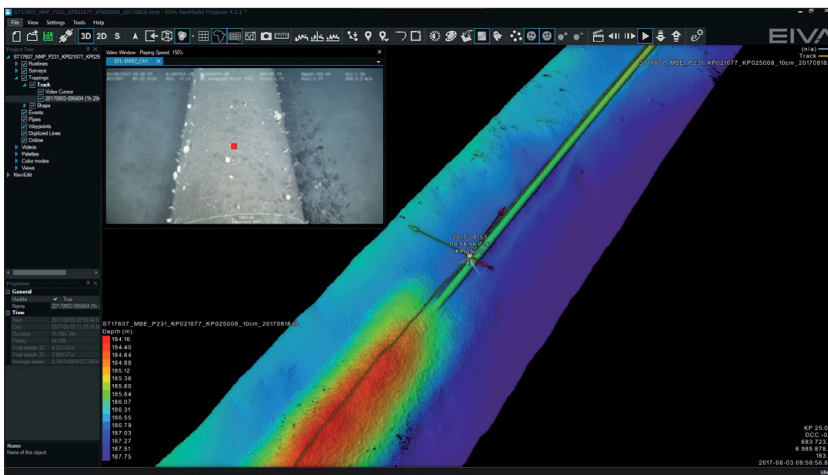


Fig. 5: The visual pipetracker navigation method involves calculating the TOP, which is marked here with a red square

can simply define the area to be scanned, as well as the first runline. Then, Coverage Assist creates the most efficient route one runline at a time. It does so by designing the shortest route to turn, and by following the outer limit of bathymetry data collected on the previous line.

In its calculations, Coverage Assist considers the vessel’s turn capabilities, as well as custom cover-

age and density requirements. In other words, it designs the optimal route for that specific vessel, with that survey’s specific requirements, and in that way adapts to ensure full area coverage (Fig. 4).

The Coverage Assist tool excels at automatically surveying a fixed area. However, surveying an area which could be positioned differently than expected, such as pipelines or a mussel net, requires more navigation-aiding. For this, we can make good use of the automatic, real-time data analysis described in the previous section.

Currently, we are developing several methods for autonomous underwater navigation aiding for a variety of applications. What these methods all have in common is that they provide automatic positioning by tracking objects or structures. We are also working on using Visual SLAM (simultaneous localisation and mapping) to provide real-time information as an input for future autonomous navigation.

2.1 If the computer can identify it, it can follow it

When you wish to navigate with respect to an object of interest, such as a pipeline, the first step is to be able to identify it. We have now covered the ways we use machine learning to teach the computer to automatically identify an object in the previous section – in the following we will dive into how to use this for navigation with respect to such objects.

In terms of navigation methods, we have made most progress in developing methods for navigating along a pipeline, as this was our first application for NaviSuite Deep Learning. We have developed two methods, based on sonar and video data. In both, the idea is to track the top of pipe (TOP) and navigate by following it (Fig. 5).

2.2 Positioning by landmarks

While it is great to be able to follow an object of interest, it is often necessary to know where you are in the world, so that object is mapped in terms of its global location. Just as you may see street

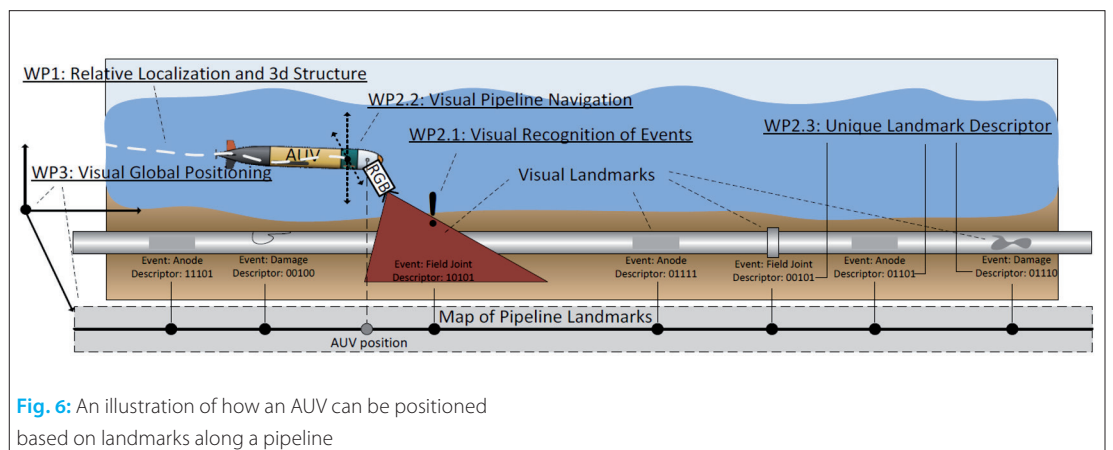


Fig. 6: An illustration of how an AUV can be positioned based on landmarks along a pipeline

names and buildings you recognise, there are landmarks under sea, which can help you navigate. These landmarks can be recognised automatically using NaviSuite Deep Learning, and then used to position your survey platform (Fig. 6). This provides a more dynamic way to perform automatic navigation.

When looking for landmarks, there are some objects under water, which we can use because we know their precise global location. These can for example be shipwrecks or points where two pipelines cross each other. Of course, we can also create such underwater landmarks ourselves if we wish, by placing a marker, or marking the position of a natural feature, such as a boulder with a recognisable shape.

There are also structures which tell us where we are relative to somewhere else. Similar to street intersections, along a pipeline there are field joints and anodes at certain intervals. By knowing the distance between these events, we have one more piece of information to map our location and speed (Fig. 7).

2.3 Navigating relative to a moving object

The object you wish to navigate with respect to may be in the water, rather than on the seabed. In this case, it is advantageous to use a forward-looking sonar (FLS). FLS is often used for obstacle avoidance, but also excels at aiding navigation, especially when you wish to approach an object without colliding with it. A useful ability, since objects floating in water rarely stay in place.

One application, in which we are using FLS, is a set-up for mussel farms. FLS is used to help navigation along mussel nets while performing video surveys of the mussels. This allows us to record a video – without colliding with the net and harming the mussels. The video can then be analysed by NaviSuite Deep Learning, which will be taught to recognise important characteristics of mussel farms, such as the amount of mussels, or occurrences of disease.

Another application in which FLS comes in handy is AUV recovery. In addition to using FLS to see the AUV, we use machine learning to track its relative location. This makes it possible to navigate towards it precisely in order to securely capture it. If the water is clear, video can also be used to track the relative location of the AUV. Both with FLS and video, the method involves using machine learning to recognise the object of interest, and then navigating with respect to its relative position (Fig. 8).

2.4 3D underwater vision with only a camera

Capitalising on recent advances in computer vision, we have developed a software tool which

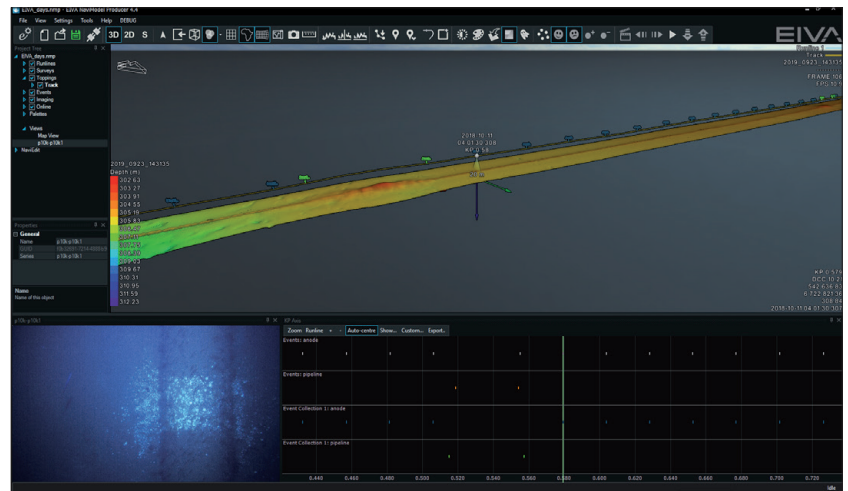


Fig. 7: NaviSuite Deep Learning recognition of anodes is used to track the position of the pipeline

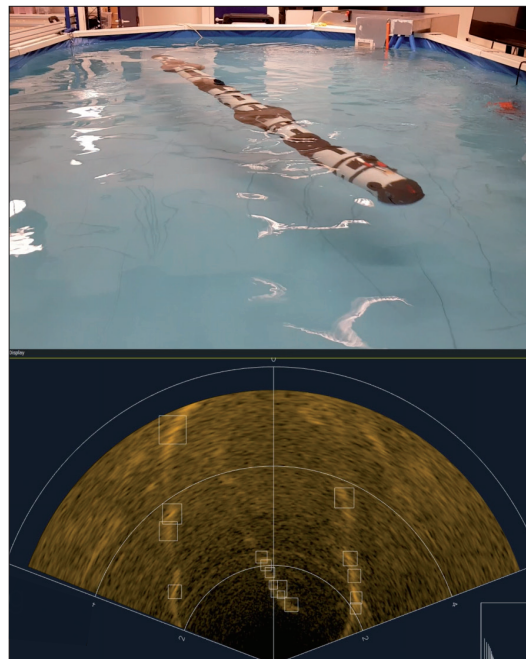


Fig. 8: In the bottom screen, you can see the FLS view of the pool with the Eelume AUV in it – the squares show where NaviSuite software uses machine learning to automatically register objects, namely the AUV in the centre, as well as interference from the sides of the pool

can create 3D reconstructions from images or videos. To achieve this, we use a combination of Visual Simultaneous Localisation and Mapping (VSLAM) and machine learning. This tool has great potential to support autonomous navigation, as it can both map the surroundings of a vehicle, as well as provide information about the vehicle's positioning.

Instead of requiring a specific hardware setup, our VSLAM software tool is designed to utilise all available equipment. With the right equipment, such as a combination of cameras and a positioning sensor, it can actually achieve higher resolu-

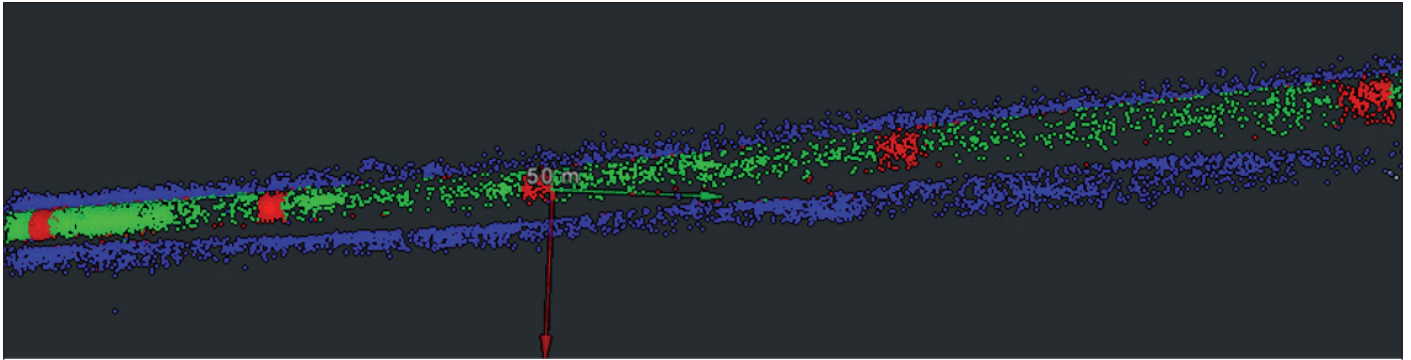


Fig. 9: A sparse point cloud of a pipeline, created using VSLAM and coloured using analysis by NaviSuite Deep Learning – the green points are the pipeline, the red are anodes and blue shows the sea bottom

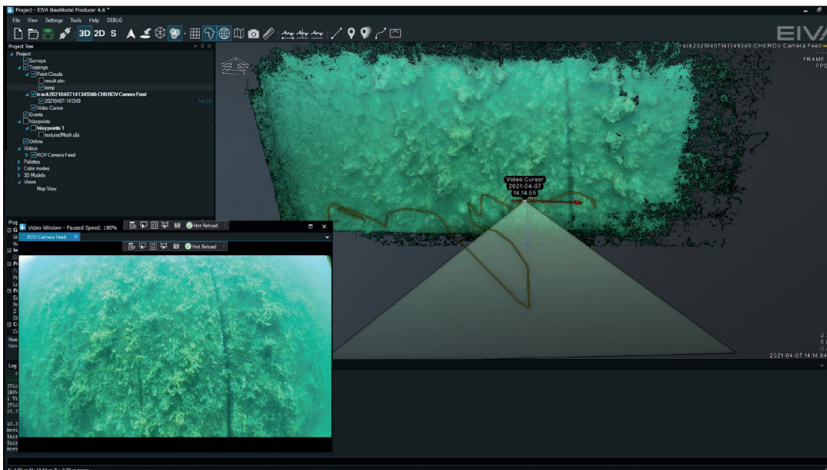


Fig. 10: A dense point cloud showing a section of harbour wall – created with VSLAM based on video data from an ROV

3 Cleaning the way

Before autonomous navigation, and even before automatic data analysis, the acquired data can be automatically cleaned. With our data cleaning feature, EC-3D, it is possible to do this by applying a filter to clean sonar data in real time, during data acquisition in NaviPac (Fig. 11).

EC-3D currently cleans data using a mix of cleaning methods, which can be combined manually to allow for precise automatic cleaning for a given set-up. Each set-up will generally have its own unique noise based on the environment and equipment, requiring this custom data cleaning. However, we aim to cut out this step with the help of machine learning. We are in the process of designing an even more automated data cleaning tool to add to the EC-3D family.

This upcoming data cleaning method uses the Density-Based Spatial Clustering of Applications with Noise (DBSCAN) algorithm. This clustering algorithm divides data points into clusters based on how dense an area is. In other words, data points

tion than sonar data. For these reasons, we expect VSLAM to play an essential role in the future of autonomous hydrographic operations in clear water (Fig. 9 and Fig. 10).

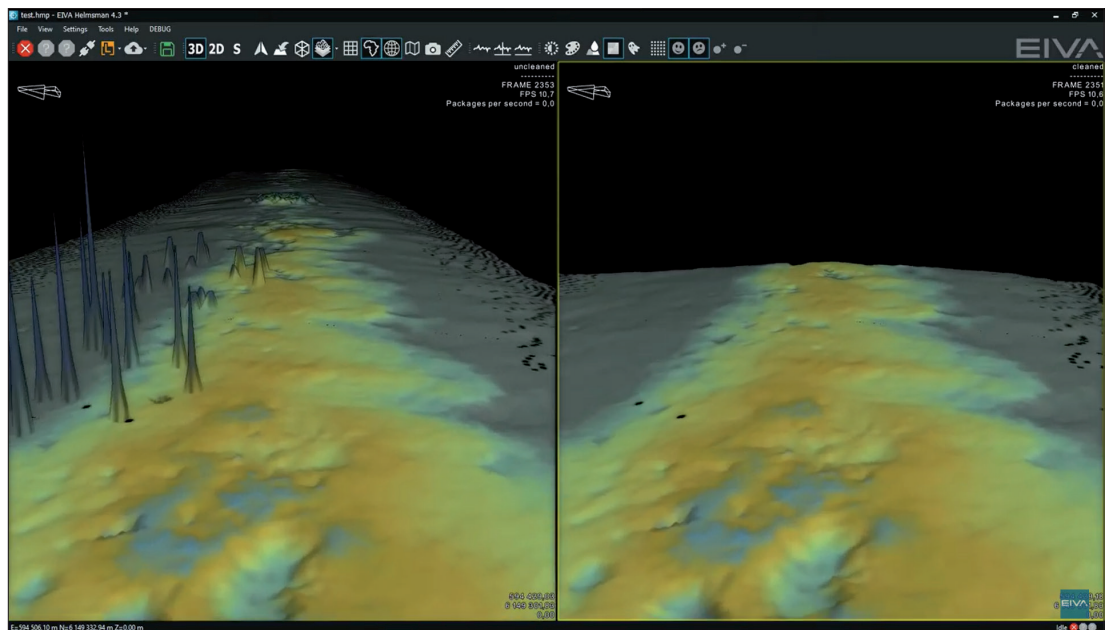


Fig. 11: An unfiltered DTM (left) and an online cleaned DTM (right) displayed simultaneously in NaviPac Helmsman's Display

which are close to each other may be grouped in clusters. You can see in the example in Fig. 12 how such clusters might look. While the seabed and pipe are grouped together, the noise around the pipe consists of many clusters, which can then all be grouped together for removal through easy instructions given in the EC-3D tool.

4 The future of autonomous hydrographic operations

Machine learning is helping us to optimise all steps in hydrographic operations, from navigation and acquisition to processing. NaviSuite supports hydrographic operations the whole way, as it is a single, complete software package for virtually any subsea task. We look forward to seeing the development of autonomous operations save NaviSuite users even more time and money.

If you want to get involved, we are more than happy to consider new projects or discuss current ones. We often need help beta-testing our solutions, so whether you are interested in trying out autonomous navigation or VSLAM computer vi-

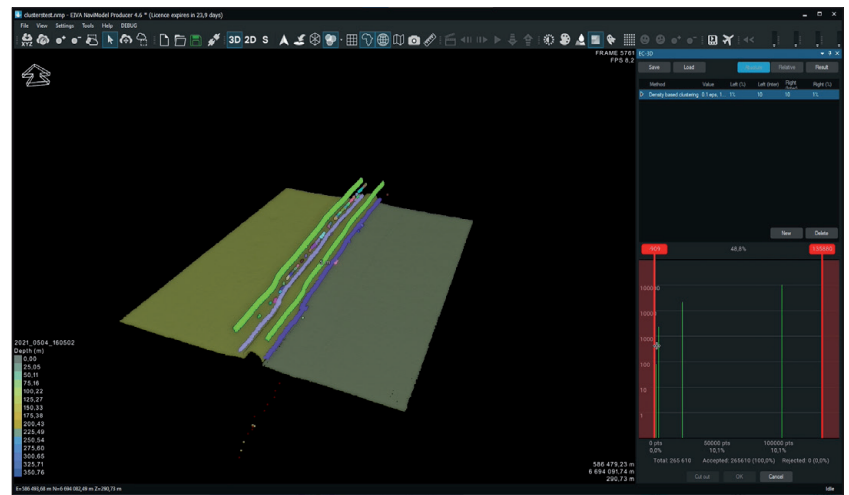


Fig. 12: Here, through the colouring, you can see the many different clusters registered by DBSCAN

sion, don't hesitate to reach out. We are also thankful for any data, which can help us to help train NaviSuite Deep Learning. This could be of pipelines, corals, mussels – or maybe you have a whole new application in mind? Get in touch. //

Fast, offshore licensed survey vessels | Cutting-edge technologies | 50 years of marine survey experience

Your data matters

AGILE OFFSHORE SURVEY SERVICES

Delivering precise hydrographic data, on demand

PRE & POST DREDGING REPORTS
TARGETED OBJECT SEARCH
UNEXPLODED ORDINANCE
CABLE DEPTH & ROUTE SURVEY

www.nicola-offshore.com
info@nicola-offshore.com

NICOLA
OFFSHORE

»Die riesigen Flächen unterhalb der Wasseroberfläche bilden das perfekte Szenario für KI-basierte Ansätze«

Ein Wissenschaftsgespräch mit ALEXANDER REITERER

Alexander Reiterer ist Professor für das »Monitoring of Large-Scale Structures« an der Universität Freiburg. Am Fraunhofer-Institut für Physikalische Messtechnik IPM erforscht und entwickelt er Multi-Sensor-Systeme und Software für die Überwachung künstlicher und natürlicher Objekte. Im Interview mit den HN schätzt der Spezialist für künstliche Intelligenz in der Geodäsie das Potenzial für KI-basierte Ansätze bei hydrographischen Anwendungen ein.

Künstliche Intelligenz (KI) | künstliche neuronale Netze (KNN) | maschinelles Lernen | Multi-Sensor-Systeme
artificial intelligence (AI) | artificial neural networks (ANN) | machine learning | multi-sensor systems

Alexander Reiterer is professor for »Monitoring of Large-Scale Structures« at the University of Freiburg. At the Fraunhofer Institute for Physical Measurement Techniques IPM, he researches and develops multi-sensor systems and software for monitoring artificial and natural objects. In the interview with HN, the specialist for artificial intelligence in geodesy assesses the potential for AI-based approaches in hydrographic applications.

Interviewer

Das Interview mit Alexander Reiterer fand im Mai per E-Mail statt. Die Fragen stellten Lars Schiller und Patrick Westfeld.

Textbearbeitung: Lars Schiller

Wir Menschen sprechen von künstlicher Intelligenz, wenn wir eine Form der Intelligenz meinen, die eben nicht die echte, die natürliche Intelligenz ist. Was ist denn an dieser unechten und unnatürlichen Intelligenz so anders?

Nun, wir haben auf der einen Seite den Menschen. Er nutzt sein Gehirn, also letztlich eine biologische Ressource, um sehr komplexe Aufgaben zu lösen – darunter sind sehr anspruchsvolle Leistungen wie Sprache, Feinmotorik, analytisches Denken usw. Auf der anderen Seite steht die Maschine, die erst einmal über keinerlei Intelligenz verfügt. Das bedeutet: Um Dinge zu tun, die auch der Mensch kann, muss sie befähigt werden. Dafür sorgt der Mensch – mit seiner natürlichen Intelligenz. Er trainiert die Maschine mit Hilfe von eigens entwickelten Lernalgorithmen und nutzt große Mengen an Daten. So lernt die Maschine, Probleme zu lösen, Entscheidungen zu treffen, also quasi-menschliche Fähigkeiten zu erlangen. Eine geistige Entwicklung im Schnelldurchlauf, wenn Sie so wollen – begrenzt auf jeweils eine bestimmte Aufgabe. Das ist ein durchaus aufwendiger Prozess, bei dem Algorithmen verwendet werden, die ein Selbstlernen ermöglichen. Bei bestimmten Aufgaben ist die Maschine nach diesem Lernen dem Menschen deutlich überlegen. Beispielsweise bei sehr langwierigen und komplexen Mustererkennungsaufgaben, bei denen Unmengen von Daten und Parametern im Spiel sind. Denken Sie nur an die Identifikation von Personen in einem Gewimmel

von Menschen – kein Mensch kann hier so schnell und zuverlässig agieren wie eine trainierte Maschine.

Wenn Sie also fragen, worin der Unterschied zwischen einer künstlichen und einer natürlichen Intelligenz liegt, dann würde ich es so formulieren: Die KI ist trainiert für eine klare Aufgabe, und zwar von Menschen. Die Kapazität einer KI kann mit der heute verfügbaren Rechenpower riesig ausgelegt werden. Das menschliche Gehirn können wir nicht erweitern und beliebig aufrüsten. Und: eine KI ermüdet nicht. Sie kann in stundenlanger Rechenarbeit sehr anstrengende Aufgaben zuverlässig erledigen, logisch richtige Entscheidungen treffen. Diese Vorteile der KI sind offensichtlich. Aber das sollte uns nicht frustrieren. Erstens, weil es jeweils Menschen sind, die eine KI erschaffen. Und zweitens, weil das menschliche Gehirn fähig ist zu Kreativität, Intuition, zu Emotionen und zu einem eigenen Bewusstsein. Darüber verfügt keine KI.

Wo liegen die Ursprünge von KI? Was war anfangs die Hoffnung?

Die grundsätzliche Vorstellung, menschliches Denken technisch nachbilden zu können, geht sehr weit zurück. Die Aufklärung beflügelte rationales, technisches Denken und die Wissenschaft. Die Vorstellung von Mensch-Maschinen, Automaten und Robotern gehen zurück bis ins 18. Jahrhundert. In der ersten Hälfte des 20. Jahrhunderts wurden dann die ersten Rechenmaschinen ent-

wickelt, die Vorläufer der Computer. Der Begriff »Künstliche Intelligenz« tauchte erstmalig in den 50er-Jahren auf. Die Hoffnungen waren teils grenzenlos und gingen bis hin zur Vorstellung, dass KI das postbiologische Zeitalter einleiten wird, in dem das biologische Gehirn dereinst durch Technik ersetzt wird. Solche Szenarien werden als »starke KI« bezeichnet – also die Vorstellung, dass KI dem Menschen immer ähnlicher und am Ende ebenbürtig wird. Viele Romane und Filme in der zweiten Hälfte des 20. Jahrhunderts zeigen ja, wie das Thema KI die Menschen inspiriert. Sie zeigen aber auch, welche Befürchtungen und Ängste es hervorruft. Die Vorstellung, eine KI könne dem Menschen immer ähnlicher werden, ihn letztendlich beherrschen, ist zu einer verbreiteten Dystopie geworden.

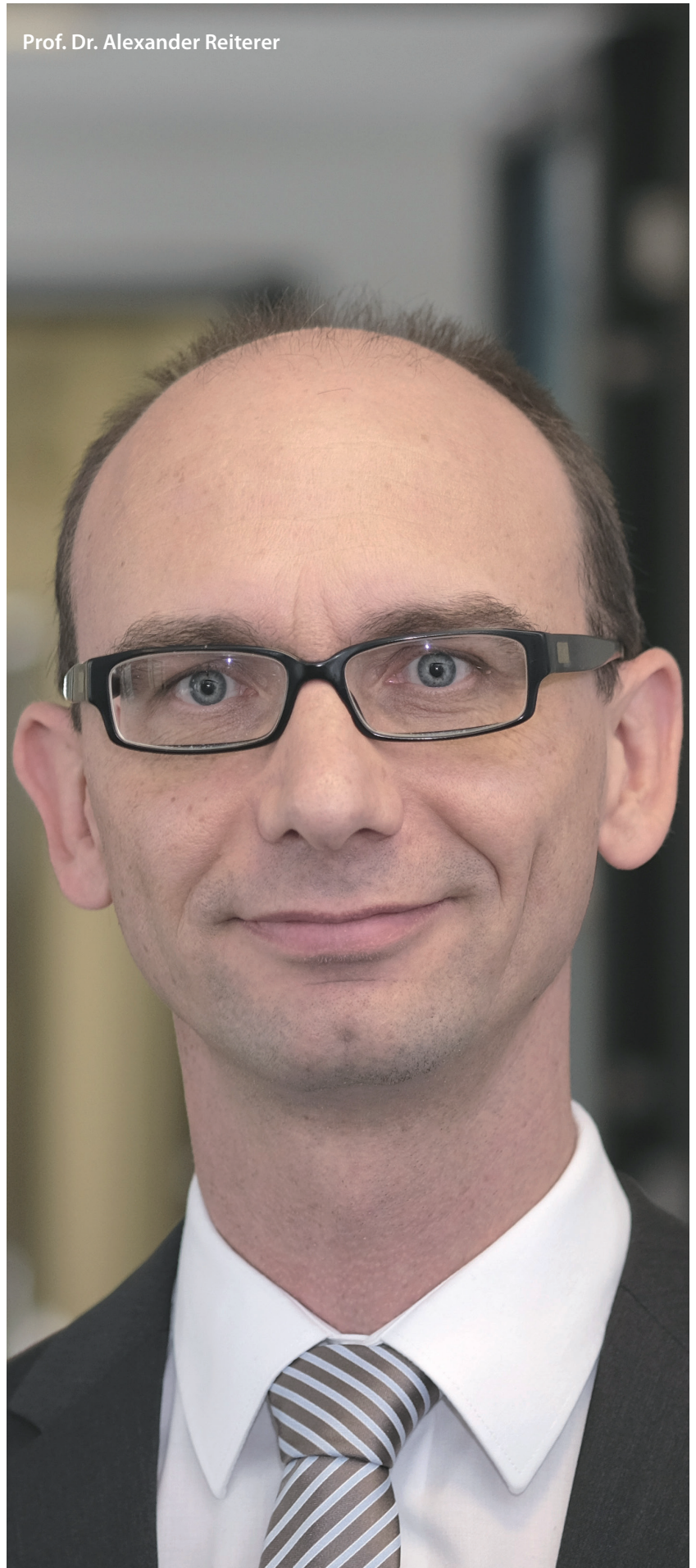
Aber Sie haben nach Hoffnung gefragt: Aus meiner Sicht liegen die Chancen in der sogenannten »schwachen KI«. Damit ist gemeint, bestimmte komplexe Aufgaben mit Hilfe von Algorithmen zu lösen. Wir sehen ja die erfolgreiche Anwendung von KI schon seit einigen Jahren. Viele von uns nutzen sie im Alltag. Denken Sie an Computerspiele oder automatische Übersetzungsprogramme. Stark ist KI in der Mustererkennung und im Auswerten großer Datenmengen. Dabei denke ich an die medizinische Diagnostik, an die Modellierung von Klimadaten oder auch an die Qualitätskontrolle in der industriellen Produktion. Hier gibt es so viele Möglichkeiten, Dinge effizienter und besser zu machen und damit den Menschen nicht nur zu unterstützen, sondern ihn zu entlasten bzw. in seiner Entwicklung sogar zu fördern.

[KI gibt es schon eine Weile, warum ist KI plötzlich so ein Hype?](#)

Das liegt ganz wesentlich an den enormen Fortschritten bei der Hardware, vor allem unglaublich leistungsfähige Grafikkarten und Prozessoren, die in den vergangenen zehn Jahren auf den Markt kamen. Die Gaming-Industrie war hier Treiber einer Entwicklung, die nun die Industrie beflügelt und der KI sehr viele Möglichkeiten eröffnet. Und natürlich wird seit geraumer Zeit sehr intensiv zum Thema KI geforscht, allen voran in den USA, in China und inzwischen auch hier bei uns. Der Hype wurde getrieben durch die Erfolge, die ja heute jedem einzelnen von uns zugänglich sind und große gesellschaftliche Relevanz haben. Methoden der KI werden heute sehr breit in den unterschiedlichsten Produkten eingesetzt – oftmals, ohne dass wir es bewusst wahrnehmen. Denken Sie an die Gesichtserkennung, die Ihr Handy entsperrt, an die Sprachsteuerung zum Beispiel bei Google-Produkten. Da ist seit den frühen 2000er-Jahren sehr, sehr viel Innovation passiert – und das ist für jedermann täglich erlebbar und nutzbar.

[Folgender Fall: Ein Mitarbeiter eines Vermessungsbüros soll 3D-Punktwolken aus einem Laserscanner klassifizieren. Bisher hat er diese Arbeit](#)

Prof. Dr. Alexander Reiterer



selbst erledigt, er ist ja vom Fach. Jetzt liegt ihm das Angebot eines KI-Dienstleisters vor, der behauptet, die Informatiker können diese Aufgabe mit Hilfe künstlicher neuronaler Netze ebenfalls erfüllen, noch dazu viel schneller. Der Kollege aus dem Vermessungsbüro ist skeptisch. Was raten Sie ihm?

Der Aufwand und damit auch die Kosten, eine KI einzusetzen, hängt sehr davon ab, ob man auf ein bestehendes KI-System aufbauen kann, das heißt, ob man für die spezifische Aufgabe auf vorhandene Trainingsdaten zurückgreifen kann. Ist das Problem noch weitgehend unerschlossen und es

»Alles unterhalb der Wasseroberfläche ist KI-technisch noch weitgehend unerschlossen. Eine riesige Chance«

Prof. Alexander Reiterer

müssen eigene Trainingsdaten erstellt werden, muss man prüfen, ob sich der Aufwand für das Trainieren der KI lohnt. Die Entwicklungskosten für gut trainierte Systeme mit hoher Zuverlässigkeit im Sinne der Lösungsfindung sind mitunter sehr hoch. Oft suchen wir aber in Messdaten auch

nach den immer gleichen Objekten, das gilt speziell für die Klassifizierung von Umfelddaten: Hier müssen immer wieder ähnliche prototypische Objekte wie Straßenlaternen, Bäume, Bordsteinkanten oder Pflastersteine erkannt werden. Darauf lässt sich eine KI sehr gewinnbringend und mit nicht allzu aufwendigen Mitteln trainieren. Ein weiterer Vorteil: Die klassifizierten Daten lassen sich automatisiert weiterverarbeiten, also zum Beispiel in Planungskarten oder Dokumentationssysteme integrieren. Die gewonnene Zeit können die Mitarbeiterinnen und Mitarbeiter des Büros damit verbringen, zum Beispiel die Qualitätskontrolle weiter zu verbessern, um dann in Zukunft noch bessere und zuverlässigere Ergebnisse erreichen zu können. Anders sieht es bei Umgebungen aus, die KI-technisch noch weitgehend unerschlossen sind. Alles unterhalb der Wasseroberfläche gehört hier meist dazu. Eine große Herausforderung, aber auch eine riesige Chance.

Sie beschäftigen sich seit vielen Jahren mit KI in der Geodäsie. Wie wird KI in der Geodäsie bisher genutzt?

Mich treibt das Thema KI seit fast 20 Jahren um. Als ich 2004 an der TU Wien im Bereich regelbasierte Systeme promoviert habe, war das Thema maschinelles Lernen gerade ziemlich out. Es bedurfte großer Überzeugungsarbeit, mich auch mit künstlichen neuronalen Netzen beschäftigen zu dürfen. Aber ich war schon damals fest überzeugt, dass KI sich für die Geodäsie absolut gewinnbringend einsetzen lässt, da bei vielen Aufgaben unglaublich viele Daten anfallen. Die Auswertung dieser Datenmengen kann mit KI nicht nur effizienter, sondern auch objektiver ablaufen. Zudem werden die Messgeräte immer leistungsfähiger und pro-

duzieren Datenmengen, die der Mensch nur noch schwer in kurzer Zeit hinreichend gut verarbeiten kann. Wir haben an unserem Institut Laserscanner entwickelt, die über zwei Millionen Messpunkte pro Sekunde erzeugen. Die Sensoren messen von mobilen Plattformen aus – von Messfahrzeugen oder inzwischen auch von Drohnen – und vermessen so sehr große Flächen. Aus den Messdaten das Maximum herauszuholen, das gelingt aus meiner Sicht nur mit Hilfe von KI. Das wird auch mehr und mehr zur gängigen Praxis. Nehmen Sie zum Beispiel das Monitoring von Infrastruktur, mit dem wir uns am Fraunhofer IPM beschäftigen: Hier vermessen die Scanner und Kameras Straßen oder Schienen – und sammeln sehr viele Daten von den immer gleichen Objekten. Diese Daten zu sichten, ist für den Menschen eine sehr monotone Arbeit, eine Quälerei ... Eine KI kann hier sehr schnell und zuverlässig gesuchte Objekte identifizieren, Fehler und Unregelmäßigkeiten finden. Anderes Beispiel: Wir haben ein künstliches neuronales Netz (KNN) auf die Erkennung bestimmter Straßenobjekte und -oberflächen trainiert. Dieses Netz wird jetzt genutzt, um Straßen für den Glasfaserausbau zu kartieren. Wo früher mehrere Menschen geschaut, gemessen und gezeichnet haben – »Wächst da ein Baum? Ist dort ein Stromverteiler? Gibt es hier Kopfsteinpflaster?« –, gibt heute das KNN diese Informationen aus. Und es speist diese Infos direkt in eine Planungskarte und errechnet daraus die günstigste Trasse für die Glasfaser. Der Planungsprozess beschleunigt sich so um ein Vielfaches. Das ist ein großer Fortschritt, möglich geworden durch KI.

Welche Anwendungsfälle sehen Sie für die KI in Hinblick auf den Untersuchungsgegenstand der Hydrographie, die Gewässer?

Was die Hydrographie betrifft, stehen wir noch am Anfang, wenn es um den Einsatz von KI geht. Ich sehe hier aber großes Potenzial. Meere und Flüsse sind als Schifffahrtswege wichtige Verkehrsadern im globalen Handel, hinzu kommt eine wachsende Unter-Wasser-Infrastruktur, vor allem in Form von Offshore-Windparks. Diese Infrastruktur muss überwacht werden. Gleichzeitig führt der Klimawandel zu Veränderungen an den Küsten. Der Küstenschutz ist also ebenfalls auf Messdaten angewiesen. Die wachsende Notwendigkeit hydrographischer Daten liegt also auf der Hand. Hinzu kommt, dass neue Messgeräte immer höher aufgelöste Bathymetriedaten liefern. Am Institut arbeiten wir beispielsweise an einem Laserscanner für Unter-Wasser-Messungen. Damit werden wir die Präzision und die räumliche Auflösung im Vergleich zu Sonarsystemen jeweils um den Faktor fünf bis zehn steigern können. Solche hochaufgelösten Daten ermöglichen und erfordern letztlich auch ganz andere Methoden der Datenanalyse. Hochaufgelöste Daten von immens großen Flächen, wie man sie unterhalb der Wasseroberfläche

naturgemäß bei vielen Anwendungen vorfinden wird, bilden das perfekte Szenario für KI-basierte Ansätze. Bei einigen Aufgaben kann man direkt auf bereits etablierte Entwicklungen anwendungsspezifischer KI aufbauen. Risse in Betonfundamenten zu identifizieren, ist bei Bauwerken an Land und im Meer weitgehend die gleiche Aufgabe – der Bewuchs der Bauwerke, der diese Aufgabe vielleicht behindert, unterscheidet sich aber sehr stark. Daneben gibt es natürlich Aufgaben, die an Land in dieser Form nicht vorkommen und sehr spezifisch für Unter-Wasser-Anwendungen sind – ein Beispiel ist die zuverlässige Erfassung und Charakterisierung von Auskolkungen.

Wie lässt sich KI für die Steuerung von Multi-Sensor-Systemen nutzen?

Derzeit verbindet man KI in erster Linie mit dem Auswerten von Daten. Dieses Auswerten kann zeitlich deutlich versetzt, also nach der eigentlichen Datenaufnahme erfolgen, oder auch möglichst zeitgleich mit der Aufnahme. Wenn wir Daten aufnehmen und direkt, also zeitgleich analysieren, können wir den sequenziellen Aufnahmeprozess steuern – auf Basis der unmittelbaren Ergebnisse der Datenanalyse. Es kann also quasi ein Regelkreis gebildet werden. Die Aufnahme der Daten kann dann beispielsweise so gestaltet werden, dass bestimmte Objekte mit ganz spezifischen Sensoren erfasst werden. Denken wir zum Beispiel ans Mobile-Mapping unterirdisch verlegter Infrastruktur: Es wäre möglich, ein Georadar-System nur dann Daten aufzeichnen zu lassen, wenn auch wirklich interessante Infrastruktur im Untergrund zu erwarten ist. Dies wäre vermutlich in der Nähe von Straßenlaternen oder Ampeln, wo unterirdische Leitungen verlegt sind. Gelingt es, die Laterne oder die Ampel in den Bilddaten oder den Laserscandaten im laufenden Erfassungsprozess zu erkennen, kann das Georadar-System sehr gezielt eingesetzt werden. In eine ähnliche Richtung geht die Anonymisierung von Daten in Echtzeit. Wir haben ja beim Messen im öffentlichen Raum immer das Problem des Datenschutzes. Ideal wäre es, wenn Bilddaten möglichst bereits vor dem Speichern im Multi-Sensor-System anonymisiert werden könnten. Dies ist ein Bereich, in dem wir am Fraunhofer IPM derzeit intensiv arbeiten und forschen. Das Ziel ist hier ein Mobile-Mapping-System, das mit jeder Sensorkonfiguration völlig datenschutzkonform im öffentlichen Raum unterwegs ist. Ein weiterer sehr spannender Bereich ist die Kalibration hochkomplexer Multi-Sensor-Systeme. Bisher kommen hier sehr komplizierte mathematische Modelle zum Einsatz. Die Bestimmung aller notwendigen Parameter für den Kalibrationsprozess ist aufwendig und mit Fehlern behaftet. Auch hier lässt sich der Prozess mit Hilfe von KI effizienter gestalten – auch daran arbeiten wir derzeit am Fraunhofer IPM und an meiner Professur an der Universität Freiburg.

Wie lange muss man ein KI-System trainieren? Woran kann man festmachen, dass genug trainiert wurde?

Das hängt direkt von der Komplexität der Aufgabe ab. Wenn wir beispielsweise von der Mustererkennung sprechen, mit der wir uns beschäftigen: Suche ich ein rotes Quadrat in einem Set unterschiedlicher Formen, so ist das eine einfache Aufgabe, bei der das neuronale Netz einige wenige Parameter lernen muss. Das geht sehr schnell. Für die Analyse von Straßenumgebungen, die ich bereits erwähnte, haben wir um die Hunderttausend Bilder ausgewertet. Laternen, Briefkästen oder Kanaldeckel können unterschiedliche Formen haben, es gibt viele Arten von Hecken, unterschiedliche Größen von Pflastersteinen – und nicht zuletzt verschiedene Jahreszeiten, und damit Bäume mit und ohne Laub ... All das müssen wir der KI antrainieren. Dazu müssen Beispielbilder »annotiert« werden, das heißt, die Objekte darin werden markiert und verschlagwortet. Das ist eine mühselige manuelle Arbeit, an der bei uns ein 50-köpfiges Team über zwölf Monate gearbeitet hat. Ein solcher Trainingsdatensatz ist daher ein wertvolles Gut. Je besser er ist, desto zuverlässiger ist die Objekterkennung. Bei unseren Straßendaten liegen wir bei einer Erkennungsgenauigkeit von über 90 Prozent. Um den Prozess effizienter zu gestalten, arbeiten wir inzwischen auch an Konzepten, um Trainingsdaten synthetisch zu erstellen. Dahinter steckt ein Ansatz mit enormem Potenzial. Wir könnten so perspektivisch sehr schnell KI-Systeme einsetzen für spezifische Aufgabenstellungen, bei denen das Erfassen und Annotieren von Trainingsdaten sehr aufwendig oder sogar unmöglich wäre. Damit werden solche Systeme in Zukunft auch für kleine und hochspezialisierte Firmen – wie sie im Bereich der Hydrographie auch existieren – erschwinglich und interessant.

»Immer höher aufgelöste Bathymetriedaten ermöglichen und erfordern ganz andere Methoden der Datenanalyse«

Prof. Alexander Reiterer

Wie stellt man sicher, dass die Ergebnisse, zu der eine KI gekommen ist, wissenschaftlich profund sind? Wie lässt sich eine Qualitätsaussage machen?

Am Ende zählt das Ergebnis, und das lässt sich in den meisten Fällen sehr gut evaluieren. Aber zugegeben: Der Aufwand für eine Evaluierung ist hoch. Prinzipiell verwenden wir Referenzsysteme oder Referenzdatensätze, um die Qualität zu beurteilen, mit der eine KI arbeitet. Insofern ist das Vorgehen vergleichbar mit der Art, wie wir die Leistung eines Menschen beurteilen. Das Referenzsystem oder der Referenzdatensatz muss die Anwendung und die gewünschte Qualität hinreichend repräsentieren. Dies kann zum Beispiel ein Datensatz von Bildern sein, in denen gesuchte Objekte von gut

Bisher erschienen:

- Horst Hecht (HN 82),
 Holger Klindt (HN 83),
 Joachim Behrens (HN 84),
 Bernd Jeuken (HN 85),
 Hans Werner Schenke (HN 86),
 Wilhelm Weinrebe (HN 87),
 William Heaps (HN 88),
 Christian Maushake (HN 89),
 Monika Breuch-Moritz (HN 90),
 Dietmar Grünreich (HN 91),
 Peter Gimpel (HN 92),
 Jörg Schimmler (HN 93),
 Delf Egge (HN 94),
 Gunther Braun (HN 95),
 Siegfried Fahrentholz (HN 96),
 G. Braun, D. Egge, I. Harre,
 H. Hecht, W. Kirchner und
 H.-F. Neumann (HN 97),
 W. und A. Nicola (HN 98),
 Sören Themann (HN 99),
 Peter Ehlers (HN 100),
 Rob van Ree (HN 101),
 DHyG-Beirat (HN 102),
 Walter Offenborn (HN 103),
 J. Schneider v. Deimling (HN 104),
 Mathias Jonas (HN 105),
 Jürgen Peregovits (HN 106),
 Thomas Dehling (HN 107),
 Egbert Schwarz (HN 108),
 Ingo Hennings (HN 109),
 Harald Sternberg (HN 110),
 Uwe Jenisch (HN 111),
 Petra Mahnke (HN 112),
 Holger Rahlf (HN 113),
 Boris Schulze (HN 114),
 Jacobus Hofstede (HN 115),
 Gottfried Mandlbürger (HN 116),
 Gerhard Bohrmann (HN 117)
 Günther Lang (HN 118)

geschulten Fachleuten markiert und vordefinierten Klassen zugeordnet wurden. Das Ergebnis der KI wird dann mit diesem Bilddatensatz verglichen und geometrische Abweichungen werden berechnet. Daraus lassen sich eindeutige Qualitätsmaße bestimmen, die objektiv und auch zwischen verschiedenen Anwendungen vergleichbar sind. Natürlich lassen sich mit dieser Methode auch KI-Systeme untereinander vergleichen. Etwas komplexer wird es, wenn sich die Unterschiede zwischen einem menschlichen Experten und der KI nicht mehr in Qualitätsparameter kleiden lassen, wenn es also kein klar definiertes Referenzsystem gibt. Denken Sie zum Beispiel an eine klassische Aufgabe aus dem Industriedesign: Was macht einen ergonomisch perfekten, ästhetisch möglichst ansprechenden, gut zu produzierenden, kostengünstigen Türgriff aus? Da gehen die Einschätzungen und Parameter auseinander, sind also verhandelbar. Das muss die KI abbilden; sie muss hier weichere Kriterien berücksichtigen. Statt einer starren Referenzbasis wird hier mit breiteren Referenzgruppen gearbeitet, sodass am Ende im Schnitt die beste, schönste, praktischste ... Lösung herauskommt, die dann als Referenz gilt. Je schwieriger die mathematische Beschreibung der Qualitätsmerkmale, desto schwerer fällt die objektive Beurteilung der Ergebnisse. Das Problem haben wir aber auch bei der Beurteilung durch menschliche Expertinnen und Experten bzw. bei Ergebnissen und Produkten, die vom Menschen geschaffen wurden.

KI hat oft etwas von einer Blackbox. Da passiert irgendwas, doch die Frage ist, was da vor sich geht und wie das Ergebnis zustande kommt. Oft weiß man es nicht, der Lösungsweg ist nicht nachvollziehbar, das Ergebnis nicht reproduzierbar. Klingt nicht gerade nach einem wissenschaftlichen Ansatz, oder?

So würde ich das nicht sehen. Mit dem gleichen Recht könnte man ein Gehirn als Blackbox beschreiben – man weiß nie recht, was der andere denkt. Wer sich auskennt, kann sehr genau wissen, was in einer KI vor sich geht: Ein Algorithmus ist anhand bestimmter Kriterien auf eine Entscheidung trainiert. Wer sich tiefer damit beschäftigt, kann diese Kriterien und die Entscheidungsvorgaben kennenlernen – wenn sie denn offengelegt werden. Natürlich braucht es dazu mathematisches Vorwissen und Wissen über die verwendeten Trainingsdaten. Aber ohne Wissen verste-

hen wir vieles nicht in unserer hochentwickelten Gesellschaft. Ohne ein gut ausgestattetes Labor und Kenntnisse in Chemie weiß ich auch nicht, was in meiner Backmischung drin ist. Es sei denn,

ich verlasse mich auf die Zutatenliste. Und was die Reproduzierbarkeit und Wissenschaftlichkeit betrifft: Die Ergebnisse einer KI-basierten Aktion sind in hohem Maße reproduzierbar und daher auch klar wissenschaftlich evaluierbar. Die meisten KI-Systeme lassen sich heute gut auf der Basis freizugänglicher Datensätze wissenschaftlich beurteilen. Aber ich verstehe, worauf Sie mit Ihrer Frage wahrscheinlich abzielen. Der Einsatz von KI, beispielsweise in den sozialen Medien oder bei der Gesichtserkennung, ist vielen Menschen unheimlich und birgt ja auch ganz klar große Risiken wie zum Beispiel Deepfakes oder Überwachung. Und natürlich ergeben sich in bestimmten Bereichen auch schwierige ethische Fragen. Das müssen wir kritisch im Blick haben. Die EU hat das Thema vor diesem Hintergrund ja auch aufgegriffen und erste Vorschläge zur Regulierung gemacht. In vielen Gebieten, in denen wir in der Wissenschaft unterwegs sind, sehe ich solche Risiken nicht. Dazu gehört auch die Messtechnik und im Speziellen die Geodäsie.

Was meinen Sie, kann KI eines Tages ganz intuitiv von allen genutzt werden? Oder ist es heute schon so weit, nur wir haben es noch nicht mitbekommen?

Letzteres, ganz klar. Jeder, der schon einmal Übersetzungssoftware, einen Schachcomputer oder ein Computerspiel genutzt hat, weiß, dass KI ganz hervorragend funktionieren kann und man intuitiv damit umgehen kann bzw. nicht wirklich merkt, warum etwas so gut funktioniert. Darum wird ja auch kein Geheimnis gemacht. Ganz im Gegenteil: Wo KI drin ist, steht heute immer öfter auch ganz groß KI drauf. Zumindest in der Wissenschaft ist das so, und das wird sich meines Erachtens auch durchsetzen, wenn klar ist, zu welchem Zweck eine KI eingesetzt wird. Um noch einmal bei der Mustererkennung zu bleiben: Was spricht dagegen, wenn eine KI ein Tomographiebild auf bestimmte Muster durchsucht, dabei wirklich minimale Abweichungen im Vergleich zu vorigen Aufnahmen findet? Abweichungen, die das menschliche Auge oder ein vielleicht übermüdeten Arzt gar nicht sehen würde. In solchen Fällen gibt es sehr gute Argumente für den Einsatz von künstlicher Intelligenz.

Wird KI zu neuen Jobs in der Geo-Branche führen?

Das wird auf jeden Fall so sein. Da gibt es eine große Dynamik, und wir müssen die Ausbildung des Nachwuchses dringend darauf ausrichten, dass wir in Zukunft Menschen mit Kenntnissen im Bereich KI rekrutieren können. Kenntnisse in diesem Bereich sollten Teil der entsprechenden Studiengänge werden. Bereits heute zeigt sich, dass Absolventinnen und Absolventen, die auch nur minimale Kenntnisse in Softwareentwicklung und speziell im Bereich KI haben, vom Markt förmlich weggesaugt werden. In meinem Team am Fraunhofer IPM

»KI-Systeme werden in Zukunft auch für kleine und hochspezialisierte Firmen der Hydrographie erschwinglich und interessant«

Prof. Alexander Reiterer

haben wir die Zahl der Mitarbeitenden in diesem Bereich in den letzten drei Jahren verdoppelt – das zeigt ganz klar, dass hier viel Potenzial vorhanden ist. Voraussetzung ist, dass die Universitäten und die Studiengänge sich dahingehend weiterentwickeln und am Marktbedarf orientieren.

Mit was beschäftigen Sie sich am Fraunhofer IPM in Freiburg?

Wir sind eines von 75 Fraunhofer-Instituten und arbeiten mit dem Schwerpunkt physikalische Messtechnik. Im Wesentlichen beschäftigen wir uns mit der Entwicklung und der Anwendung optischer Messsysteme. In meinem Bereich sind dies vor allem laser- oder kamerabasierte Systeme zur 3D-Vermessung großer Strukturen, etwa von Infrastruktur – Schienen, Straßen, Bauwerke oder großer Vegetationsflächen. Die Messsysteme messen in der Regel von mobilen Plattformen aus – also von Straßen- oder Schienenfahrzeugen oder auch von Drohnen. Seit einiger Zeit arbeiten wir auch am Einsatz der Systeme auf Unter-Wasser-Fahrzeugen. Was die Messtechnik-Hardware angeht, sind wir bei einigen Systemen bereits an der Grenze

des physikalisch Möglichen angelangt: Wir messen überaus genau mit sehr hohen Punktdichten und höchster Präzision. In den vergangenen Jahren wurde es immer wichtiger, Daten aus verschiedenen Quellen zu fusionieren, um bei der Interpretation noch mehr Information zur Verfügung zu haben und damit belastbare Interpretationsergebnisse zu generieren. Das heißt, die Themen Dateninterpretation und -visualisierung haben gegenüber der Datenerfassung deutlich an Bedeutung gewonnen. KI ist hier ein wesentlicher Treiber und der Enabler für viele Anwendungsbereiche.

Was würden Sie gerne besser können?

Da gibt es zu viele Dinge, als dass ich sie alle aufzählen könnte.

Was wissen Sie, ohne es beweisen zu können?

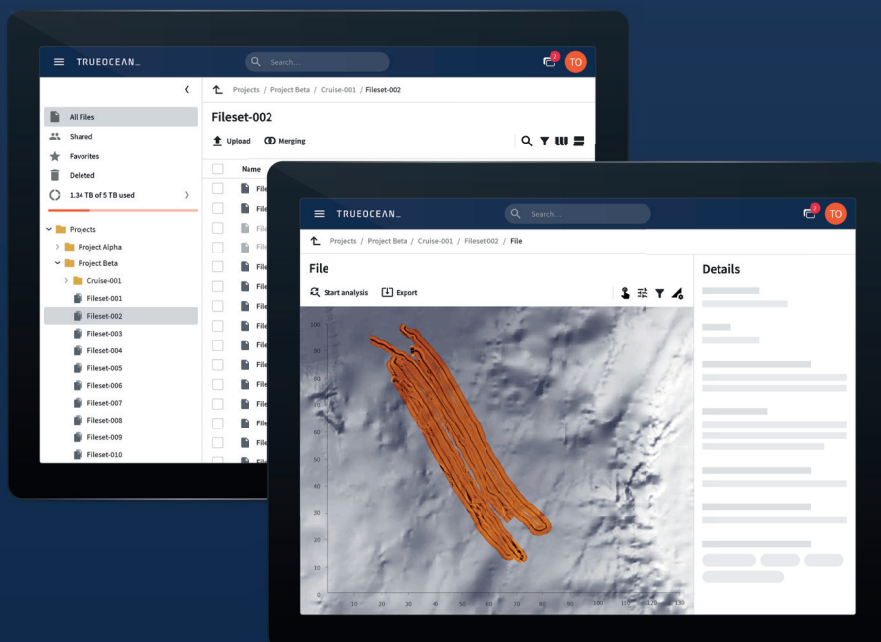
Die Weltformel ist im Kaffeesatz versteckt. //

»Dateninterpretation und -visualisierung gewinnen gegenüber der Datenerfassung deutlich an Bedeutung. KI ist hier ein wesentlicher Treiber und Enabler«

Prof. Alexander Reiterer

Your ocean data **service.**

TrueOcean is a safe and collaborative platform for your marine sensor data. Available, everywhere at any time and designed for big data volumes to gain better information.



Management Processing Collaboration

Visualisation AI-based analysis

Large variety sensors & file formats

We enable the digital transformation of the maritime world. Be an innovator and connect with us:

www.trueocean.io | info@trueocean.io

Interactive processing of MBES bathymetry and backscatter data using Jupyter Notebook and Python

An article by SOPHIE ANDREE

This work explores the potential of Jupyter Notebook and Python to create an interactive processing tool for multibeam bathymetry and backscatter data. For this purpose, a Kongsberg EM 122 data set was used to identify and implement the required processing steps. Special attention was paid to the integration of freely available open source libraries to meet the performance requirements. The result is a modular approach that first decodes the required raw data, then computes the bathymetry and backscatter point clouds and finally applies semi-automatic filters to clean the bathymetry from outliers and visually correct the backscatter. Validation with data already processed on board confirmed the general feasibility of the approach. However, minor inconsistencies were encountered in the preprocessing of the bathymetry, which should be addressed in further work. Additionally, the tool can be extended for tidal correction and navigation processing.

Python | Jupyter Notebook | multibeam processing | bathymetry | backscatter | open source
Python | Jupyter Notebook | Verarbeitung von Fächerlotdaten | Bathymetrie | Backscatter | Open Source

Diese Arbeit untersucht das Potenzial von Jupyter Notebook und Python zur Erstellung eines interaktiven Tools zur Verarbeitung von Fächerlot-Bathymetrie- und -Rückstreudaten. Zu diesem Zweck wurde ein Kongsberg-EM-122-Datensatz verwendet, um die erforderlichen Verarbeitungsschritte zu identifizieren und zu implementieren. Besonderes Augenmerk wurde auf die Integration von frei verfügbaren Open-Source-Bibliotheken gelegt, um den Leistungsanforderungen gerecht zu werden. Das Ergebnis ist ein modularer Ansatz, der zunächst die benötigten Rohdaten decodiert, dann die Bathymetrie- und Rückstreupunktewolken berechnet und schließlich halbautomatische Filter anwendet, um die Bathymetrie von Ausreißern zu bereinigen und die Rückstreuung visuell zu korrigieren. Die Validierung mit bereits an Bord verarbeiteten Daten bestätigte die generelle Machbarkeit des Ansatzes. Allerdings traten kleinere Unstimmigkeiten bei der Vorverarbeitung der Bathymetrie auf, die in weiteren Arbeiten behoben werden sollten. Zusätzlich kann das Tool für die Gezeitenkorrektur und die Navigationsverarbeitung erweitert werden.

Author

Sophie Andree holds a M.Sc. degree in Geodesy with specialisation in Hydrography from HafenCity University in Hamburg.

sophie-andree@web.de

Introduction

Today, multibeam echo sounders (MBES) are the most common and efficient method of conducting hydrographic surveys for the collection of bathymetry and backscatter data. Due to the challenging conditions in the marine environment and the complex MBES system setup, both types of data require various processing steps to provide reliable results. Conventionally, proprietary software suites with purchasable licenses are used for this purpose. While these leave little to be desired in terms of functionality and reliability, it is often semi-transparent what processing is applied to the data. In various areas of geomatics, there is a movement towards openness: keyword open source. Particularly in the university environment, open source and the use in teaching can be combined well in order to give students an understanding

of the fundamental interrelationships. With this in mind, the idea was formed to investigate the possibilities of processing MBES data in order to develop an interactive tool based on Jupyter Notebook and Python. The exemplary data was acquired using a Kongsberg EM 122 MBES aboard the research vessel *Sonne* on a transit cruise (SO268-3) from Vancouver to Singapore, which is also available on PANGEA (Kinne et al., 2019).

Why Python and Jupyter Notebook?

As a dynamically typed, interpreted programming language, Python requires relatively little code to express a high level of functionality. Therefore, the code is usually easy to read and quick to debug and review. When it comes to executing code, programming languages that are compiled in advance tend to be faster. However, especially for

non-professional programmers, the readability and efficiency of code implementation in Python is often comparatively more productive than faster code execution. This is perhaps one of the reasons why Python has become particularly popular in the data science community (Carbannelle 2020). This leads to another aspect that should be considered: The open source community for Python is large. Libraries and packages already exist for many different applications to solve a wide variety of tasks. In addition, Python can be used to extend and embed other languages such as C or C++. In this context, it can be understood as a »glue« language. Performance-critical parts of a program can be written in or adapted from faster languages, while Python is used for code control and adaptation (van Rossum and Drake 2003).

Jupyter Notebook is a free, open source, interactive web tool that is structured like a notebook. Software code, computational results, explanatory text and multimedia resources can be combined into a single document. Originally, the Jupyter project grew out of the IPython (interactive Python) project, with the goal of supporting interactive data science and scientific computing (Perkel 2018). In teaching, Jupyter Notebooks are particularly well suited for interactive software guides. IPython widgets (GUI controls) can be used to execute code specifically on user input without having to modify the actual code. In this way, a graphical user interface can be created with little effort.

Input data

Kongsberg provides MBES data in the binary decoded ALL format. The individual sensor measurements (echo sounder, position system, motion sensor, etc.) are streamed to the output file as sequential datagrams. There are two different datagram types for both, bathymetry and backscatter data. For bathymetry, the choice is between the XYZ datagram and the raw range and angle datagram. The former includes the local Cartesian coordinates per beam computed in real time. Ship motion, sound velocity at the transducer face, and ray bending through the water column have already been corrected (Kongsberg 2018). The XYZ datagram was chosen for the first implementation, even though it disables corrections to the individual sensor data. The raw range and angle datagram could be integrated in a later stage.

For the backscatter, the choice was between the single value per beam reflectivity provided as part of the XYZ datagram or the beam time series written to the seabed image datagram. The single values are typically determined as some sort of average of the beam time series. This has the effect of discarding much of the original resolution. However, while the individual values are already georeferenced via the associated beam bathymetry, the individual beam time series samples must

be georeferenced via the swath bathymetry in an additional processing step. Since the resolution of the backscatter data is very important, the seabed image datagram is used.

For georeferencing, the position datagram is needed as well (Fig. 1). The three identified datagrams can be decoded using the PyALL module written and published on GitHub by Kennedy (2016). Afterwards, the bathymetry is transformed from local Cartesian ship coordinates to global geographic coordinates using the navigation information. Then, the beam time series backscatter data are georeferenced by interpolating between the bathymetry soundings. Subsequently, the bathymetry and backscatter data are available as point clouds in a global coordinate reference frame. As a next step, a semi-automatic filtering of the bathymetry point cloud and visual image corrections for the backscatter data follow.

Concept development

During concept development, a database approach was initially considered. As already discussed, the raw data are provided in different datagram types that have to be handled individually. However, the datagram timestamps are not always sequential because individual sensors sometimes output their measurements with a delay. For these types of tasks, a database-based approach offers an optimal solution. The basic idea is to store the data itself, the different processing stages, but also metadata and survey information across files in a project database. In this way, for example, a bathymetry sounding can be traced back through the processing to the original datagrams (XYZ and position). Likewise, it would be possible to query which soundings were measured in equidistant mode or to find all soundings between specific coordinates or dates.

However, during the database setup, it became clear that a complex database management was critical for both data integrity and processing performance. This phase proved to be extremely time consuming and there were only few exist-

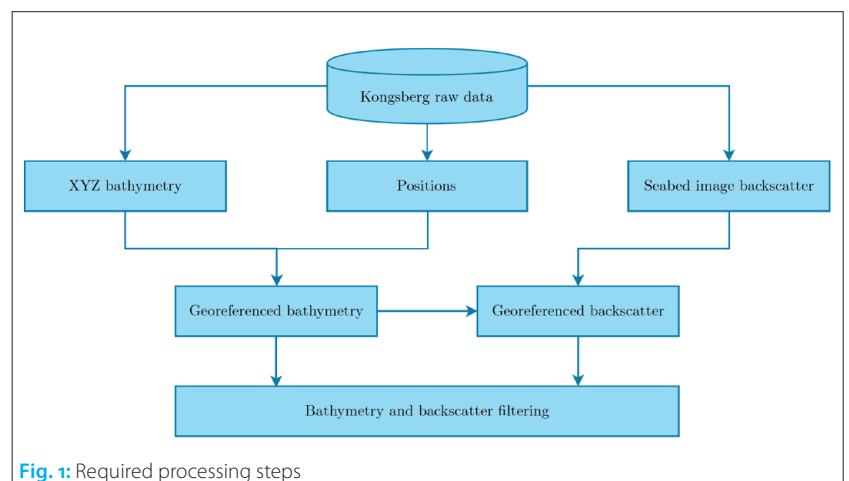


Fig. 1: Required processing steps

ing libraries that could have been effectively integrated. As a result, the approach failed in terms of performance. Firstly, performance in terms of the implementation itself, but also because the data volumes could not be handled without performance orientation.

The important lesson learned from the first approach was to move from an isolated monolithic approach based on a project database to a modular approach with less tightly coupled code. The individual modules must be specialised for processing large volumes of spatial data. In best case, the modules should come from established, open source libraries and may also come from performance-optimised programming languages such as C or C++ due to Python's ability to embed other languages.

With regard to the above criteria, a combination consisting of PDAL, Entwine and Potree was taken. PDAL (Point Data Abstraction Library) is a C++ based library for processing point clouds (PDAL Contributors 2020). The basic concept behind PDAL is the compilation of individual processing steps into pipelines. For example, spatial outlier filters can be assembled for bathymetry cleaning or attribute-based filters for backscatter correction. Entwine is a point cloud organisation software that uses an octree-based storage format (Hobu 2019). An octree is a tree data structure used for spatial indexing (Fig. 2). Individual points are indexed by incrementally dividing cuboids into eight child cuboids. Using a spatial index can speed up the processing of point clouds. The Entwine format can be read into PDAL pipelines and visualised in Potree. The latter is an interactive, WebGL-based point cloud renderer for large point clouds (Schütz 2020). It can be embedded in Jupyter Notebook, as it is also web-based and uses Entwine's Octree structure for efficient visualisation.

The compiled open source libraries are used to provide decoding of the identified datagrams from the raw Kongsberg data (PyALL) on the one hand,

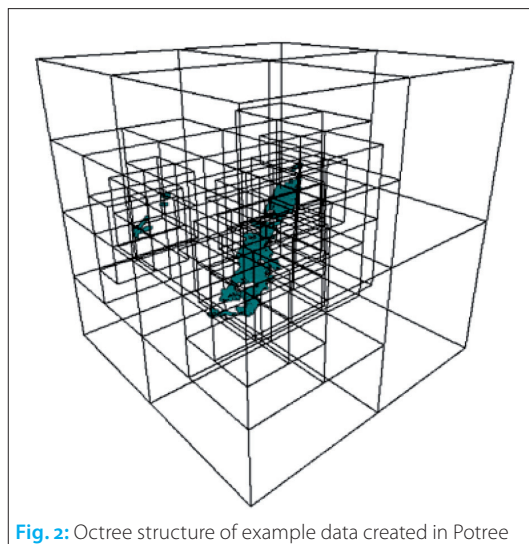


Fig. 2: Octree structure of example data created in Potree

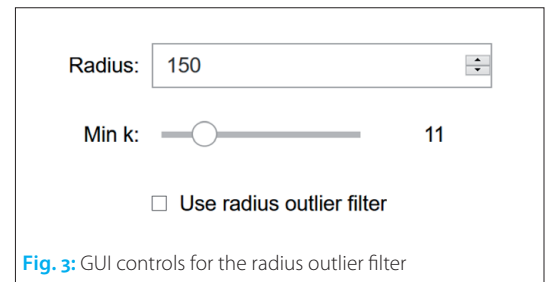


Fig. 3: GUI controls for the radius outlier filter

and bathymetry and backscatter point cloud filtering (PDAL, Entwine and Potree) on the other. To connect the two components, the raw data needs to be processed into point clouds by georeferencing. For this purpose, a separate Python module was written. The first step is to interpolate the ship positions to the ping timestamps. The heading is then used to transform the Cartesian coordinates of the individual soundings into the superior geographic coordinate system. For georeferencing the backscatter time series, the samples belonging to the bottom detection are identified. Since the georeferencing of the bottom detections is given by the bathymetry, the other samples can be georeferenced by rearranging the beam time series between the bottom detections and interpolating between the bottom detection samples.

As previously mentioned, no corrections are applied to the individual sensor data, which can significantly degrade the data quality. To address this problem, the processing was divided into two phases: First, a preprocessing Python module from raw Kongsberg data to point clouds. If any corrections would need to be applied, this step may be conducted within another software. The raw point clouds can then be imported as ASCII files and processed in a Jupyter Notebook in which they are further filtered to outlier-cleaned bathymetry and visually corrected backscatter. Thereby the filters can be configured via GUI controls. For the bathymetry outlier cleaning, a combination of a depth window filter, an extended local minimum (ELM) filter, a radius (Fig. 3) and a statistical outlier filter can be used. For the backscatter corrections, a constant offset or multiplier can be applied, a median absolute deviation (MAD) filter used for despeckling and Poisson sampling for anti-aliasing.

Results

To act in the spirit of open source, the tool has been released on the code hosting platform GitHub under the MIT license (Andree 2021). There is also a documentation/manual in the repository that provides a good overview if there is interest in the code itself and how to use it. For now, only the results of the bathymetry and backscatter processing are considered here. For evaluation, the grids created during the cruise from manually cleaned soundings and backscatter mosaics are taken.

The result of the bathymetry processing (Fig. 4)

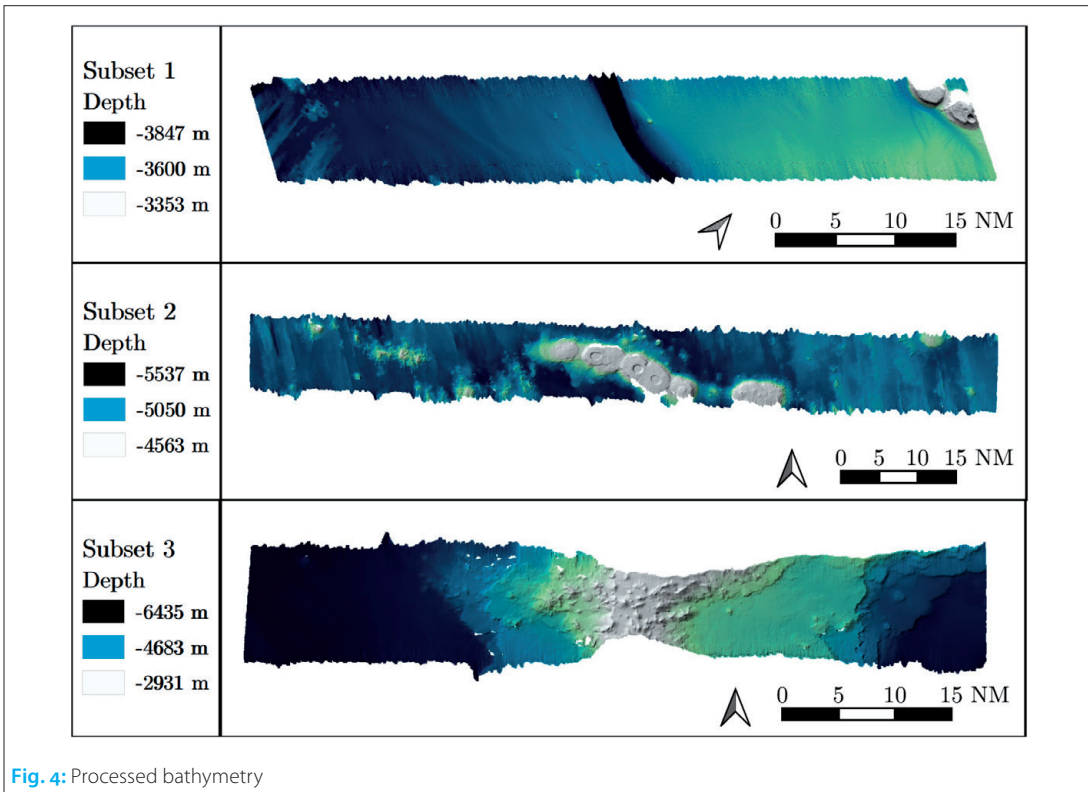


Fig. 4: Processed bathymetry

looks consistent. Most of the outliers could be filtered well except for areas where they accumulate. When compared to the on-board processed bathymetry (Fig. 5 and Fig. 6), two patterns were noted: There are clearly recognisable offsets around

bathymetric features and in the areas of the outer beams.

The pattern is seen in all analysed data subsets and appears to be related to the travel direction of the ship. At this point, it is not clear at which step

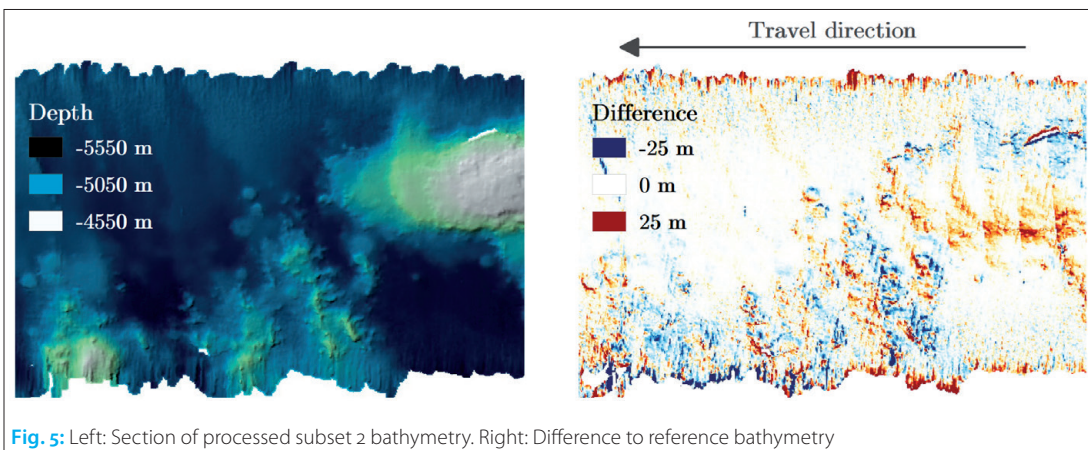


Fig. 5: Left: Section of processed subset 2 bathymetry. Right: Difference to reference bathymetry

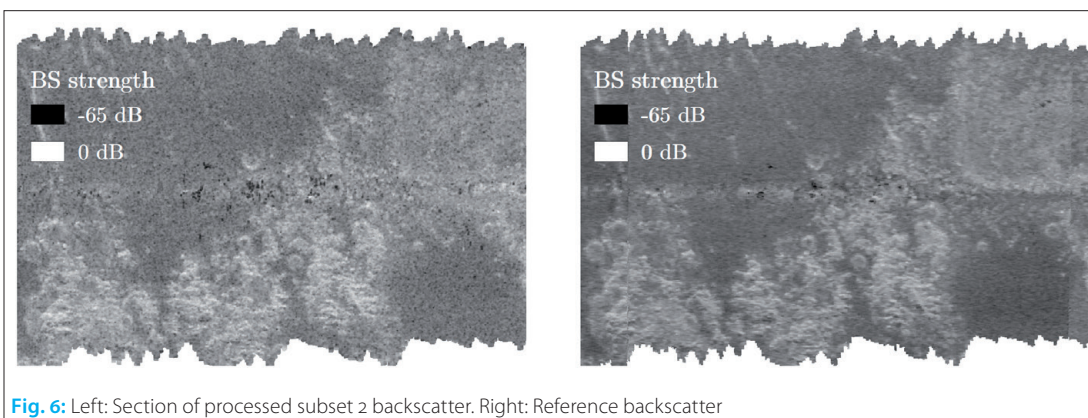


Fig. 6: Left: Section of processed subset 2 backscatter. Right: Reference backscatter

this deviation occurs. Presumably, it is due to a difference in preprocessing. Based on the correlation with the direction of travel, the cause can probably be narrowed down to a time or pitch offset. A possible pitch offset could be caused by a difference in the handling of the dual-swath mode. A time offset could result from a discrepancy in the definition of the exact measurement time or the position interpolation itself.

The georeferencing of the beam time series looks plausible and correctly represents bathymetric features. Since only visual and no comprehensive radiometric corrections were applied, strictly speaking the two data sets cannot be compared. Nevertheless, the visual corrections served their purpose (Fig. 6). In addition, the Kongsberg real-time corrections were found to give very pleasing results. Compared to the reference grid, it can be seen that the overall backscatter range is slightly different and that the result is more noisy and speckled with some remaining artefacts around the centre beam area.

Conclusion and outlook

The idea of this work was to develop a tool for processing bathymetry and backscatter data from Kongsberg EM series MBESs. This could be realised using freely available open source libraries. The advantages of the concept are the modular ap-

proach especially in terms of long-term maintainability and adaptability. The entire tool is purely open source and can therefore be used by anyone. By integrating C++ libraries, the performance requirements could be met.

The disadvantages of this approach are that interactivity comes at a high price in terms of complexity. GUI programming must be well thought out to avoid becoming clumsy. Also, Jupyter Notebook is not designed for pure GUI programming, as the code execution is very flexible. It is practical and fast for small programs but cannot be scaled up arbitrarily. Potentially, the dependence on existing libraries can also be disadvantageous since the functionality is so externally determined.

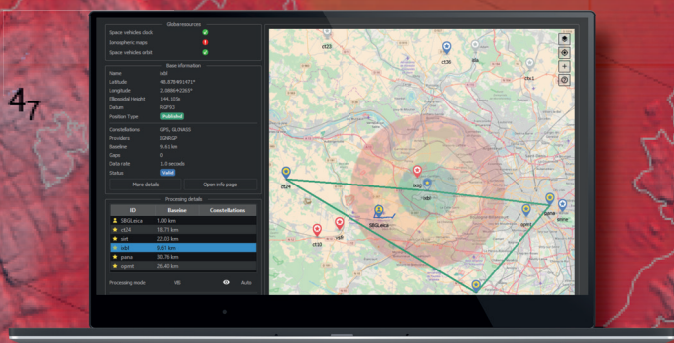
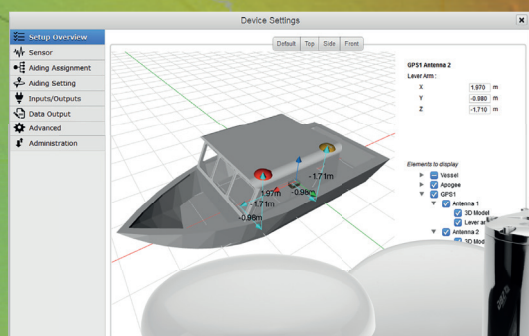
Overall, the use in teaching is advantageous in that the students work much closer to the raw data and have a closer contact to programming. In this context, it may also be useful to reduce the GUI programming. The tool that was developed in the course of this work can be understood as a rough framework, which can be optimised in the following. Important successive steps would be the identification and elimination of the position offset in the bathymetry. In addition, further filters for both bathymetry and backscatter can be added very easily. More profound improvements could be the integration of tide correction possibilities and navigation processing. //

References

- Andree, Sophie (2021): Interactive MBES processing. <https://github.com/SophieHCU/Interactive-MBES-processing>
- Carbannelle, Pierre (2020): PYPL. Popularity of Programming Language index. <https://pypl.github.io/PYPL.html>
- Hobu, Inc. (2019): Entwine. Version 2.1. <https://github.com/connormanning/entwine>
- Kennedy, Paul (2016): PyALL. Version 1.50. <https://github.com/pktrigg/pyall>
- Kinne, Stefan; Annika Jahnke et al. (2019): MICRO-FATE – Characterization of the fate and effects of microplastic particles between hotspots and remote regions in the Pacific Ocean, MORE-2 – Measuring Ocean REferences (of aerosol, clouds and trace-gases for evaluations of satellite retrievals and model simulations) – part 2. SONNE-Berichte, Cruise SO268-3, 30.05.2019–05.07.2019, Vancouver–Singapore
- Kongsberg (2018): EM Series. Multibeam echo sounders. Datagram formats
- PDAL Contributors (2020): PDAL. Point Data Abstraction Library. Version 2.2.0. <https://github.com/PDAL/PDAL>
- Perkel, Jeffrey M. (2018): Why Jupyter is data scientists' computational notebook of choice. Nature, DOI: 10.1038/d41586-018-07196-1
- Schütz, Markus (2020): Potree. Version 1.7. <https://github.com/potree/potree>
- van Rossum, Guido; Fred L. Drake (2003): An introduction to Python. Release 2.2.2. Network Theory Ltd.

Making Hydrographers' Tasks Easier

Courtesy of CADDEN



Navsight Marine Solution

State-of-the-art Motion & Navigation Solution

Qinertia

The Next Generation INS/GNSS Post-processing Software

OFFICIAL DISTRIBUTOR

MacArtney
UNDERWATER TECHNOLOGY

MacArtney Germany GmbH

Wischhofstrasse 1-3
Geb. 11
D-24148 Kiel
Germany

Phone: +49 431 535500 70
Email: hydro@macartney.com
Web: www.macartney.de



Comparison of different sub-bottom profiling systems to be used in very shallow and tide-influenced areas

A case study in the backbarrier tidal flat of Norderney, Germany

An article by CIGDEM ASKAR

Shallow waters are the transition zones between land and sea where human activities are dominant, such as building infrastructures and oil digging. Therefore, there is always a great interest in the stratigraphy of the sub-bottom in shallow waters. However, working in shallow waters is more complex than deep waters. Various seismic methods are used in subseafloor investigations, such as sparkers and air guns. Yet, these methods operate generally towed behind the vessel, which becomes challenging in very shallow waters. On the other hand, sub-bottom profilers operate mounted on the vessel; hence, more suitable for shallow waters. This article summarises findings from the Master Thesis that compared three sub-bottom profilers in very shallow and tide-influenced areas in the German Wadden Sea. The study was completed during an internship at the NLWKN Forschungsstelle Küste (FSK) Norderney.

sub-bottom profiler | shallow water | tidal flats | chirp SBP | parametric SBP
Sedimentecholot | Flachwasser | Watt | CHIRP-SBP | parametrisches Sedimentecholot

Flache Gewässer bilden die Übergangszone zwischen Land und Meer, wo menschliche Aktivitäten dominieren, wie z. B. der Bau von Infrastrukturen und Ölbohrungen. Daher besteht ein großes Interesse an der Stratigraphie in flachen Gewässern. Allerdings ist die Arbeit in flachen Gewässern komplexer als in tiefen Gewässern. Bei der Untersuchung des Bodenaufbaus werden verschiedene seismische Methoden eingesetzt, wie z. B. Sparker und Airguns. Diese Geräte werden jedoch in der Regel hinter dem Schiff geschleppt, was in sehr flachen Gewässern zu einer Herausforderung wird. Dahingegen arbeiten Sedimentecholote vom Schiff aus und sind daher für flache Gewässer besser geeignet. Dieser Artikel fasst die Ergebnisse einer Masterarbeit zusammen, in der drei Sedimentecholote in sehr flachen und tidebeeinflussten Gebieten im deutschen Wattenmeer verglichen wurden. Die Studie wurde während eines Praktikums beim NLWKN Forschungsstelle Küste (FSK) Norderney durchgeführt.

Author

Cigdem Askar is Research Assistant at HafenCity University in Hamburg.

cigdem.askar@hcu-hamburg.de

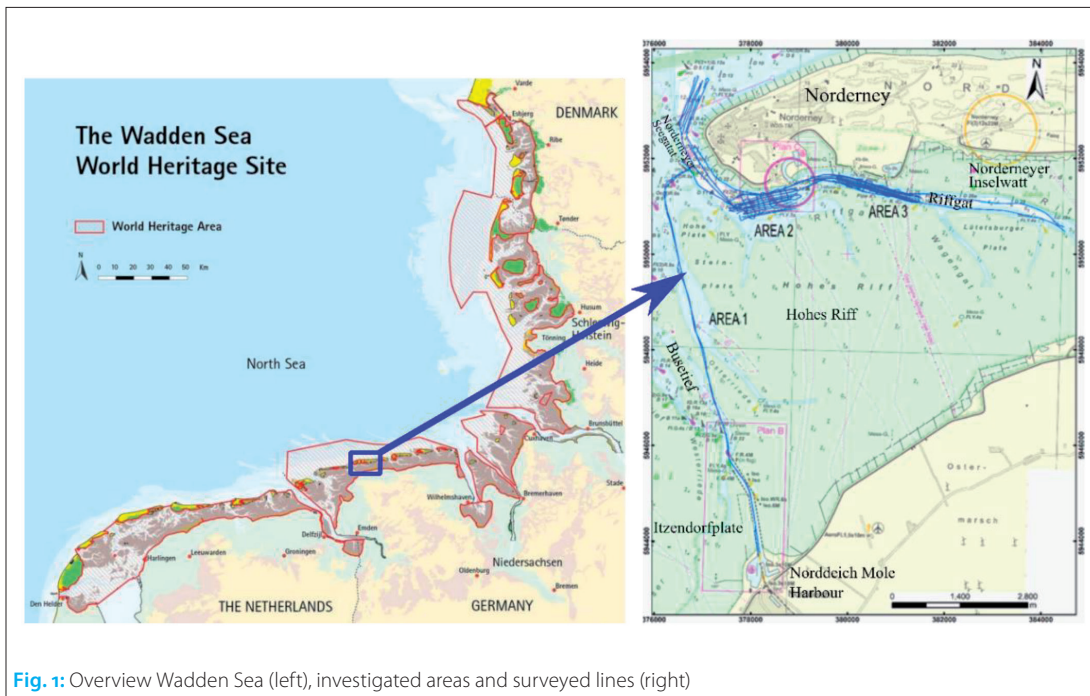
Introduction

The challenge of shallow water surveys is their dynamic environment. Fierce wave actions, strong currents, shallow water depths, and a large tidal range are some factors that induce technological problems in shallow waters (Missiaen et al. 2018). The Wadden Sea is an example of such areas, an intertidal zone that extends along the south-eastern part of the North Sea and covers approximately 10,000 km² between the Frisian Islands and the coast of the Netherlands, the German Bight, and the Danish coast. The Wadden Sea system consists of large tidal flats, tidal gullies, inlets and sandy barrier islands (Hofstede 2005). Varying tidal ranges and meteorological circumstances work continuously on its geomorphology. While not all

acoustic sub-bottom investigation methods are well suited for such environments, sub-bottom profiling works well.

Sub-bottom profiling is an acoustic technique used for investigating the characteristics of the seabed and the sub-surface layers and detecting buried objects, e.g. pipes or archaeological remnants. The method is similar to a single-beam echo sounder (SBES). An acoustic signal is vertically sent into water, then the echoes, which are reflected (not the backscattering) from the seabed and sub-surfaces, are recorded. Compared to SBESs, which operate at frequencies from 12 kHz up to 200 to 400 kHz, sub-bottom profilers (SBP) work at lower frequencies up to 10 kHz (Lurton 2010).

Parametric and chirp systems are commonly



Source: Common Wadden Sea Secretariat, CWSS, 2017

Fig. 1: Overview Wadden Sea (left), investigated areas and surveyed lines (right)

used SBPs. The parametric SBP uses a nonlinear concept, the so-called parametric array, which produces the desired frequency using the nonlinearity in the medium. It sends two slightly different high frequencies (primary frequencies) into the water under high sound pressure. Due to the medium's nonlinearity, new frequencies (secondary frequencies) are generated, such as difference and sum. The difference is the low frequency used in parametric systems and can penetrate deeper into the seafloor while keeping the low horizontal resolution of the high primary frequencies. The chirp SBP transmits chirp signals, wide-band, frequency-modulated (FM) signals that sweep a wide range of frequencies, mostly varying from 2 to 20 kHz. Upon reception, chirp signals are correlated with a copy of the transmitted signal, and the envelope of the correlation's output is detected (Lurton 2010). This process is called pulse compression, which refers to producing a temporal response narrower than the received signal's duration by matched filtering (Abraham 2017). The vertical resolution depends on the output pulse width of this process rather than the received echo width.

This thesis compared three sub-bottom profilers, Echoes 10000 (iXblue), SES-2000 Quattro (Innomar) and Topas PS 120 (Kongsberg). Table 1 summarises specifications of each instrument.

Data acquisition and processing

The data was collected between March and May 2019 in cooperation with the FSK, which also provided this study with the supplementary data, like sediment cores, grab samples, bathymetric and backscatter data sets. The investigated region consisted of three different areas (Fig. 1) in the German Wadden Sea's Norderney tidal inlet. Area 1 had a very shallow water depth of less than 10 m. The seabed was covered mainly by coarser sediment or showed an irregular surface in parts due to some marine organisms. The sub-seabed here had alternating layers of marine and terrigenous sediments. The peat layers were one of the frequent deposits. Area 2 was located at the Riffgat channel entrance, close to the open sea and affected by strong tidal currents, waves and wind. Therefore, the sub-bottom consisted of a very compact glacial Pleistocene base under a very thin recently accumulated sediment, and coarser sediments covered the seabed. Area 3 had an irregular seabed due to the tide-induced ripples and high dunes along with coarse sediments. Also, the sub-bottom comprised a homogenous type of deposits in this area.

The instruments were not used simultaneously but on different dates due to the planning with other parties. The systems were pole mounted

Instrument	Manufacturer	System	Pulse form	Operating/secondary frequency	Primary frequencies	Vertical resolution
Echoes 10000	iXblue	Chirp	Chirp	5–15 kHz	–	8 cm
SES-2000 Quattro	Innomar	Parametric	Ricker, CW	4, 5, 6, 8, 10, 12 kHz	85–115 kHz	up to 5 cm
Topas PS 120	Kongsberg	Parametric	Ricker, Chirp, CW	2–30 kHz	70–10 kHz	less than 5 cm

Table 1: Instruments' specifications

on the port side of the vessel, MS *Burchana*. The same motion sensor and dual-antenna positioning system provided motion and navigation data. For a better comparison, the acquisition parameters were kept as constant as possible. Since the region experiences semi-diurnal tides, surveys were performed during both high tides and low tides. The wind mainly was strong on the survey days due to the season. As a result of the wind and tidal currents, the vessel speed changed from 5 knots to 7 to 7.5 knots, although the intention was to keep it less than 5 knots.

The data was post-processed with the Delph Seismic Interpretation software from iXblue. The sound velocity was applied as constant 1,500 m/s, and the tide was corrected. Furthermore, a matched filter was applied to the Echoes 10000 data while a bandpass filter was applied to the Topas PS 120 data. No filter was applied to the

SES-2000 Quattro data. The absorption loss was balanced by applying some gain during processing. Lastly, the data was heave corrected, if not corrected during the acquisition, and backscatters from the water column were removed.

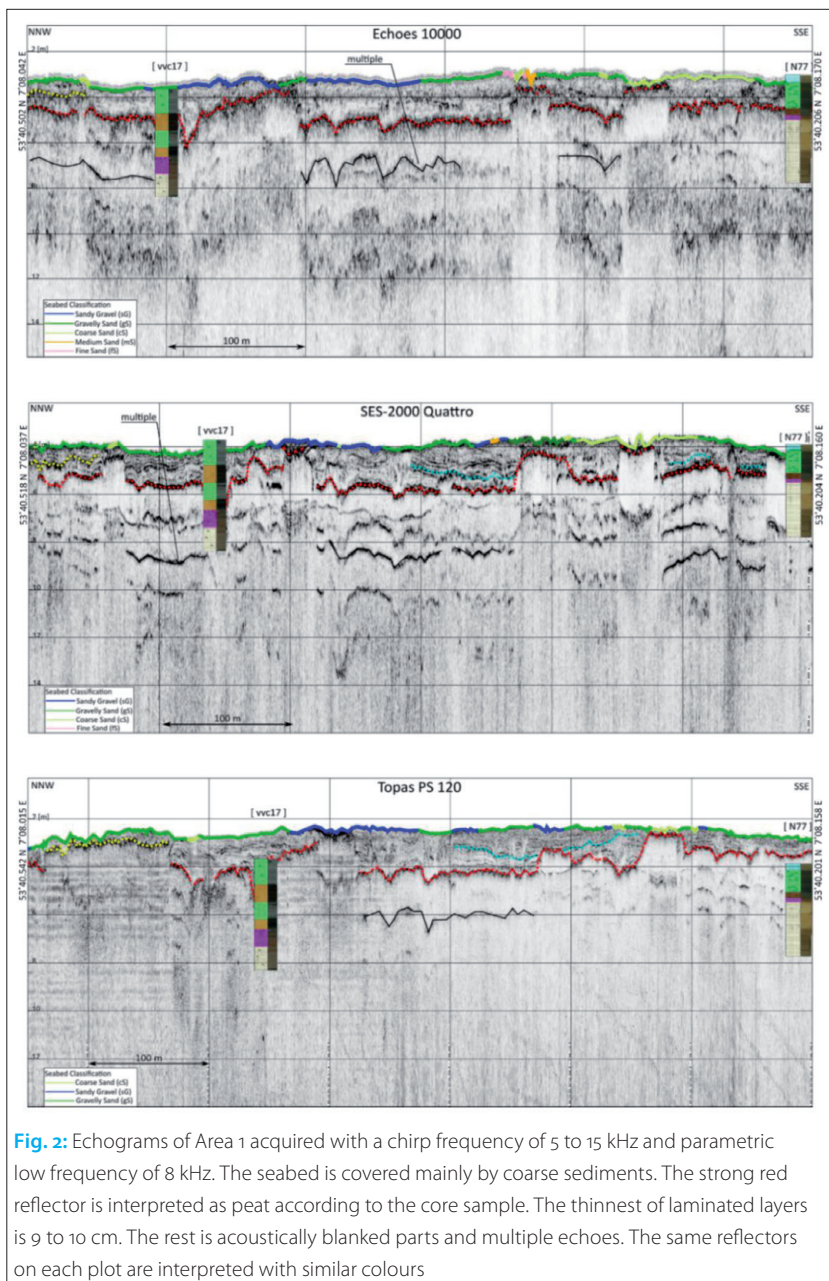
Each system's data was evaluated against the specialities of the surveyed areas concerning systems' technique by focusing on the penetration depths, visual quality of the plots and vertical resolution. The FSK mainly conducts surveys for geophysical investigations, which demands deeper penetration capacity with sufficient resolution. Therefore, penetration capability was an important criterion in comparison. On the other hand, the sub-bottom profiler data interpretation is not fully automated yet and demands quite a lot of time. Hence, the final image's visual quality is of importance for an effortless interpretation and was another essential criterion of the comparison. Besides, there is a constant sedimentation cycle and transport in the Wadden Sea, resulting in changes in the tidal channel and creeks. These events happen both in the noticeably short and long term. A good vertical resolution, therefore, is paramount to trace these events over time.

Results

In Area 1 (< 10 m, coarse sediment), the systems achieved a maximum penetration of 2 to 4 m; yet, it was sometimes not exceeding 0.5 m (Fig. 2). Beneath these depths, there were transparent zones and multiples on the echo plots. Partly, there were laminated reflectors, the thinnest of which was measured as 9 to 10 cm. Visually, the echo plots from the parametric systems SES-2000 Quattro and Topas PS 120 demonstrated slightly better performance, especially in displaying thinly layered sediments.

In Area 2 (compact sub-bottom sediments topped by a thin layer of Holocene sediments), the average penetration depth was around 3 to 4 m in the deep channel for all systems (Fig. 3). In the shallow part, an old channel and fillings were visible on the plots. Here, the penetration was slightly deeper than in the channel centre, about 5 m, marking the old channel bed. SES-2000 Quattro penetrated slightly deeper, approximately 7 m below the seabed. The vertical resolution was 8 cm for each system. Visually, reflectors on the Echoes 10000 and Topas PS 120 were in parts weak that needed more effort to interpret. However, Echoes 10000 provided a good result in the very shallow tidal flat, considering it is a chirp system.

In Area 3 (homogeneous sediments, sand dunes and ripples), while the systems reached only down to 1 m from the seabed in the channel (Fig. 4), the penetration was around 3 m on the flanks. The Echoes 10000 and SES-2000 Quattro achieved similar penetrations along the longitudinal survey lines, while the Topas PS 120 displayed slightly fewer re-



flectors. However, the SES-2000 Quattro provided slightly better visualisation of the reflectors than the Echoes 10000. Also, the SES-2000 Quattro's performance along the transversal survey lines was moderately ahead of the Echoes 10000 and Topas PS 120 regarding penetration and visualisation of the reflectors. In Area 3, the ripples and the coarse sediment cover on the seabed blocked the systems' penetration of the seabed in the northern part of the channel.

Discussion

In Area 1, the systems were affected by the gaseous peat deposits, very shallow water depths and coarser sediments on the seabed. Peat is made of organic matters (such as mosses, grasses, shrubs), which do not entirely decompose due to water excess (Bozkurt et al. 2001). During the Wadden Sea region's transgression times, the barrier and tidal inlet system advanced landward, which resulted in flooding and subsiding of the peat areas due to the high-water content. Increased space of the inlet system led to an increase in the tidal prism, resulting in further subsiding of the peat areas due to the heavy deposits of clay brought by storms (Vos and Knol 2015). As a result of alternating transgressions and regressions, there are multiple peat layers in Area 1. In shallow water deposits, gas primarily results from the biogenic decomposition of organic matter (Floodgate and Judd 1992). The gaseous sediments are easily detected in the acoustic data because of their distinctive reflections. Higher acoustic and elastic contrast than the surrounding non-gaseous medium characterise gas-bearing deposits (Jaśniewicz et al. 2019). The gaseous sediments attenuate most acoustic energy and prevent further penetration; hence strong reflectors with a transparent zone underneath mark these sediments.

Besides the gaseous sediments, very shallow water depths affected the systems. Caused by the shallow water depths, multiples led to problems in interpreting the sub-bottom structures (Hung et al. 2010). Lastly, the seabed characterisation in Area 1 is attributed to another factor for limited penetration. On the echo plots, the first strong reflection represents the seabed where the acoustic impedance differs in the water-sediment border, and bottom sediments strongly affect the penetration depth (Hurtado et al. 2013). After most acoustic energy is reflected and scattered on the surface, the rest will penetrate the seabed. Jones et al. (2017) state that tens of metres of penetration in soft sediments will severely diminish within sand or rock in parametric systems. In chirp systems, the penetration might be as low as 3 m within coarse sediments. In contrast, it can be up to 200 m in soft sediments (Jones et al. 2017), depending on the water depth. Coarse sediments cause stronger scattering than the finer sediments

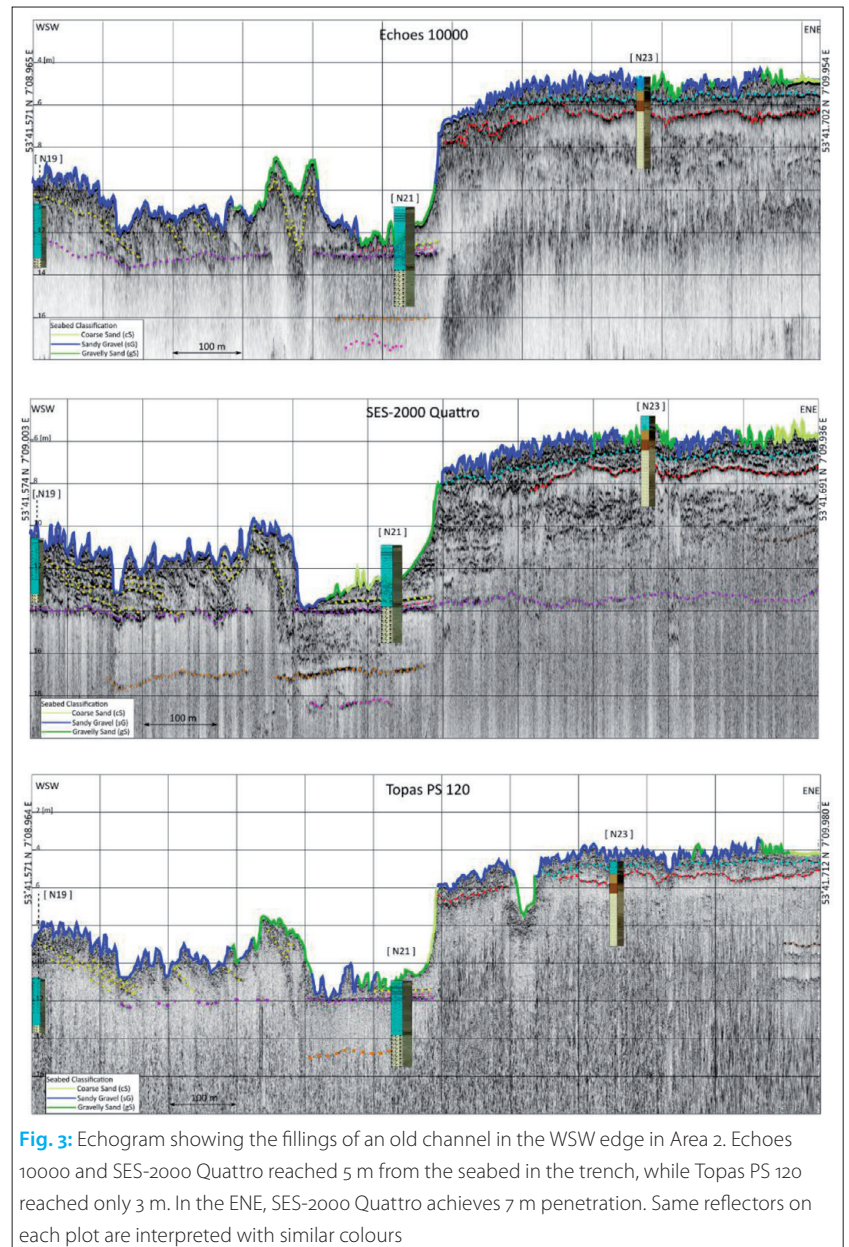


Fig. 3: Echogram showing the fillings of an old channel in the WSW edge in Area 2. Echoes 10000 and SES-2000 Quattro reached 5 m from the seabed in the trench, while Topas PS 120 reached only 3 m. In the ENE, SES-2000 Quattro achieves 7 m penetration. Same reflectors on each plot are interpreted with similar colours

due to their bigger grain size; hence, less signal penetrates through the medium. Some marine species, like *Lanice conchilega* in Area 1, increases seabed roughness, which results in higher scattering of the acoustic energy.

In Area 2, the systems performed on a very compact seabed covered by coarse sediments in the channel and shallow water depths with peat deposits in the tidal flats. The Holocene deposits in the channel of Area 2 are scoured out due to the strong currents in the Riffgat channel's mouth. Hence, the sub-bottom layers are very compact. As stated in McGee (1995), consolidated sediments demonstrate strong scattering and lessen the seabed acoustic signal penetration. Besides the packed bottom, coarser sediments on the seabed also increased the scattering, and less energy is transmitted to the seabed. In the southern part of the area, where there was a thicker Holocene deposit, the systems performed better. However,

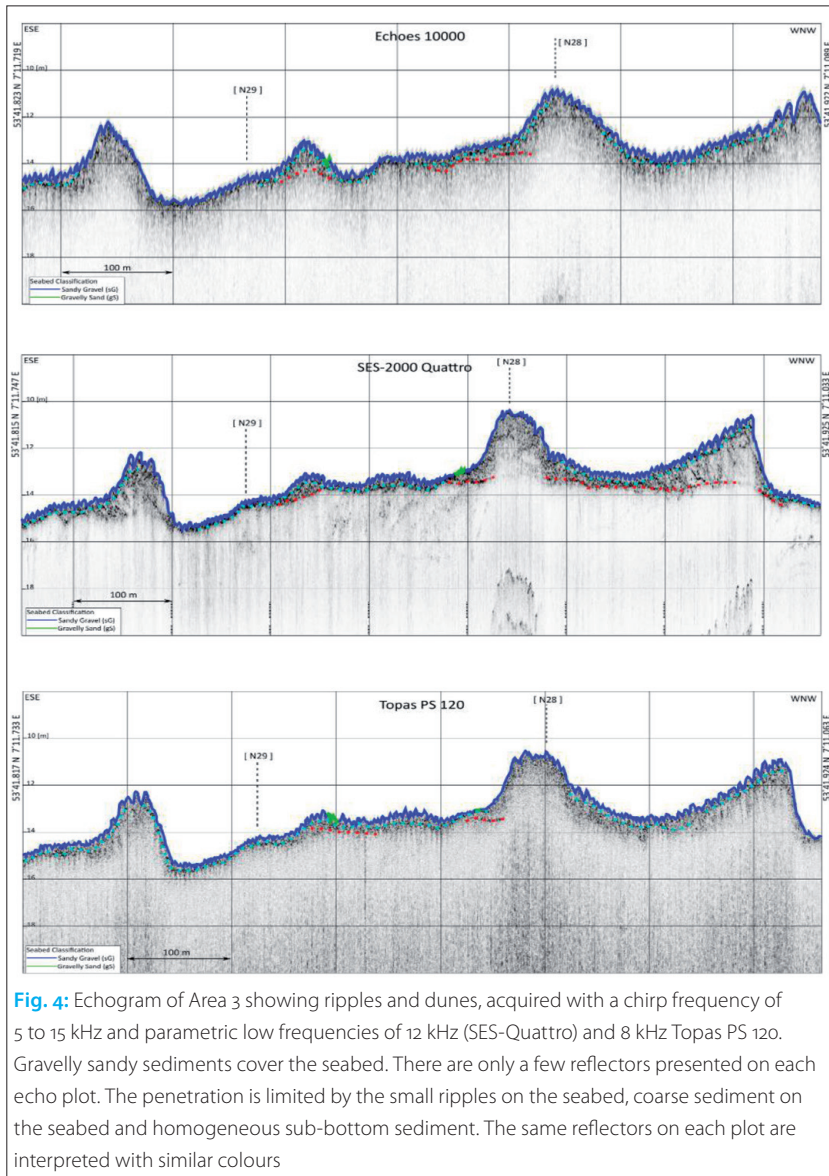


Fig. 4: Echogram of Area 3 showing ripples and dunes, acquired with a chirp frequency of 5 to 15 kHz and parametric low frequencies of 12 kHz (SES-Quattro) and 8 kHz Topas PS 120. Gravelly sandy sediments cover the seabed. There are only a few reflectors presented on each echo plot. The penetration is limited by the small ripples on the seabed, coarse sediment on the seabed and homogeneous sub-bottom sediment. The same reflectors on each plot are interpreted with similar colours

penetration was affected by the shallow waters in the tidal flats and the peat deposits.

In Area 3, irregular seabed with ripples and high dunes, the coarse sediment cover and the homogeneous type of sub-bottom deposits impact the systems' performance. Rough surfaces spread the scattering in all directions while strongly attenuating the specular reflection (Lurton 2010). The increased scattering results in less energy transmitted into the sub-bottom. Besides that, the core samples suggest a homogenous type of sediment for the upper few metres, which means no change in the acoustic impedance. Therefore, no strong reflection is recorded until the signal encounters a border between mediums of different densities.

Conclusion

These results showed that shallow waters, especially areas under tide influence, are challenging to work with. Each system used in the study promised a reliable performance according to their specifications; although, they were affected

by the surveyed areas' complex settings. The systems' capabilities in achieving deeper penetrations, visual representations of reflectors and the vertical resolution, performances in revealing thin layers of sediments were the main criteria in the comparison.

The parametric SES-2000 Quattro provided better penetration capability while maintaining a good resolution. The parametric Topas PS 120 and chirp system Echoes 10000 performed similarly in the penetration they achieved. The visual representation of reflectors on Echoes 10000 was weaker than on the parametric SES-2000 Quattro, whereas the parametric Topas PS 120 also provided a weak visualisation. This, for Echoes 10000, arose from the used power levels, which were preferred in order not to cause reverberation in the shallow environment of the study area. It operated at a lower transmission power level (1 to 3 ms pulses at 10 to 20 % power level) compared to its optimal configuration (~10 ms pulse at 50 to 70 % power level). For Topas PS 120, it is attributed to the higher vessel speed, which was higher than the suggested speed, 3 to 5 knots, as stated in the instrument manual. Regarding the vertical resolution, all systems performed well due to the narrow beam pattern of parametric systems and the chirp system's broad frequency range. The thinnest layers displayed by each profiler were as thin as 7 to 8 cm.

Besides their performances, the setup and the handling of the software during data acquisition/processing were straightforward for all systems. The user guides thoroughly explain the steps of installation, data collection and processing, and sub-bottom profiling technique. There was no interruption during the surveys that stemmed from system malfunctions. Also, the transducers' compact sizes make them handy for operating in shallow waters; however, one has to be careful in waters shallower than 3 m, especially in the presence of strong currents, not to run aground with the system on the pole. //

Acknowledgements

I would like to express my sincere gratitude to my examiners Prof. Dr.-Ing. Harald Sternberg (HafenCity University) and Dr. Francesco Mascioli (the FSK) for their support. I want to thank Tina Kunde (the FSK) for guiding me tirelessly throughout my internship and thesis process and Tanja Dufek (HafenCity University) for helping me to get this internship. I would like to thank the MS *Burchana* team, Captain Hugo Martens and the crew members Jens Voß, Winfried Bruns and Alexander Heidenreich. Lastly, my sincere thanks to Innomar and iXblue for supporting me and my thesis by providing their survey instruments. Particularly, my sincere thanks to Jens Lowag from Innomar and Philippe Alain from iXblue for their participation and guidance in surveys and sharing their knowledge.

References

Abraham, D. A. (2017): Signal Processing. In: Leif Bjørnø, Thomas Neighbors, David Bradley (Eds.): Applied Underwater Acoustics. Elsevier, pp. 743–807

Bozkurt, Sila; Marco Lucisano et al. (2001): Peat as a Potential Analogue for the Long-term Evolution in Landfills. Earth-Science Reviews, DOI: 10.1016/S0012-8252(00)00036-2

CWSS (2017): Wadden Sea Quality Status Report. Common Wadden Sea Secretariat (CWSS). <https://qsr.waddensea-worldheritage.org/reports/introduction>

Floodgate, George D.; Judd, Alan G. (1992): The Origins of Shallow Gas. Continental Shelf Research, DOI: 10.1016/0278-4343(92)90075-u

Hofstede, Jacobus (2005): Danish–German–Dutch Wadden Environments. In: Eduard A. Koster (Ed.): The Physical Geography of Western Europe. Oxford University Press, pp. 185–205

Hung, Barry; Kunlun Yang at al. (2010): Shallow Water Demultiple. ASEG Extended Abstracts, DOI: 10.1081/22020586.2010.12041899

Hurtado, O. Z.; T. Missiaen et al. (2013): SeArch – Archaeological Heritage in the North Sea – Comparative Review of Techniques WP 1.1.5. www.sea-arch.be/sites/sea-arch.be/files/public/docs/resultaten/Algemeen%20overzicht%20technieken_WP1.1.5.pdf

Jaśniewicz, Damian; Zygmunt Klusek et al. (2019): Acoustic Investigations of Shallow Gas in the Southern Baltic Sea (Polish Exclusive Economic Zone) – A review. Geo-Marine Letters, DOI: 10.1007/s00367-018-0555-5

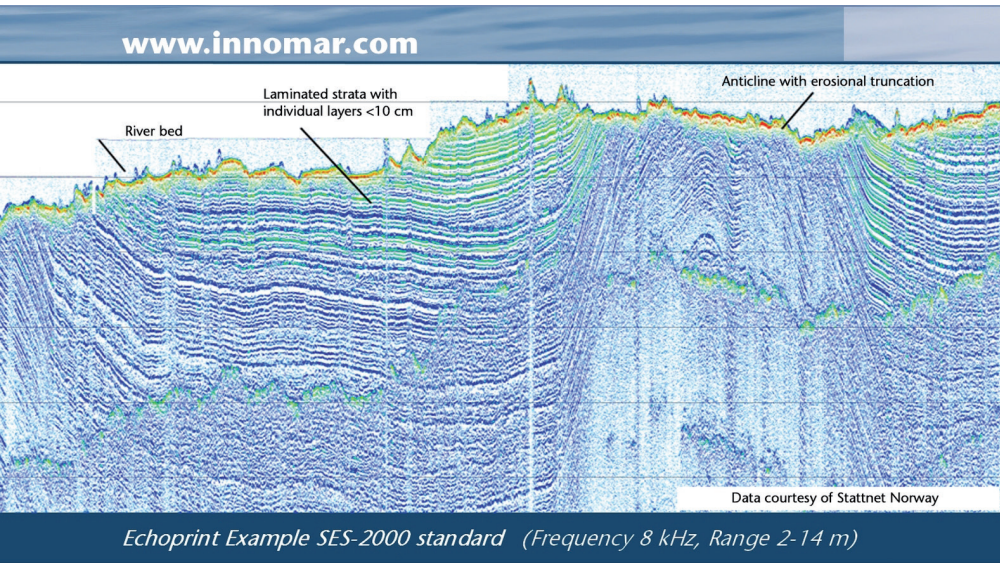
Jones, G. E.; Victor J. Abbott et al. (2017): Acoustic Seabed Survey Methods, Analysis and Applications. In: R. J. Uncles, S. B. Mitchell (Eds.): Estuarine and Coastal Hydrography and Sediment Transport. Cambridge University Press, pp. 54–91, DOI: 10.1017/9781139644426.004

Lurton, Xavier (2010): An Introduction to Underwater Acoustics: Principles and Applications. Springer

McGee, Thomas M. (1995): High-resolution Marine Reflection Profiling for Engineering and Environmental Purposes. Part A: Acquiring Analogue Seismic Signals. Journal of Applied Geophysics, DOI: 10.1016/0926-9851(95)90046-2

Missiaen, Tine; Dimitris Evangelinos et al. (2018): Archaeological Prospection of the Nearshore and Intertidal Area Using Ultra-High Resolution Marine Acoustic Techniques: Results from a Test Study on the Belgian Coast at Ostend-Raversijde. Geoarchaeology, DOI: 10.1002/gea.21656

Vos, Peter C.; Egge Knol (2015). Holocene Landscape Reconstruction of the Wadden Sea Area Between Marsdiep and Weser. Netherlands Journal of Geosciences – Geologie En Mijnbouw, DOI: 10.1017/njg.2015.4



Echoprint Example SES-2000 standard (Frequency 8 kHz, Range 2-14 m)



SES-2000 Parametric Sub-Bottom Profilers

Discover sub-seafloor structures and embedded objects with excellent resolution and determine exact water depth

- ▶ Different systems for shallow and deep water operation available
- ▶ Menu selectable frequency and pulse width
- ▶ Two-channel receiver for primary and secondary frequencies
- ▶ Narrow sound beam for all frequencies
- ▶ Sediment penetration up to 200m (SES-2000 deep)
- ▶ User-friendly data acquisition and post-processing software
- ▶ Portable system components allow fast and easy mob/demob
- ▶ Optional sidescan extension for shallow-water systems



Meeting requirements for new types of on-demand survey campaigns

An article by *ANDRES NICOLA and DANIEL ESSER*

In March 2021, the newly founded Nicola Offshore GmbH started its work. The company specialises in services for marine survey campaigns. The fast workboats of the partner ProMarine BV guarantee the shortest transit times to the site. This means that the orders can be completed quickly.

Nicola Offshore | workboat | offshore wind farm | UXO
Nicola Offshore | Arbeitsboot | Offshore-Windpark | Kampfmittelaltlasten

Im März 2021 hat die neu gegründete Nicola Offshore GmbH ihre Arbeit aufgenommen. Das Unternehmen ist auf Dienstleistungen für maritime Vermessungskampagnen spezialisiert. Die schnellen Arbeitsboote des Partners ProMarine BV garantieren kürzeste Transitzeiten zum Einsatzort. So können die Aufträge rasch erledigt werden.

Authors

Andres Nicola and Daniel Esser are Managing Directors of Nicola Offshore in Halstenbek.

a.nicola@nicola-offshore.com

We are all well aware that hydrography is a technical process requiring highly trained professionals operating complex, expensive equipment with a common goal: to measure what lies below the surface of the water for industrial, commercial and scientific purposes. We can create high-resolution maps of the seafloor to centimetre accuracy, quantify rates of erosion around underwater infrastructure and pinpoint the smallest hazards or features on the seafloor.

With the ability to capture such precise data efficiently and from diverse environments, the subsea survey industry in Germany and globally is well-positioned to guide energy and marine construction companies to develop infrastructure projects that are both safe and sustainable. New technologies and cloud-based workflow innovations continue to provide an even stronger foundation for improvements in data and finished product quality.

The survey industry is an essential and well-oiled machine, certainly. But as the expansion of offshore renewable energy continues globally, there are still some areas that the industry is playing catch-up. This is most noticeable in how marine contractors and survey companies optimise their services for offshore working, especially for projects where the actual survey time is minimal, but the time it takes to organise and transit to site is anything but.

While not new applications at all, there are certain types of survey jobs that are becoming more commonplace because of the upturn in the construction of offshore wind farms, which over the last two decades have seen a steady increase in the distance from shore, with new installations regularly happening between 30 to 40 kilometres out.

In just 20 years, the average distance from shore of a wind farm has increased circa 700 % and be-

cause of this, the transit time and cost of service vessels has become a major consideration in relation to the wind farm operations and maintenance (O&M) budget.

It's also why new, Hamburg-based marine survey company Nicola Offshore has chosen to provide specialist survey services with focus on using fast workboats as an operational platform. The company, which opened for business in March 2021 and has already completed multiple contracts, was founded by Nicola Engineering GmbH, a German marine survey company operating for 50 years, and ProMarine BV, a highly regarded Dutch manufacturer of fast workboats.

The founders formed Nicola Offshore to act like an »emergency responder« for organisations needing fast access to expert offshore survey capabilities. With support from exclusive hydroacoustic technology partner Subsea Europe Services GmbH, Nicola Offshore has placed the spotlight on its capabilities for specific survey types that are becoming more in demand in the North Sea and Baltic sea as new wind farms are built or existing installations expanded.

Specialist survey services

Pre and post dredging reports and cable depth surveys are of course a staple of its work with offshore contractors and energy companies, but Nicola Offshore also specialises in object search and surveys covering very specific targets. This comes from the growing number of incidents during offshore construction when tools, equipment or components are lost over the side of workboats. If the lost item is integral to the project, it can cause significant delays and non-productive time of assets mounts up quickly. Checking data anomalies prior to starting a project also falls into this category.

Unexploded ordnance, aka UXO, is another key work stream for Nicola Offshore. UXO is a very real issue as more infrastructure gets built offshore in northern Europe. There are an estimated 1.6 million tons of conventional UXO still on the seafloor of the North Sea and Baltic Sea region, which is causing significant issues for Germany's expanding offshore wind ambitions.

UXO already creates challenges within the tourism industry, with many WWII relics known to be close to busy tourist areas. These need to be detected and cleaned to ensure safety, especially for larger cruise ships with thousands of people on board. Nicola Offshore's sister company Nicola Engineering has been heavily involved in this activity and is now providing a foundation of expertise for similar work, only further offshore at new wind farm locations.

While the Nicola Offshore team – which has already grown to 17 marine survey experts and support staff – will use AUV and/or ROV systems when appropriate, the company has introduced innovative vessel systems to ensure safety and performance on UXO jobs. Operating on a no-risk policy and leveraging the appropriate technologies, Nicola Offshore is employing cutting-edge new solutions, such as a unique UXO detection frame, on its vessel *Nautical Explorer* (Fig. 1).



Fig. 1: Workboat *Nautical Explorer*

projects and collect high-quality data while meeting strict deadlines, often under extreme offshore conditions. And with transit times to the survey site being much shorter due to the speed of Nicola Offshore's survey boats, costs can be lowered.

A job that may require a day's transit to the site, a day on site and a day travelling back to port for a standard survey vessel can easily be completed in a single day, with a faster vessel. *Nautical Explorer* for instance, can cover 30 kilometres in less than 30 minutes, with its top speed of 44 knots. It's a simple approach, but as it is already permanently fitted with a high-performance multibeam package, Nicola Offshore can be on site next day and, in many cases, even have the needed data in the client's hand on the same day.

The benefits to the efficiency of offshore wind construction projects are very clear. Should an issue halt work, the assets and professionals in place could get back to work much sooner if the data needed to overcome an issue can be delivered quickly.

The concept of agility that drives Nicola Offshore is already proven. The partners saw the rise in demand for unplanned, short surveys with long transit times growing and together they completed several successful »on-demand« campaigns in 2020. This ultimately led to Nicola Offshore opening as a full-time provider of agile survey services for offshore oil & gas installations and wind farms.

Close cooperation with Offshore Energy companies, vessel providers and technology leaders is helping the new firm to achieve the best results based on the latest technologies and professionally educated staff, while at the same time respecting the fragile marine environment, preventing pollution and committing to continuous improvement in order to increase efficiency.

Nicola Offshore has started its business in its home market, the North- and Baltic Sea, with the aim to expand in-line with the offshore renewable business and to approach new emerging markets within the Asia Pacific and North America region. Since its official opening, the fledgling survey company has already secured contracts in its home market and has received significant interest in the European offshore wind markets. //

Speed matters

While Nicola Offshore's UXO work highlights its specialist approach, it's the choice to build a fleet of high-speed vessels which gives the team a unique ability in the market to optimise the time and cost of transiting to offshore wind farms for ad-hoc or on-demand surveys.

Nicola Offshore's ability to respond to requests for urgent and challenging surveys quickly – the company's goal is to get the job done in days rather than weeks while still retaining the highest safety standards, professionalism and efficiency – comes in part from its advanced marine data acquisition platform based on ProMarine fast vessels fitted with flexible and easily configured integrated hydroacoustic packages.

In addition to the 12.5 metre *Nautical Explorer*, the fleet includes *Nautical Surveyor*, a 14 metre survey catamaran with a still very respectable top speed of 27 knots. Two further vessels will join the fleet in 2021, one of the PROCAT 1200 OBC design used by *Nautical Explorer* and a 14.5 metre aluminium boat with an integral A-Frame. As part-owner of Nicola Offshore, there are also three Fast Workboats in different models on standby at ProMarine in Holland. These are ready to be deployed as survey platforms should the Nicola Offshore team need them.

Integrated hydroacoustic technology and fast boats allow Nicola Offshore's experienced team of hydrographers to tackle the toughest survey

100 years of international cooperation in hydrography

An article by PETER EHLERS

Peter Ehlers was supposed to give a speech at the Assembly 2020 in Monaco planned for the anniversary of the IHO. Unfortunately, this did not happen, the words remained unsaid. But because he has something to say, we publish the manuscript of the speech here.

IHO | IHB | IHC | EIHC | GEBCO | RHC
IHO | IHB | IHC | EIHC | GEBCO | RHC

Bei der zum Jubiläum der IHO für 2020 geplanten Assembly in Monaco hätte Peter Ehlers eine Rede halten sollen. Dazu kam es leider nicht, die Worte blieben ungesagt. Doch weil er was zu sagen hat, drucken wir das Manuskript der Rede an dieser Stelle ab.

Author

Prof. Dr. Dr. h.c. Peter Ehlers was President of the Federal Maritime and Hydrographic Agency (BSH) until 2008 and is co-author of the anniversary book »Measuring and Charting the Seas and Oceans« published by the IHO.

Peter.Ehlers@gmx.de

I. Call for cooperation

Maybe that some time in future the past 100 years will be noticed as the initial period of globalisation. The bad experiences from two world wars led to ever closer international cooperation, which aimed to maintain peace, but also intensified the exchange of information on many technical issues and promoted common, uniform standards. The different parts of the world came closer and closer together. This was particularly evident in the economic relationships that were characterised by ever-increasing world trade. Since world trade is predominantly carried out by sea, safety of navigation has become increasingly important, also in the interest of protecting the marine environment. A basic requirement is the availability and provision of current and precise hydrographic information. While in old times states used to keep hydrographic information more like a secret treasure – it is no coincidence that the first Danish hydrographer Jens Sorensen was called »Spy and Hydrographer« – since the end of the 19th century the voices increased that advocated closer international cooperation. At international maritime conferences 1889 in Washington and St. Petersburg in 1908 and 1912 the advantages of uniformity in nautical charts and publications through international cooperation were highlighted. However, only after the First World War time had come for a first International Hydrographic Conference (IHC), which was initiated by the British and French hydrographers and held in London in 1919.

II. The IHB Statutes

The 1919 conference in principle adopted a proposal to establish an International Hydrographic Bureau (IHB) as a permanent international body to maintain a close association among the par-

ticipating hydrographic offices. For preparing the statutes and specific directions of the IHB a special committee was appointed which after the conference elaborated draft Statutes. By April 1921 they were approved by 19 States. The Statutes formally established the IHB and defined as its object a close and permanent association between the hydrographic services of the Member States to coordinate their efforts with a view to rendering navigation easier and safer in all the seas of the world, causing the national offices to adopt the rules taken by an international hydrographic conference, obtaining uniformity as far as possible in hydrographic documents, and advancing the theory and practice of the science of hydrography. In order to discuss questions concerning hydrography and in particular to review and guide the work of the IHB, an ordinary IHC was to be arranged originally every six years, but it was changed to five years before the first instance. The IHB, which was a consultative body only should be controlled by a Directing Committee, composed of three Directors of different nationalities, elected by the IHC, a Secretary General and further staff. The director elected with the highest number of votes should be the President of the Committee, acting as primus inter pares. The expenses should be borne by subscriptions from the Member States, divided into shares which are dependent on the total tonnage of a Member State. English and French are determined as official languages. The Statutes declared that Monaco should be the official seat, following an invitation of Prince Albert I. These Statutes did not create an international organisation in the modern understanding but were restricted to jointly setting up and operating a bureau to be led by a triumvirate with decisive powers and su-

pervised only in long intervals by meetings of the »owners« who acted as shareholders. From the very beginning the question as to whether such a construction was adequate and efficient for international cooperation was raised again and again.

III. Start-up and persistence in hard times

Following the approval of the Statutes the first three Directors were elected by postal ballot. The counting of the ballots took place on 21 June 1921 at a meeting of the special committee in London in the presence of representatives of several States. This date has to be seen as the official date of the establishment of the IHB. The Directors immediately moved to Monaco and started work, concentrating in particular on internal administrative measures. A quite urgent issue was the relationship with the League of Nations. On 5 October 1921 the Council of the League adopted a resolution stating that the IHB »shall be placed under the direction of the League«. Step by step the general and technical work of the IHB progressed including the collection of surveys carried out, their methods and progress, studies relating to navigation, lights, tides and magnetism as well as information on the methods and processes used for compilation, updating and publication of charts and other nautical documents. For distributing all relevant information about new developments to hydrographic offices (HO), the IHB started in 1923 to publish the *International Hydrographic Review*, and to edit Special Publications. On specific technical and administrative subjects Circular Letters were sent out. Annual Reports describing progress made, including a business and financial report, provided further information and were complemented from 1927 by an IHB Yearbook. In addition, from 1928 prompt information was disseminated by the *International Hydrographic Bulletin*, which initially was published monthly. A Repository of Technical and Administrative Resolutions was gradually built up.

The first IHC organised by the IHB, which was counted as the second IHC after 1919, took place in the Oceanographic Museum of Monaco in 1926 with the participation of 42 delegates from 21 of 22 Member States and two non-Member States. The conference agenda addressed 69 topics, including charts, sailing directions, lists of lights, notices to mariners, catalogues, geographical names, instruments, ocean currents, tides and hydrographic surveys, but also modifications of the Statutes, the financial administration and the election of the Directors and the Secretary General for the next five-year period. As not all issues could be fully examined a Supplementary Conference, counted as the first Extraordinary International Hydrographic Conference (EIHC), was held in April 1929 discussing among other issues for the first time the problem of copyright of hydrographic publications. During the conference, the founda-

tion stone for new premises of the IHB was laid. After completion the building was inaugurated by Prince Louis II of Monaco on 14 January 1931, so that in 1932 the 3rd IHC could be held in the chartroom of the IHB premises. At that conference a specific proposal dealt with the definition of hydrography as the »science by which data concerning the true configuration of the earth, as far as navigation demands, are determined and laid down in charts, Sailing Directions and appertaining publications«. This definition reflects the perception at that time that hydrographic data were relevant for navigation only. The conference also accepted responsibility for the production of the General Bathymetric Chart of the Oceans (GEBCO), originally initiated by Prince Albert I, which since then has been a subject of particular interest.

In the 1930s the IHB negatively suffered from the world economic crisis and adverse political developments. Several Member States withdrew from the IHB. A considerable decrease of the contributions decreased forced the IHB to reduce salaries and the expenses for publications. The difficult financial situation dominated the 4th IHC in 1937, which was only attended by 20 representatives from twelve of 17 Member States. Amongst the various resolutions adopted, was the decision to compile a standard dictionary of hydrographic terms, a task that has quickly proved to be permanent, and therefore continues to this day.

The situation became far more difficult with the outbreak of World War II. Four more States withdrew their membership, two Directors went to their home countries, several staff members left the IHB. The one remaining IHB Director, Pierre de Vanssay de Blavous (France), carried on conducting and maintaining the work as best possible under wartime constraints despite of discussions to suspend all activities and to stop the payment of contributions. In December 1943 and August 1944 the building was severely damaged by bombing, but recovery plans were initiated soon and repairs were carried out by August 1945.

IV. Securing a firm basis

At the end of 1945 the IHB could return to normal operation. The Hydrographic Dictionary was published in which hydrography was now defined more comprehensive, but still concentrating on navigational purposes. Relations with other international organisations were renewed or newly established. In spring 1947 the 5th IHC could be held, 16 of 17 Member States participated together with observers from seven former Member States as well as from the recently established United Nations, UNESCO and some other international organisations. Spanish was introduced as a third conference language. Initiatives to considerably re-organise the IHB resulted in a revised version of the Statutes without changing the legal character,

the leading principles and the general structure. A proposal to become an integrated entity within the framework of the United Nations was rejected as the conference was in favour of having an independent international organisation of mere technical character, free from general political issues. In the following years quite a number of States returned to IHB membership. The 6th IHC in 1952 was attended by 26 out of then 30 Member States, two non-Members and twelve international organisations, proving the great interest in the work of the IHB. The conference was also used to disseminate broader information by lectures given by participants and by an exhibition of instruments, which as a side effect became increasingly important at following IHCs.

At the 7th IHC in 1957 again items relating to constitutional and administrative issues were brought forward, in particular concerning the legal status of the IHB. Therefore, the burdensome process for elaborating a formal convention to achieve recognition of the IHB as an intergovernmental organisation was initiated. After laborious inter-sessional approaches, the issue was re-discussed at the 8th IHC in 1962 with participants from 35 of now 41 Member States and three non-Member States. The conference approved that a convention should be prepared to be adopted some months later on an extraordinary IHC. However, it took additional five years before the 9th IHC in 1967 finally approved the text of an IHO convention. The legal adoption process took further three years, but at last on 22 September 1970 the IHO Convention entered into force. And by this the IHO came into existence as a truly intergovernmental organisation with its own juridical personality. The convention maintained full continuity with the preceding IHB Statutes by taking up their substantial principles, basic objects, goals and functions. The IHC became now the assembly of the members of the organisation and the IHB, composed of the Directing Committee and the professional staff, the executive body or secretariat of the organisation, whereas the additional post of Secretary General was waived. As the Convention was more or less restricted to some main principles and provisions, it was supplemented by General Regulations and Financial Regulations, containing specific rules of procedure. In addition, a Host Agreement was drawn up, which after lengthy negotiations was signed by Monaco and France in 1978.

V. Consolidation in a changing world

Although the period after 1957 was essentially marked by the struggle for a convention, a new focus was also set on other topics. In the 1960s and 1970s great significance was attached to the improvement of hydrographic surveys. This included specifications for hydrographic survey operations, the compilation of an index of those

areas, which had not been surveyed to a standard appropriate for modern navigation requirements, but also the development of a curriculum reflecting the basic standards of excellence, which should be common to all surveys. Together with the International Federation of Surveyors (FIG) a joint International Advisory Board on Standards of Competence for Hydrographic Surveyors was established.

At the 9th IHC in 1967 a first step was made to establish an international charting system, initially confined to charts at small scale. After the publication of the first INT charts in 1972, the 10th IHC extended the concept to medium and large scale charts, so that international shipping could navigate along all the major sea routes and enter all major ports of any country by using standardised INT charts.

It became more and more obvious that hydrographic data and information were not required for navigation only, but also for other purposes related to the use and protection of the seas and as a basic tool for countries to manage their marine areas. Whereas the fishery industry had since long been interested in specific hydrographic data, the increasing offshore activities, aiming at the exploitation of hydrocarbons, created a growing need for precise hydrographic data.

Another issue that took more and more prominence was technical assistance in the field of hydrography. The 10th IHC in 1972 explicitly decided that the IHB should serve as a source of technical advice and as a coordinating body for the promotion of measures to establish or strengthen the hydrographic capabilities of developing countries, taking into account that at least 50 coastal States had no hydrographic services at all, whereas the hydrographic capabilities in many other developing countries were extremely limited.

In the field of navigation and oceanography cooperation with other international organisations became more and more important. The IHO closely collaborated inter alia with the IMCO, now the IMO, the IOC of UNESCO, IALA, WMO, and also participated in the UN conferences on the law of the sea, starting in 1973 with the aim to elaborate a new convention. To strengthen the cooperation between neighbouring HOs the 9th IHC formally accepted and encouraged the establishment of Regional Hydrographic Commissions (RHC) to cooperate in the solution of common regional problems of charting, research or data collection. At the beginning of the 1970s six RHCs were active. The IHO membership steadily increased and in 1972 reached 43, the 10th IHC was attended by 37 of then 43 Member States, six non-Member States and 24 intergovernmental and other international as well as national organisations and associations. Due to the large number of participants the IHC could no longer be held at the IHB premises, but

was organised in the »Centre des Rencontres Internationales«. As an important platform for the hydrographic community the conference was supplemented by lectures, an exhibition of hydrographic, oceanographic and navigational instruments and products, and the visit of several hydrographic vessels. In 1977 the 11th IHC introduced Russian as a fourth working language together with English, French and Spanish.

As the workload steadily grew, the IHB made more and more use of the knowledge and experience by groups, formed of specialists from Member States. If appropriate such groups were established in partnership with cooperating international organisations. Confusingly, the naming of these bodies differed between working groups, ad hoc groups, commissions, committees and even advisory boards. Due to increasing tasks and responsibilities in the 1960s the IHB staff, not including the Directing Committee, had been expanded to 19 persons, but in the 1970s was reduced again to 15 persons because of economic menaces, despite considerable increase in contributions to be paid by the Member States.

VI. New challenges

In the 1980s the IHO had to face new challenges. Hydrographic activities were more and more influenced by technological developments, in particular by the increasing use of computers, which opened a wide field for digitisation. Close international cooperation gained further weight. The workload of expert groups constantly became heavier. In the mid-1980s there existed ten commissions, committees, sub-committees and working groups in total. A decade later the working load had further increased. The 1993 Annual Report cited 24 commissions, committees and working groups of the IHO, including joint bodies with other organisations, and contacts with 37 international organisations and associations. Yet the now existing eight RHCs also took on specific projects, which they carried out for the benefit of the whole hydrographic community, in particular as concerns INT charts. Additionally, because of increasing activities in Antarctica, in 1992 the 14th IHC established a Permanent Working Group on Cooperation Concerning Hydrographic Surveys and Charting in Antarctica. The efforts were in-

RIEGL VQ-840-G

TOPO-BATHYMETRISCHER LASERSCANNER



- ideal für die Datenaufnahme von UAVs oder Helikoptern aus
- grüner Laserstrahl mit mehr als 2 Secchi Tiefen Wasserdurchdringung
- Messrate von 50 kHz bis zu 200 kHz
- hochauflösende Digitalkamera und INS/GNSS System vollintegriert

UAV-BASIERTE VERMESSUNG VON
KÜSTENGEBIETEN UND FLACHWASSERZONEN



QR-Code
scannen und
RIEGL VQ-840-G
Video ansehen!

www.riegl.com

Weitere topo-bathymetrische Laserscanner
und Systeme finden Sie auf www.riegl.com

[f](#) [t](#) [in](#) [w](#) [y](#) [v](#) [n](#) [e](#) [n](#) [s](#) [r](#) [o](#) [o](#) [m](#) [.riegl.international](#)



tensified to increase awareness in developing countries that hydrography was needed for the safety of navigation as well as for tasks relating to the marine environment, coastal research and coastal engineering. These technical assistance activities included contacts with Governments, expert missions and workshops together with other organisations, training courses at several maritime academies and the encouragement of HOs to transfer excess equipment to needy nations.

The setting up of a committee on the exchange of digital hydrographic and charting data between HOs by the 12th IHC (1982) may be marked as the very beginning of the development of an electronic chart system. Some time later the considerations led to the creation of an IMO/IHO Harmonization Group on ECDIS. At the beginning of the 1990s the development of ECDIS became a major issue of the work of the IHO and resulted in the elaboration of precise standards and specifications. The 14th IHC (1992) set up a special committee to examine matters related to the establishment of a Worldwide Electronic Chart Data Base (WEND) as an indispensable prerequisite to introduce Electronic Navigational Chart (ENC) services. In November 1995, the IMO Convention on Safety of Life at Sea was amended for an electronic chart display and information system to be accepted as satisfying the chart carriage requirements, referencing the IHO performance standards for ECDIS. An important milestone in the history of hydrography and navigation was the introduction of the first operational ENC service, offered by the regional electronic navigational chart centre PRIMAR in Norway in 2000, which was opened by King Harold of Norway.

Another crucial issue was the publication of nautical documents by private publishers, resulting in the decision that no HO may grant permission for reproduction, if the area in question includes data collected by another HO, as the data belong to the originator.

Since the entry into force of the IHO Convention the IHC repeatedly discussed internal matters of the organisation, in particular concerning the most effective structure and composition of the Directing Committee. The 13th IHC (1987) even amended the convention to introduce a new election procedure. However, this amendment never came into effect, as the necessary quorum for formal approval was not achieved. Another issue were the service conditions which at the 14th IHC led to the approval of further convergence with the relevant conditions in the UN system.

In the 1980s the annual income of the IHO grew steadily because of increasing membership. At the end of the decade 57 States were members of IHO. Yet the workload of the IHB and all the different expert bodies significantly increased accordingly.

The output of publications informing about the results of the various activities tripled, not the least thanks to the acquisition of modern printing equipment and computerisation that speedily advanced in the 1990s. The internet dramatically facilitated communication. More and more digital versions of publications and documents were made available. The use of the Spanish language was enhanced, when the 14th IHC tasked the IHB to use Spanish for certain periodical publications, Circular Letters and correspondence.

VII: Facing the third millennium

In late 1996, 75 years after its inauguration, the IHB premises were moved to the opposite side of the harbour to the new location 4 Quai Antoine 1er. This heralded a phase of great change. With about 300 delegates from 52 of 63 Member States, 18 non-Member States and 15 organisations and associations the 15th IHC (1997) was larger than ever before. The conference was marked by the growing awareness that changing and adapting to new developments had become more and more urgent in order to survive in the future. A more systematic internal structure of the IHO and a clear strategic orientation were needed. The conference adopted clear principles for the formation of inter-sessional subsidiary bodies and general guidelines for the creation of RHCs, which were understood as part of the IHO. With regard to the question of how to cope with future challenges in the field of hydrography to be prepared for entering the 21st century, an inter-sessional Strategic Planning Working Group (SPWG) was established.

Acknowledging that the copyright of the data belongs to the HO that is the originator of the data which are included in a chart or a nautical publication, the 15th IHC approved principles to be applied by HOs when permitting private publishers to reproduce charts or nautical publications. Furthermore, new rules for the exchange and the reproduction of nautical products on the basis of bilateral agreements between HOs were accepted.

The growing importance of assisting countries in developing hydrographic capabilities was reflected in 1998 by a UN General Assembly Resolution on oceans and the law of the sea, which on the occasion of the International Year of the Ocean for the first time made reference to hydrography and explicitly invited States to carry out hydrographic surveys and to provide nautical services. The IHO concentrated on capacity building activities by conducting technical assistance visits and accompanying development projects to be implemented with the support of donor organisations. Not the least these activities encouraged additional States to establish hydrographic services and to become members of the IHO. In 2000 the

membership had increased to 69 Member Governments. At the same time twelve Regional Hydrographic Commissions and the Committee for Antarctica existed, covering most of the major sea areas worldwide.

In a time of globalisation when maritime transport was steadily growing and the risks for the marine environment in case of casualties were expanding, accurate hydrographic information became more important than ever for safe navigation. It was only logical that the IMO in 2000 revised Chapter V of the International Convention for the Safety of Life at Sea (SOLAS) to introduce new regulations that oblige Contracting Governments to carry out nautical and hydrographic services in the manner most suitable for navigation. Charts and nautical publications must be issued by or on behalf of a relevant Government institution. These regulations, which entered into force in 2002, may be seen as a quantum leap for HOs. For the first time international law created an obligation for States to maintain hydrographic services, as well as a firm commitment to cooperate, standardise and coordinate activities on a worldwide scale. The in-

creasing interest in hydrographic matters was also shown when in 2001 the IHO, though for good reasons still not interested in becoming a UN organisation, was granted observer status to the UN General Assembly.

Based on an analysis of the strengths and weaknesses of the organisation and the opportunities and threats facing it, the SPWG developed strategic goals and priorities of IHO, examined necessary structural or constitutional changes to enhance the future effectiveness, proposed a strategic planning cycle and presented a strategic plan. To speed up the process the results of the SPWG were discussed at a supplementary conference, the 2nd EIHC, in 2000. The conference adopted the proposed new Strategic Plan, which highlighted as main strategic issues the transition to the digital era, a global hydrographic data coverage, the response to developments of Government policy, the adequate funding for the provision of hydrographic services, the building up of effective national organisations and the provision of services other than for navigation. For implementing this plan, a work programme for the next five-year pe-



OBTAIN **COMPREHENSIVE** **HYDROGRAPHIC DATA** **IN DEEP WATER** **AND COASTAL REGIONS**

We draw on our vast experience and extensive resources, including a fleet of dedicated survey vessels and airborne systems, to deliver a high-quality service that meets your data objectives.

To find out more visit
fugro.com

riod and the future planning cycle were approved. The SPWG continued to study especially the need of structural changes and was tasked by the 16th IHC (2002) to carry out a study on the need to revise the IHO Convention.

Considerations, which had started in the 1970s, that hydrographic data were not only important for navigation, became more and more evident. The demand grew for hydrographic data for other purposes, especially for fishing, offshore activities, coastal protection, harbour construction, and marine scientific research; non-navigational applications had to include the determination of national maritime boundaries, coastal zone management, modelling of marine areas, study of habitats, assessment of the state of the marine environment and exercise of national rights in maritime zones. Accordingly, the IHO understood the provision of hydrographic data for geomatic applications as an important new policy direction.

VIII. Renewing the IHO

The work to reform and modernise the IHO, especially done by the SPWG, came to a conclusion

by a 3rd EHC in 2005 in agreeing on far reaching amendments of the IHO Convention. The main objectives of the amendments were to maintain the strengths, eliminate the weaknesses, achieve the vision, mission and objectives of the IHO and establish a more effective and cost-effective system. The new version of the convention clarifies that the IHO is the competent international organisation for hydrography and defines its vision, mission and objects. The organisational structure and procedures are drastically changed. The IHC is now named the Assembly, being the principal organ of the IHO, and has all the powers of the organisation unless otherwise regulated. The period between ordinary sessions of the Assembly is reduced to three years. In addition to the Assembly a Council is created. It is composed of one fourth, but not less than 30 Member States. The functions of the Council are to guide and coordinate the IHO activities during the inter-Assembly period. The term International Hydrographic Bureau (IHB) is replaced by the term Secretariat, which comprises of a Secretary General as the chief administrative officer, Directors and other personnel.

DHyG-Sonderpublikationen

Sophie Andree:

Interactive processing of MBES bathymetry and backscatter data using Jupyter Notebook and Python
DHyG-Sonderpublikation Nr. 003
DOI: 10.23784/DHyG-SP_003

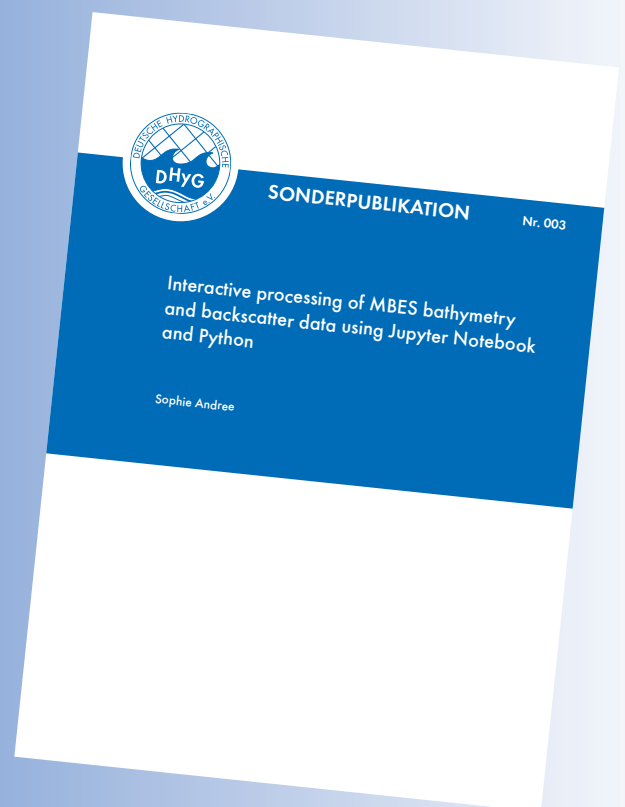
Hannes Nübel:

Bathymetry from multispectral aerial images via Convolutional Neural Networks
DHyG-Sonderpublikation Nr. 002
DOI: 10.23784/DHyG-SP_002

Patrick Goffinet:

Neue Bewertung der harmonischen Analyse im Vergleich zur Darstellung der Ungleichheiten am Beispiel der Deutschen Bucht
DHyG-Sonderpublikation Nr. 001
DOI: 10.23784/DHyG-SP_001

www.dhyg.de/index.php/hydrographische-nachrichten/sonderpublikationen



Supplementary detailed provisions were adopted by the 17th IHC in 2007, including General Regulations and Rules of Procedures for the Assembly, the Council and the Finance Committee. In anticipation of the Convention amendments, which had not yet entered into force, the 17th IHC also decided on a new structure for the subordinate bodies by establishing the Hydrographic Services and Standards Committee (HSSC) and the Inter-Regional Coordination Committee (IRCC) as main committees. The hitherto unclear legal nature of the existing 15 RHCs was explicitly regulated, as being regional bodies established by Member States, but recognised by the Assembly. A special status was maintained for the Hydrographic Commission on Antarctica.

Capacity building, in particular, gained more and more importance and was strongly influenced by the RHCs and further enhanced by annual UN General Assembly Resolutions on the Law of the Sea, which repeatedly welcomed the work of the IHO and its Regional Commissions. The importance of international cooperation and the support for developing States in building up hydrographic capabilities became highly obvious after the tsunami disaster in December 2004 and was reconfirmed in response to the earthquake and tsunami in Japan in 2011. The 18th IHC in 2012 agreed on revised guidelines and procedures with the aim of helping Member States to develop contingency plans in case of anticipated disasters.

In 2005 the UN General Assembly explicitly welcomed the adoption by the IHO of a «World Hydrography Day» to be celebrated annually on 21 June, as the date of creation of the IHB, with the aim of giving suitable publicity to its work and of increasing the coverage of hydrographic information on a global basis.

Especially concerning ECDIS, the collaboration with IMO became even more intensive, as the work of the IHO depended on the acceptance of performance standards and carriage requirements to be determined by IMO. As a first step, in 2006 the IMO made the carriage of ECDIS mandatory for high speed craft. Three years later in 2009 the mandatory carriage for other than high speed craft was introduced by IMO in a phased manner from 2012 onwards. In the light of this development the 17th (2007) and 18th IHC (2012) underlined the importance of full ENC coverage and the need in many parts of the world for improving the collection, quality and availability of hydrographic data.

In order to manage the many different seaborne uses and interests, the need for precise marine data became more and more evident, not the least as an indispensable basis for the development of marine spatial planning programmes. Hydrographic data were seen as an important part of an adequate marine data infrastructure. HOs had

to move from map production as their primary focus to the management and operation of, or the participation in, marine spatial data infrastructures (SDI) from which nautical charts and other products were derived. The 4th EIHC (2009) adopted a Marine Spatial Data Infrastructure Policy, in 2011 the IHB launched a specific IHO Publication on «Spatial Data Infrastructure – the Marine Dimension», which explained the way that HOs might provide hydrographic-related data as part of the national SDI.

Another further remarkable step towards the modernisation of the IHO was made by the 4th EIHC. The starting point was a new definition of hydrography as «the branch of applied sciences which deals with the measurement and description of the physical features of oceans, seas, coastal areas, lakes and rivers, as well as with the prediction of their change over time, for the primary purpose of safety of navigation and in support of all other marine activities, including economic development, security and defence, scientific research, and environmental protection». The broad new definition was reflected in the revised Strategic Plan that was not a mere updating of the earlier version but introduced a new systematic approach and the use of modern management tools, which was to be implemented by a new structured Working Programme, including annual performance monitoring. The 4th EIHC also invited the relevant RHCs to encourage through appropriate liaison bodies the consistent use of hydrographic standards and mutual cooperation for the enhancement of safety in navigable inland waters within and between regions, as no other organisation was in a position to foster this harmonisation.

In the 2000s cooperation with private industry steadily became closer. The exchange of information and experience with stakeholders from academia, industry, government and non-governmental organisations was intensified through stakeholders' forums. A special information session, held at the 5th EIHC (2014), in particular dealt with the collection of bathymetric data collated by private crowd-sourcers, as new technologies could be used by private entities leading to the development of open-sea-map behaviours.

The conferences in 2012 and 2014 devoted particular attention to the progressively increased workload and scope of the IHO, which was mainly due to the rising number of Member States, more RHCs and more regular RHC meetings, secretariat functions for IHO bodies, the implementation and management of the capacity building programme, the maintenance of the very comprehensive IHO documentation and website, the introduction of programme performance monitoring, the involvement in outreach activities and the active recruitment of new Member States, implementation measures related to ECDIS, participation in the de-

velopment of the IMO e-navigation strategy and representation in a number of new intergovernmental initiatives. At the same time the transition from paper to digitally-based hydrographic products and the broader use of the IHO data transfer standard placed an increased responsibility and obligation on the IHO to ensure the reliable maintenance of the standard.

IX. IHO today

After twelve years the necessary quorum for the approval was met and the Protocol of Amendments to the IHO Convention entered into force on 8 November 2016. The new structure of the IHO was put in place without significant problems. The IHC now became the IHO Assembly. As an additional powerful organ, the Council was established to act in operational control of the organisation for the inter-sessional period. And the former IHB was renamed to IHO Secretariat. The now 87 Member States held the first Assembly meeting in spring 2017, adopted the necessary organisational and procedural adaptation measures, approved the composition of the Council, and elected Mathias Jonas, the former head of the Nautical Hydrographic Department of the BSH (Federal Maritime and Hydrographic Agency, Germany) as Secretary General as well as two assisting Directors. The Assembly also dealt with numerous technical issues, such as the use of ECDIS, information to mariners about submarine cables, improvement of the availability of bathymetric data worldwide, including crowd sourcing, and participation in geospatial information management activities. Some months later the Council started its annual meetings, focusing on strategic planning, the Work Programme and financial control, including the approval of the budget for the following year. Due to the global

effects of the Covid-19 pandemic the second Assembly was moved from April to November 2020 and was only conducted as a remote event by combining Assembly Circular Letters to be decided on in advance and virtual assembly sessions. This hybrid format resulted in 52 decisions, including the future of the paper chart, the further development of the technical standardisation of ENC's, as well as the Work Programme and budget for the next three year-period. Thus, IHO's ability to remain agile and decisive under extraordinary conditions was demonstrated, though the paramount benefit of in-person meetings was recognised by all online participants.

X. Conclusion

At its 100th anniversary the IHO, which has begun as a Bureau with 19 shareholders, has become the competent global organisation for hydrography, comprising of 94 Member States from all parts of the world, and with an annual budget that increased from originally 242,000 Swiss francs to 3.6 million euros. Over the past 100 years, IHO has consistently succeeded in modernising itself, adapting and expanding its range of tasks and activities in the light of new developments and challenges. Despite all changes and modifications, however, an unbroken continuity has been maintained. It has been proved advantageous that the IHO is not a political, but a technical organisation only. Nor has it been a hindrance that the IHO is of consultative nature only, as technical standards reflect the state of the art and therefore in the end are accepted and applied even if they are not legally binding. While the IHO, for well-considered reasons, is not part of the UN system, it is nevertheless an indispensable element in global efforts concerning safety of navigation and the sustainable development of the oceans. //



SIMPLIFY MARINE DATA ACQUISITION

NEW – integrated Hydrographic Survey System (iHSS) includes
MULTIBEAM · WORKSTATION · SOFTWARE · INS · MOUNTING SOLUTION

» **OPTIMISE YOUR HYDROGRAPHIC WORKFLOW – TURNKEY SOLUTION**

» **EASY TO INSTALL, CALIBRATE AND OPERATE – OFFSHORE OR INLAND**

» **FLEXIBLE AND COST-EFFECTIVE PLANS – RENT, SUBSCRIBE OR BUY**

iHSS-Standard

Based on R2Sonic 2024 Multibeam
Echo Sounder depth rated to 4000 m

iHSS-Compact

Based on R2Sonic 2020 Multibeam
Echo Sounder depth rated to 100 m

Both available as Dual head system allowing for more than 200 degrees of swath coverage



**CHECK OUT OUR EXTENSIVE RENTAL POOL FOR HIGH
AVAILABILITY ON COMPONENTS, SYSTEMS AND PACKAGES**

SCAN WITH YOUR SMARTPHONE

*Subsea Europe Services GmbH is a hydrographic survey
technology provider based in northern Germany. We offer:*

» **FAST-TRACK DELIVERY ANYWHERE IN EUROPE**

» **REMOTE TECH AND ON-BOARD SURVEY SUPPORT**

» **IN-HOUSE POST PROCESSING EXPERTISE**



Präzise 3D-Positionierung mit GNSS und Polarmessverfahren

Die Leica GNSS-Instrumente empfangen und verarbeiten die Signale aller aktuellen und zukünftigen Navigationssysteme.

Höchste Präzision bei voller Automatisierung der Messabläufe garantieren die Leica Polarmesssysteme.



Leica Geosystems GmbH Vertrieb
www.leica-geosystems.de



- when it has to be **right**

Leica
Geosystems